

Analysis of SUMOylation in human Adenovirus large E1B proteins

Dissertation

with the aim of achieving a doctoral degree at the
Faculty of Mathematics, Informatics and Natural Sciences,
Department of Biology,
University of Hamburg

submitted by

Viktoria Kolbe

January 2019 in Hamburg

Tag der Disputation: 15. März 2019

Erster Gutachter: Prof. Dr. Thomas Dobner

Zweiter Gutachter: Prof. Dr. Nicole Fischer

Declaration on oath

I hereby declare on oath that I have written the present dissertation myself and have not used any sources or aids other than the ones indicated.

Hamburg,

Signature



HPI

Heinrich Pette Institute
Leibniz Institute for Experimental Virology

HPI • Martinistraße 52 • D-20251 Hamburg

Timothy Soh, Ph.D.

Research Department of
"Structural Cell Biology of Viruses"

Phone: +49 (0) 40 480 51-273
timothy.soh@leibniz-hpi.de

Page 1 of 1

Hamburg, Jan 11, 2019

Viktoria Kolbe's Ph.D. thesis entitled "**Analysis of SUMOylation in human Adenovirus large E1B proteins**" is written in fluent and proper English. I confirm that the language is clearly written and properly articulated.

Kind regards,

"There's more to the picture than meets the eye."

Neil Young

Table of content

Abbreviations	X
Abstract	XII
1 Introduction	14
1.1 Adenoviruses	14
1.1.1 Classification and pathogenesis.....	14
1.1.2 Structure and genome organization.....	16
1.1.3 Infectious life cycle of HAdV	17
1.1.4 Early region 1B protein	19
1.1.5 Transforming potential and oncogenicity of HAdV.....	22
1.2 The cellular post-translational modification (PTM) machinery.....	23
1.2.1 Pathways of cellular PTM.....	23
1.2.2 Modification by the small ubiquitin-like modifier (SUMO).....	24
1.2.3 Post-translational modification of viral pathogens.....	26
1.2.4 HAdV-C5 E1B-55K as a target of the cellular PTM machinery.....	27
2 Material.....	30
2.1 Cells	30
2.1.1 Bacterial Strains.....	30
2.1.2 Mammalian cell lines.....	30
2.2 Viruses	31
2.3 Nucleic acids	31
2.3.1 Oligonucleotides	31
2.3.2 Vector plasmids.....	33
2.3.3 Recombinant plasmids.....	33
2.4 Antibodies	36
2.4.1 Primary antibodies	36
2.4.2 Secondary antibodies	36
2.5 Standards and markers	37
2.6 Commercial systems.....	38
2.7 Chemicals, enzymes, reagents, equipment.....	38
2.8 Software and databases	38
3 Methods	40

3.1	Bacteria.....	40
3.1.1	Culture and storage	40
3.1.2	Chemical transformation of <i>E. coli</i>	40
3.2	Mammalian cells.....	41
3.2.1	Cultivation and passaging.....	41
3.2.2	Storage.....	42
3.2.3	Transfection of mammalian cells.....	42
3.2.4	Cell harvesting	43
3.2.5	Transformation of pBRK cells.....	43
3.3	Adenovirus.....	44
3.3.1	Infection of mammalian cells	44
3.3.2	Propagation and storage of high-titer virus stocks.....	44
3.3.3	Titration of virus stocks	44
3.4	DNA techniques.....	45
3.4.1	Preparation of plasmid DNA from <i>E. coli</i>	45
3.4.2	Quantitative determination of nucleic acid concentrations.....	46
3.4.3	Agarose gel electrophoresis.....	46
3.4.4	Polymerase Chain Reaction (PCR).....	47
3.4.5	Site-directed mutagenesis.....	47
3.4.6	DNA sequencing.....	48
3.5	Protein techniques	48
3.5.1	Preparation of total cell lysates.....	48
3.5.2	Quantitative determination of protein concentrations.....	49
3.5.3	SDS polyacrylamide gel electrophoresis (SDS-PAGE).....	49
3.5.4	Western Blot analysis	50
3.5.5	Denaturing purification and analysis of SUMO-conjugates	51
3.5.6	Indirect immunofluorescence	53
3.5.7	Reporter gene assay.....	53
4	Results.....	55
4.1	K101 regulates SUMOylation of HAAdV-C5 E1B-55K	55
4.1.1	HAAdV-C5 E1B-55K K101R is highly SUMOylated in transient transfection and during infection.....	55
4.1.2	HAAdV-C5 E1B-55K K101R localizes to the nucleus in transient transfection	61
4.1.3	HAAdV-C5 E1B-55K K101R localizes to structures resembling viral replication center (VRC) during infection.....	64

4.2	HAdV-C5 E1B-55K K101R leads to a “gain-of-function” in transiently transfected cells	68
4.2.1	HAdV-C5 E1B-55K K101R shows increased repression of p53-stimulated transcription.....	68
4.2.2	HAdV-C5 E1B-55K K101R leads to enhanced focus formation in pBRK cells	70
4.2.3	Acetylation of HAdV-C5 K101 might downregulate SUMOylation at K104	72
4.3	SUMOylation of E1B-55K is conserved amongst HAdV species	73
4.3.1	K101 is specific for E1B-55K of species C HAdV	73
4.3.2	E1B-55K from different HAdV species are highly SUMOylated at a conserved SCM.....	75
4.3.3	Nuclear localization of E1B-55K from different HAdV species is dependent on SUMOylation	79
4.3.4	Several E1B-55K proteins from HAdV species are able to repress p53- stimulated transcription in a SUMO-dependent manner	85
4.3.5	E3-SUMO-ligase function of HAdV E1B-55K is not conserved throughout different species	88
5	Discussion.....	91
5.1	K101 is a novel regulator of HAdV-C5 E1B-55K SUMOylation.....	91
5.2	SUMOylation of E1B-55K is conserved among HAdV species	98
6	Literature	102
	Zusammenfassung.....	CXX
	Publications.....	CXXII
	Danksagung.....	CXXIII

Abbreviations

aa	Amino acid
ab	Antibody
AdV	Adenovirus
APS	Ammonium persulfate
bp	Base pair
BRK	Baby rat kidney cells
BSA	Bovine serum albumin
CAR	Coxsackie / Adenovirus-receptor
DAPI	4',6'-diamidine-2'-phenylindole dihydrochloride
DDR	DNA damage response
DMEM	Dulbecco's Modified Eagle Medium
ds	Double-stranded
<i>E. coli</i>	<i>Escherichia coli</i>
EBV	Epstein-Barr Virus
<i>et al.</i>	And others (et alii, lat.)
EtOH	Ethanol
FCS	Fetal calf serum
<i>ffu</i>	Fluorescence forming unit
Fig.	Figure
fwd	Forward
h p.i.	Hours post infection
h p.t.	Hours post transfection
HAdV	Human Adenovirus
hCMV	Human Cytomegalovirus
HRP	Horseradish Peroxidase
kb	Kilobase
kDa	Kilodalton
LB	<i>Luria-Bertani</i>
MLTU	Major late transcription unit
MOI	Multiplicity of infection
NES	Nuclear export signal
NEM	N-ethylmaleimide

PBS	Phosphate buffered saline
PCR	Polymerase chain reaction
PEI	Polythylenimine
PFA	Paraformaldehyde
PTM	Post-translational modification
rev	Reverse
rpm	Rounds per minute
RT	Room temperature
SCM	Consensus SUMO conjugation motif
SCS	SUMO conjugation site
SDS	Sodium dodecyl sulfate
SIM	SUMO interacting motif
SUMO	Small ubiquitin-like modifier
TBS-BG	Tris-buffered saline with BSA and glycine
TBE	Tris/Borate/EDTA buffer
wt	Wild type
(v/v)	Volume per volume
(w/v)	Weight per volume

Abstract

The human adenovirus (HAdV) type 5 from species C (HAdV-C5) early region 1B 55 kDa (E1B-55K) is a multifunctional protein that plays an important role throughout the entire viral replication cycle. E1A, the first viral protein that is expressed, induces the cell to enter S-phase, thereby stabilizing the apoptotic cellular protein p53 and supporting viral replication. E1B-55K evolved several mechanisms to counteract this stabilization of p53. On the one hand, E1B-55K acts as an E3-SUMO-ligase for p53 promoting nuclear export of the protein. Thus, activation of proapoptotic p53-dependent genes is inhibited. On the other hand, E1B-55K forms an E3-ubiquitin-ligase together with E4orf6 and other cellular proteins that degrade not only p53, but also other factors involved in the DNA damage response (DDR) and transcriptional regulation (Mre11, SPOC-1, Daxx). Thus, antiapoptotic and proviral functions grant E1B-55K an oncogenic potential. Post-translational modifications (PTMs) of E1B-55K additionally contribute to the functional diversity of the protein. E1B-55K is a phosphoprotein and a target of the SUMO conjugation machinery and phosphorylation at the C-terminus is a prerequisite for efficient SUMOylation at lysine 104 (K104). Interestingly, many functions of E1B-55K are regulated by its SUMOylation, indicating that this PTM is essential for the protein. To further investigate SUMOylation of E1B-55K, a site-specific SUMO proteome was performed. Thereby, a lysine at position 101 (K101) was revealed as a potential new site for SUMO conjugation. K101 is in close proximity to the main SUMO conjugation motif (SCM) around lysine 104 (K104), therefore being an interesting new target and thus subject of this work.

In the first part, lysine 101 (K101) was identified as a regulator for E1B-55K SUMOylation. Remarkably, inactivation of this site via an amino acid exchange (K101R) resulted in an increased SUMOylation of the protein. In concert with previous studies, higher SUMOylation revealed a mainly nuclear retention of the protein and a clear localization to structures resembling viral replication centers (RCs) in infection experiments. Consequently, as SUMOylation promotes E1B-55K functions, stronger repression of p53-stimulated transcription and increased *focus* formation in transformation experiments with the K101R-mutant was observed.

The second part of this work concentrated on E1B-55K from different HAdV species. Here, a conserved SCM in E1B-55K from nearly all HAdV species was identified. Furthermore, K101 is specific for HAdV-C, since other HAdV species with a SCM contain an arginine at the corresponding site. Comparable to HAdV-C5 E1B-55K K101R, E1B-55K from almost all species analyzed in this work revealed a high SUMOylation together with a mainly nuclear localization. However, E1B-55K-dependent repression of p53 transactivation is rather conserved among HAdV species, whereas E3-SUMO1-ligase function is not. Moreover, SUMOylation functions as a regulator for E1B-55K in most, but not all HAdV species. The results of this work suggest that E1B-55K evolved conserved functions across HAdV species that slightly differ depending on the species and possibly pathogenicity.

1 Introduction

1.1 Adenoviruses

1.1.1 Classification and pathogenesis

Adenoviruses were first isolated in 1953 from adenoid tissue [1] and named according to their origin [2]. Although the virus was then found to be the causative agent for acute diseases of the respiratory tract, it is known today that only a small percentage of respiratory illnesses are related to Adenovirus [3, 4].

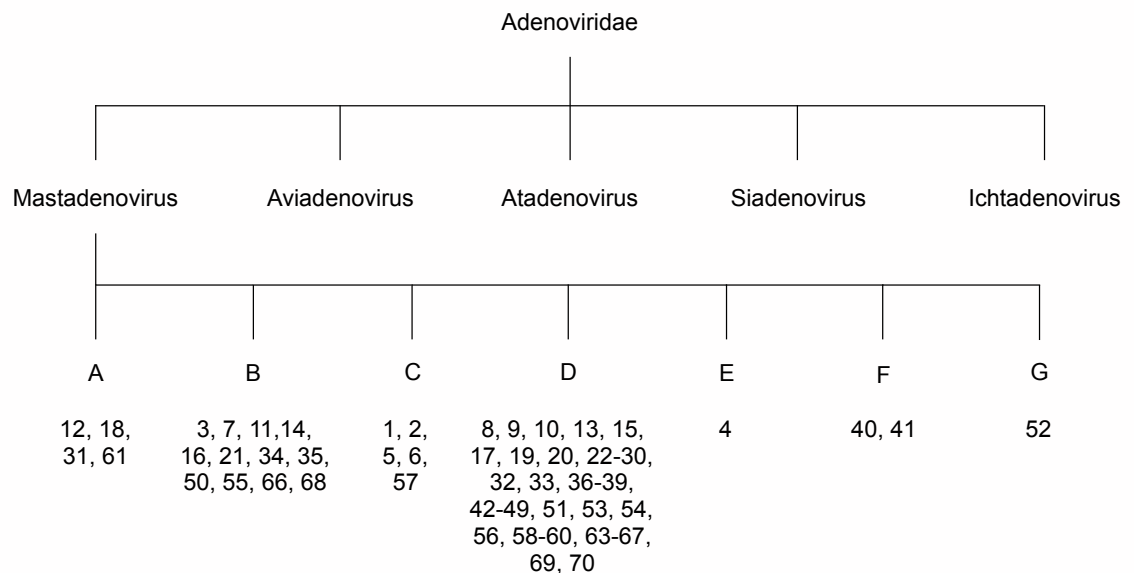


Fig. 1: Classification of human Adenoviruses (HAdVs). Schematic illustration of the family of *Adenoviridae* and the genus *Mastadenovirus*. The letters A-G indicate the HAdV species and the numbers 1-70 specify the so far investigated HAdV types according to Davison *et al.* and the International Committee of the Taxonomy of Viruses (ICTV) [5].

Adenoviruses belong to the family of *Adenoviridae*. They are clustered into 5 genera according to their host specificity and thus able to infect a wide range of vertebrates. Mastadenoviruses and Aviadenoviruses originate from mammals and birds, respectively. Atadenoviruses were isolated from reptiles, birds, ruminants and marsupials and Siadenoviruses infect avian and amphibian hosts [5, 6]. So far, only one adenovirus type belongs to the last genus, the Ichtadenoviruses, and was isolated from fish [7] (Fig. 1).

Human Adenoviruses (HAdVs) belong to the Mastadenoviruses. They consist of 7 species (A-G) that are further divided in currently more than 70 different types [8, 9] (Fig. 1). Types 1-51 were classified based on the serum neutralization and hemagglutination. More recently, genomic and bioinformatic data are used to analyze and identify novel HAdV [10–13]. More precisely, the assignment to a specific HAdV species and type involves analysis of the phylogenetic distance, genome organization, GC-content, oncogenicity in rodents as well as number of virus-associated (VA) RNAs [8].

HAdV have a broad tissue tropism and primarily target differentiated epithelial cells [13–16], causing pneumonia (species A, E), hemorrhagic cystitis (species A, B, E) keratoconjunctivitis (species D) and gastroenteritis (species F) [11, 17–22]. HAdVs usually cause mild infections that are self-limiting. In immunocompetent patients, diseases of the eye, the respiratory and gastrointestinal tract typically have a mild outcome [13]. Nevertheless, cases in which HAdV infections had a fatal outcome are reported in immunocompetent patients suffering from lower respiratory tract infections or myocarditis [23, 24]. In immunocompromised patients, HAdV infections result in severe outcomes leading to acute pneumonia, hepatitis or encephalitis [25, 26]. These severe diseases are observed in patients with primary immune deficiencies and more often in transplant recipients, especially in children [27–30]. Additionally, high prevalence of HAdVs, mainly from species C, are found in children [31]. Together with the fact that many children receiving organ transplants suffer from severe HAdV infections, the virus is thought to persist and reactivate upon immunosuppression. In fact, persistent infections with species C HAdVs have been observed in cell culture systems as well as in humanized mouse models [32, 33].

Generally, HAdVs are used as a great model system to discover important molecular mechanisms as well as virus-host interactions. Possibly, the most prominent example is the discovery of mRNA splicing in 1975 [34, 35]. Finally, HAdVs are classified as DNA tumor viruses since the discovery that HAdV-12 from species A causes tumors in newborn hamsters [36]. Although this virus is still not linked to tumor formation in humans, many studies on HAdVs have revealed important aspects of viral oncogenesis.

1.1.2 Structure and genome organization

HAdVs are dsDNA non-enveloped viruses with an icosahedral capsid. Virion particles are 80-110 nm in diameter and consist of 240 capsomers formed by hexon trimers. At each of the 12 vertices of the icosahedron there is a penton base with a fiber protein attached to it (Fig. 2) [4, 37]. Usually, HAdVs encode one fiber protein; only HAdV-40 and HAdV-41 from species F as well as HAdV-52 from species G encode two fiber proteins. Either one or the other is presented on the outer protein shell of the virion, probably enabling the virus to enter a broader range of cells [4, 11]. After all, penton and fiber proteins are important for the attachment to the host cell via receptor binding. HAdVs mainly bind to the coxsackie/adenovirus receptor (CAR), yet most HAdVs from species B attach to the host cell via CD46 [38, 39]. Whereas hexon, penton and fiber are considered to be the major capsid proteins, other so-called minor capsid proteins (proteins pIIIa, pVI, pVIII, pIX) are important for efficacious capsid formation as well [40]. Indeed, further studies on HAdV capsid formation and the structural proteins involved revealed that the capsid is “not just a shell” [16] but provides important functions regarding virus-host interactions [16, 41]. Besides the capsid proteins, HAdVs express other structural proteins that are associated with the genomic core of the virus, thus called core proteins [16]. Proteins pV, pVII and μ condense the viral DNA in the core [42, 43] and the terminal protein (TP) is covalently bound to the 5' end of the viral genome [44, 45]. Furthermore, TP acts as a primer for viral DNA replication [46].

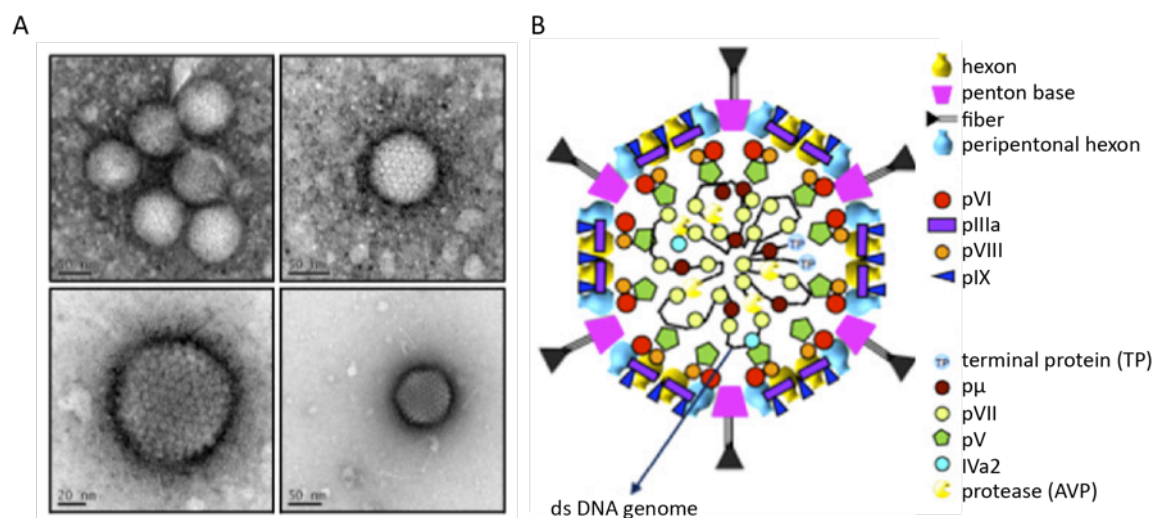


Fig. 2: Structure and schematic organization of the HAdV virion. (A) Electron microscope images of the icosahedral structure of adenoviral particles (Department of Electron Microscopy, Heinrich Pette Institute, Leibniz Institute for Experimental Virology, Hamburg). (B) Schematic

representation of the HAdV virion structure depicting the different capsid and core proteins. Protein names are shown on the right side. The structure is corresponding to the current model based on X-ray studies (adapted from [47]).

HAdV contain a linear, dsDNA genome of 26-45 kb in size. Inverted terminal repeats (ITR) at the end of the genome are between 36-200 bp long and mark the origin of DNA replication. Furthermore, the genome is divided into early, intermediate and late transcription units. The early transcription unit consists of the five early regions E1A, E1B, E2, E3 and E4 that are involved in activation of transcription, blocking of apoptosis, DNA replication as well as transcriptional and translational regulation, respectively. The intermediate transcription unit contains the four regions IX, IVa2, L4 intermediate and E2 late, whereas the late transcription unit comprises the major late transcription unit (MLTU) that is processed into five late mRNAs (L1-L5). Together, these transcription units encode for approximately 40 different structural and regulatory proteins as well as one or two VA RNAs, depending on the HAdV type (Fig. 3) [4].

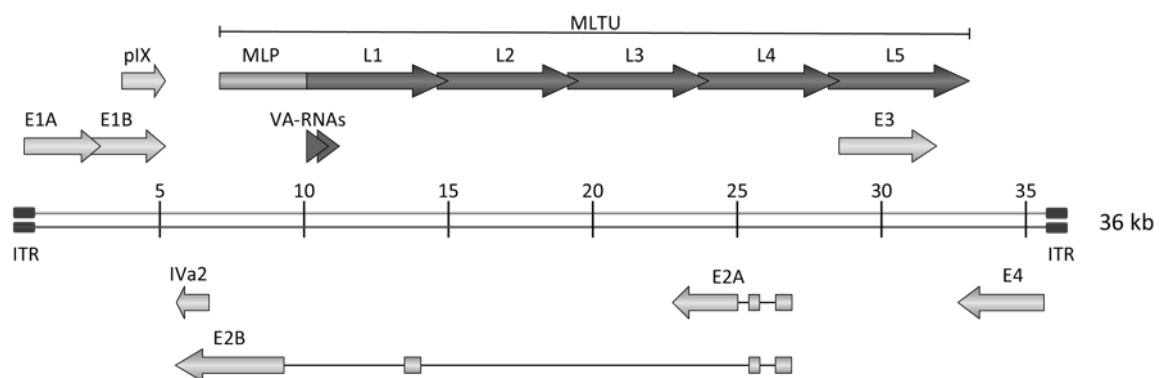


Fig. 3 Genome organization of HAdV-5. Schematic representation of the viral genome of HAdV-5. Arrows indicate the transcriptional direction of the early (E1A, E1B, E2A, E2B, E3, E4), delayed (pIX, IVa2) and late (MLTU, L1-L5) transcription units. All viral genes are transcribed by polymerase II, except for the VA-RNAs that are transcribed by polymerase III. The late genes are under control of the common promoter MLP. ITR: inverted terminal repeats; MLTU: major late transcription unit; MLP: major late promoter; VA-RNAs: virus associated RNAs.

1.1.3 Infectious life cycle of HAdV

1.1.3.1 Adsorption and entry

Most HAdVs attach to the host cell via the CAR receptor, a component of the tight junctions from epithelial cells found in the heart, CNS, lung, liver and intestine, but not in hematopoietic cells [48, 49]. Only HAdVs from species B have evolved a different mechanism for host cell binding and use CD46, a component of the complement system that is present on most cells, including

hematopoietic cells [38]. After binding to CAR, the penton base of the virion interacts with integrins α -3 and α -5, leading to receptor mediated endocytosis via clathrin-coated vesicles [4]. Again, HAdVs from species B were shown to enter the cell by a different mechanism, namely macropinocytosis [50, 51]. Following endosome acidification, the partially disassembled virion is released into the cytosol. Viral particles are transported to the nuclear pores by the cellular microtubular machinery. Thereafter, viral DNA is released through the nuclear pore complex (NPC) into the nucleus where viral DNA replication takes place [52].

1.1.3.2 Early and late phase of infection

Once the viral DNA enters the nucleus, the early phase of infection begins. E1A, the first protein that is transcribed during infection induces the cell to enter S-phase, thus creating a favorable environment for viral replication. E1A binds to retinoblastoma (Rb) proteins that suppress transcription factors of the E2F family. Consequently, E2F is released, which activates the transcription of E2F responsive genes, some of them inducing entry of the cell into S-phase [53–55]. Moreover, E1A stimulates the transcription of the other early regions (E1B, E2, E3 and E4), which have evolved different strategies to protect the virus from antiviral host defenses [4]. E1B encodes the two proteins E1B-19K and E1B-55K. Both are involved in the inhibition of apoptosis induced by the tumor suppressor p53. E1B-19K is a homolog of BCL-2 and binds to the proapoptotic factors BAK and BAX in order to prevent the release of apoptogenic proteins from mitochondria [56, 57]. E1B-55K developed several mechanisms to interact with p53 that will be described in more detail later in this work. Briefly, E1B-55K interferes with p53 through direct binding, SUMOylation as well as proteasomal degradation [58–62]. The E2 region encodes for proteins that are essential for viral DNA replication, namely the preterminal protein (pTP), the HAdV polymerase and the DNA binding protein (DBP) E2A [4]. Proteins from the E3 region are associated with the evasion of the host cell immune response, such as blocking cell surface expression of HLA-I [63, 64]. Finally, the E4 region encodes proteins that are involved in the DNA damage response (DDR) and transcriptional activation. E4orf3 inhibits DNA double-strand break responses (DSBR) by sequestering proteins of the Mre11-Rad50-Nbs1 (MRN)-complex into so-called promyelocytic leukemia (PML)-tracks [65, 66]. E4orf6 forms an E3-Ubiquitin-ligase together with E1B-55K as well as cellular components,

leading to the proteasomal degradation of cellular antiviral factors, such as Mre11, SPOC-1 and p53 [61, 62, 67–69]. E4orf6/7 dimerizes E2F transcription factors, thus increasing their affinity to E2 early promoters [70].

The onset of viral DNA replication initiates the late phase of infection. Five late viral mRNAs (L1-L5) are generated from a major late promoter (MLP) through alternative splicing and mainly encode for the structural proteins involved in virus assembly [71, 72]. The late phase of infection induces the host cell shut-off. While export and translation of cellular mRNAs are blocked, viral mRNAs are selectively transported out of the nucleus and are efficiently translated [73]. The infectious life cycle of HAdVs ends with lysis of the cell and release of about 10^4 viral particles [4].

1.1.4 Early region 1B protein

1.1.4.1 HAdV-C5 E1B-55K in lytic infection

E1B-55K is an adenoviral protein of 496 aa that is expressed early in infection (approx. 8 h p.i.) and is important throughout the life cycle. This protein contains several domains that are responsible for its numerous functions (Fig. 4). The leucine-rich nuclear export signal (NES) is located at the N-terminus of the protein at L83/87/91 followed by a classical SCM around K104 [74, 75]. Binding sites for p53 and E4orf6 are located between aa 224-354 or aa 143 and aa 262-326, respectively [76, 77]. They are both overlapping with the cysteine/histidine-rich region (C/H-rich region) between aa 282-456 [78]. Furthermore, there is a putative Elongin B and C-Box (B/C-Box) between aa 179-188 that is involved in the formation of the E3-Ubiquitin-ligase together with E4orf6 [79]. Finally, a C-terminal phosphorylation region (CPR) is located at the very end of the protein, namely at aa 490-495 [80, 81].

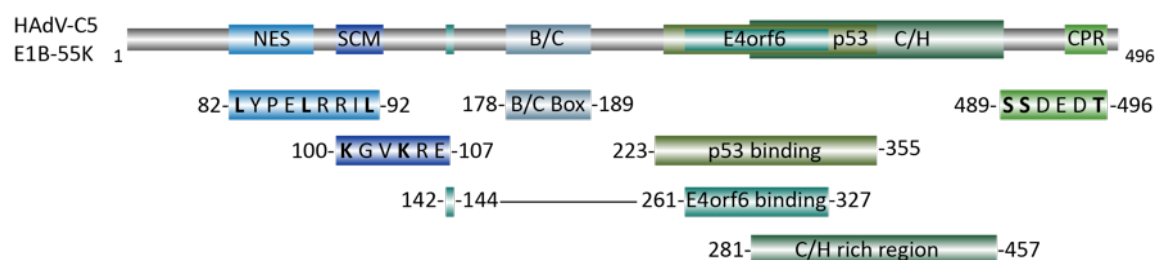


Fig. 4: Functional domains of HAdV-C5 E1B-55K. Schematic representation of the different functional domains of E1B-55K from HAdV-C5 including the nuclear export signal (NES) between aa 83-91, the SUMO conjugating motif (SCM) around K104, the putative Elongin B and C-Box (B/C-Box) between aa 179-188, the E4orf6 binding site at aa 143 and aa 262-326, the p53

binding domain between aa 224-354, the cysteine/histidine-rich region (C/H-rich region) between aa 282-456 and the C-terminal phosphorylation region (CPR) at aa 490-495 [74-77, 79, 81].

Functions of E1B-55K include the regulation of viral and cellular gene expression, cell cycle control, apoptosis, DNA damage response as well as intrinsic and innate immunity. Binding of E1B-55K to p53 was one of the first interactions described for E1B-55K and eventually led to the discovery of p53 as a tumor suppressor [58]. Since then, it has been shown that E1B-55K established different ways to inhibit the transcriptional functions of p53, all of them contributing to the oncogenic potential of HAdVs (see 1.1.5). On the one hand, E1B-55K binds p53 and sequesters it from the nucleus into perinuclear and cytoplasmic structures [82]. These so-called aggresomes are accumulations of misfolded proteins that are transported to the microtubule-organizing center (MTOC) by dynein-dependent transport [83]. On the other hand, attachment of E1B-55K to p53 presumably leads to a conformational change of p53 resulting in a higher affinity to DNA binding sites. This leads to the recruitment of E1B-55K to p53-dependent promoters where it can inhibit their activation [84, 85]. Furthermore, E1B-55K post-translationally modifies p53 by conjugating the small cellular protein SUMO-1, acting as an E3-small Ubiquitin-like modifier (SUMO)-ligase [59]. SUMOylated p53 is then transported to PML-nuclear bodies (PML-NBs), where its nuclear export is facilitated [60].

At late time points in infection, p53 is a target of the E3-Ubiquitin-ligase that is formed by E1B-55K together with E4orf6 and the cellular factors Elongin B and C, Cullin 5 and Rbx-1 [61, 62, 86]. This complex promotes ubiquitination followed by proteasomal degradation of their target proteins. It is suggested that E4orf6 forms the E3-Ubiquitin-ligase together with the cellular components while E1B-55K recruits the target proteins [79]. Apart from p53, many other cellular factors are degraded by the E3-Ubiquitin-ligase. This includes proteins involved in the DDR and DNA double strand break (DSB) repair, such as Mre11, a major component of the MRN-complex, SPOC-1 (survival-time associated PHD protein in ovarian cancer 1), DNA ligase IV as well as Bloom helicase (BLM) [68, 69, 87, 88]. Furthermore, integrin α -3 was identified to be a target of the E3-Ubiquitin-ligase [89]. Interestingly, degradation of a newly identified protein, the death domain-associated protein (Daxx) was shown to be independent of E4orf6 [90]. Moreover, interaction of E1B-55K and E4orf6 has been shown to be involved in the host cell shut-off. Here, viral mRNA is

preferentially exported out of the nucleus while cellular mRNA transport is partially blocked [91–94].

Another role of E1B-55K is the interaction with components of PML-NBs like PML and Speckled protein 100kDa (Sp100). PML-NBs are aggregations of regulatory proteins that are involved in replication and transcription, DDR, apoptosis and cell cycle regulation. Moreover, PML-NBs are thought to be a “platform for post-translational modification (PTM)” (reviewed in [95]). E1B-55K binds different PML isoforms and localizes to PML-NBs. Binding of E1B-55K and PML was shown to be regulated by other viral proteins as well as by SUMOylation of E1B-55K [96]. Additionally, E1B-55K dissociates Sp100 isoforms B, C and HMG from PML-NBs. However, Sp100A associates with PML-tracks formed by E4orf3 to maintain HAdV gene expression during infection [66, 97, 98]. Additionally, E1B-55K interacts with the cellular heterochromatin-associated transcription factor KRAB-associated protein 1 (KAP1). KAP1 is inactivated through de-SUMOylation of E1B-55K leading to chromatin decondensation and enhanced viral gene transcription [99]. In conclusion, E1B-55K exhibits functions that act on the transcriptional as well as translational level, making it an important factor in HAdV life cycle.

1.1.4.2 Early region 1B proteins from other HAdV species

Most of the investigations on HAdV E1B functions were conducted in HAdV-C5. Recently, studies concentrated on the analysis of the large E1B proteins from other HAdV species revealed conserved functions as well as heterogeneity. For instance, E3-Ubiquitin-ligase complexes of E1B and E4orf6 are highly conserved. However, they differ in composition and also evolved distinct target specificities. It has been shown that the large E1Bs from six of the seven HAdV species bind to their respective E4orf6. E3-ligase complexes are mainly Cul5-based (HAdV-B34, HAdV-C5, HAdV-D9, HAdV-E4), whereas HAdV-A12 and HAdV-F40 form a Cul2-based E3-ligase complex and HAdV-B16 is even able to use both Cul2 and Cul5 [100]. The only so far known cellular target of the E3-Ubiquitin-ligase complex that is degraded from all tested species is DNA ligase IV. The p53 protein is only efficiently degraded by HAdV-A12, HAdV-C5 and HAdV-F40, although almost all of the large E1B proteins bind to it (except HAdV-E4) [100, 101]. Another group observed the accumulation of transcriptionally inactive p53 by E1B proteins from species B

[102]. Other cellular targets that are differentially degraded among HAdV species are Mre11, integrin α -3 and BLM [100, 101].

Blanchette *et al.* analyzed the localization as well as the aggresome formation of several E1B types [103]. They showed that large E1B proteins are mainly located in nuclear dots, only HAdV-A12 showed a diffuse localization throughout the cell and HAdV-C5 was seen in the cytoplasm. Nevertheless, all large E1B proteins bound to PML and mostly co-localized with PML in the nucleus. However, aggresome formation was only observed in HAdV-B16, HAdV-C5, HAdV-D9 and HAdV-E4 [103]. These findings are summarized in the table below (Table 1).

Table 1: Functions of large E1B proteins from different HAdV species. The table compares the E1B proteins from different HAdV species with regard to the formation of an E3-Übiquitin ligase, degradation of cellular targets, aggresome formation and localization. Based on [100, 101, 103].

HAdV	E3-Übi- ligase (Cullin base)	Degradation of cellular targets					Aggre- some formation	Locali- zation
		p53	Mre 11	DNA ligase IV	Inte- grin α -3	BLM		
A 12	+(Cul2)	+	+	+	+	+	-	diffuse
B1 16	+(Cul2/5)	-	+	+	-	+	+	nuclear
B2 34	+(Cul5)	-	+	+	-	+	-	nuclear
C 5	+(Cul5)	+	+	+	+	+	+	cytoplasm
D 9	+(Cul5)	-	+	+	-	-	+	nuclear
E 4	+(Cul5)	-	-	+	+	+	+	nuclear
F 40	+(Cul2)	+	+	+	+	+	-	nuclear

In summary, analysis of large E1B proteins revealed functional diversity among different HAdV species.

1.1.5 Transforming potential and oncogenicity of HAdV

In 1962, HAdVs were discovered to cause tumors in newborn hamsters [36] and are ever since classified as DNA tumor viruses. The two viral proteins that are mainly associated with HAdV oncogenicity are E1A and E1B-55K. It is assumed that viral transformation of HAdV follows the classical concept, in which the viral oncogenes persist in the transformed cells and can later be detected [104]. In fact, several groups have observed transformation of rodent cells by E1A and E1B-55K in cell culture systems [105–107]. Complete transformation of rodent

cells is a two-step process. First, binding of E1A to p300 and/or Rb proteins leads to the stabilization of the tumor suppressor and transcription factor p53 followed by induction of apoptosis [108, 109]. Second, E1B-55K has developed several mechanisms to counteract p53 as well as other factors involved in apoptosis, DNA repair and transcription (see 1.1.4.1). Among all, p53 degradation through the E3-Ubiquitin-ligase and p53 translocation through binding and shuttling by E1B-55K are the most important functions involved in the transformation process [110]. Additionally, it has been shown that degradation of Daxx by E1B-55K is necessary for transformation of baby rat kidney cells (pBRKs) [111]. Consequently, the growth arresting functions of E1A in permissive cell lines that promote viral replication do not account for non-permissive rodent cells. There, E1A rather induces immortalization and partial transformation [112]. The pro-apoptotic functions of E1A are furthermore prevented by E1B-55K so that complete transformation can take place.

So far, only small amounts of viral DNA were found in tumors of humans. For example, HAdV DNA was detected in pediatric brain tumors, small-cell lung carcinomas, mantle cell lymphomas and human sarcomas [113–116]. Recently, transformation of primary human mesenchymal stroma cells (hMSC) has been observed, hence indicating association of HAdV with human oncogenesis by mediating cellular transformation [117].

1.2 The cellular post-translational modification (PTM) machinery

1.2.1 Pathways of cellular PTM

PTMs of proteins occur via covalent binding of an enzyme from the PTM machinery. PTM is a versatile regulator involved in cell cycle progression, cell growth, DDR, signal transduction, protein stability as well as protein-protein interaction [118–120]. Furthermore, PTMs have been shown to interact and interfere with pathogens, such as viruses and bacteria (reviewed in [121, 122]).

Ubiquitin, the best-studied protein involved in PTMs, was found in the late 1970s to modify proteins on lysine residues [123]. To date, the group of ubiquitin-like proteins (Ubl) comprises a number of members, for instance neural precursor cell expressed developmentally down-regulated protein 8 (NEDD8), interferon stimulated gene 15 (ISG15) and small ubiquitin-like modifier (SUMO) [124].

Another PTM that plays an important role in regulating cellular processes is CK2 phosphorylation. CK2 is a serine/threonine kinase that phosphorylates a broad number of target substrates involved in many different functions such as cell-cycle control, DNA replication and transcription, DDR and apoptosis [125–128]. On this regard, increased levels of CK2 have been linked to cancer formation, since CK2 is able to suppress apoptosis (reviewed in [129]). Similar to ubiquitin and Ubls, CK2 phosphorylation is also known to modify viral proteins. For example, phosphorylation of EB2 from Epstein-Barr virus (EBV) regulates the nuclear export of cellular mRNA. NS2 from hepatitis C virus (HCV) is marked for proteasomal degradation upon phosphorylation by CK2 [130, 131]. CK2 Phosphorylation occurs at the consensus motif *S/TXXE/D* and phosphoryl donors can be either ATP or GTP [132].

Besides CK2 phosphorylation, acetylation is another major PTM that occurs in proteins. Thereby, an acetyl group (CCH₃) is transferred via an acetyl co-enzyme A (Ac-CoA) to a protein. Either, the acetyl group is attached by N-acetyltransferases (NATs) to the α -amino group at the N-terminus of the protein, or the acetyl group is transferred to the ϵ -amino group of a lysine residue by histone-acetyltransferases (HATs). HATs were named after the first discovery of acetylation on histones and now they are mainly termed as lysine-acetyltransferases (KATs) [133]. Acetylation of lysine residues can be reversed by lysine-deacetylases (KDACs) (reviewed by [134]).

Finally, several groups observed a crosstalk between the different PTMs. For example, it has been shown that the acetylation of the tumor suppressor p53 inhibits its ubiquitination [135]. Furthermore, SUMOylation of another tumor suppressor, HIC1 (hypermethylated in cancer 1), stimulates interaction with metastasis associated protein 1 (MTA1), whereas its acetylation blocks this interaction [136]. Finally, inactivation of PML IV SUMOylation at K490 has been shown to increase acetylation of the protein at K487 [137].

1.2.2 Modification by the small ubiquitin-like modifier (SUMO)

SUMO was discovered in 1996 by two groups working on the targeting of RanGAP1 to the nuclear pore complex [138, 139]. Currently, five isoforms of SUMO are known. SUMO-1 shares 50 % sequence identity with SUMO-2 and SUMO-3, whereas the latter have a similarity of 97 %, only differing in three residues at the N-terminus. Therefore, they are mostly referred to as SUMO-2/3

[124, 140]. Moreover, SUMO-2/3 contains an internal SUMO consensus site (SCS) ΨKxE , whereas Ψ is a hydrophobic amino acid and x refers to any amino acid, enabling the protein to form chains. In contrast, SUMO-1 is lacking this internal SCS and only binds to substrates as a monomer [141]. SUMO-4 and -5 are the latest SUMO isoforms identified. SUMO-4 was detected mainly in the kidney and it is associated with type I diabetes mellitus [142]. However, there are reports stating that SUMO-4 is one of the many pseudogenes of the SUMO-family [124, 143]. SUMO-5 was found to be involved in PML-NB formation, on the one hand, and PML-NB disruption, on the other hand [144].

Conjugation of SUMO to a protein is a three-step enzymatic pathway that is very similar to the ubiquitination pathway (Fig. 5). SUMOylation occurs at a SCM $\Psi KxE/D$, whereas Ψ is a hydrophobic amino acid and x refers to any amino acid [145]. The SUMO protein has to be activated in order to undergo the enzymatic cascade. Therefore, Sentrin specific proteases (SENPs) cleave off the C-terminus of the protein and reveal a Gly-Gly motif [120]. The first step of the SUMOylation pathway is the activation by an E1 activating enzyme (SUMO activating enzymes 1 and 2; SAE1/SAE2). Hereby, SUMO forms a thioester bond with the active site cysteine of SAE2 in an ATP-dependent manner [146, 147]. Second, the C-terminal carboxy group of SUMO is linked via a thioester bond to the catalytic cysteine of an E2 conjugating enzyme (ubiquitin carrier protein 9; Ubc9) [148, 149]. So far, there is only one E2 conjugating enzyme known for SUMO, whereas there are over 20 known for ubiquitin [150]. Finally, SUMO is transferred to the substrate, where it forms an isopeptide bond via the Gly-Gly motif with a lysine residue on the target. This last step is often facilitated by SUMO-E3-ligases that act as a catalyzer for the process. Multiple HECT-domain E3-ligases have been described for ubiquitin [150]. However, SUMOylation requires different E3-ligases. So far, SUMO-E3-ligases can be differentiated into three groups. A first group contains E3-ligases with a RING-finger motif, which includes the protein inhibitor of activated STAT (PIAS)-family [151]. The second group consists of RanBP2 and the third one comprises the polycomb group (PcG) protein Pc2 [152, 153]. SUMOylation of proteins is reversible. The turnover of SUMOylation and deSUMOylation is very high. SUMO cleavage is mediated by SENPs, thereby releasing the substrate as well as free SUMO [154, 155].

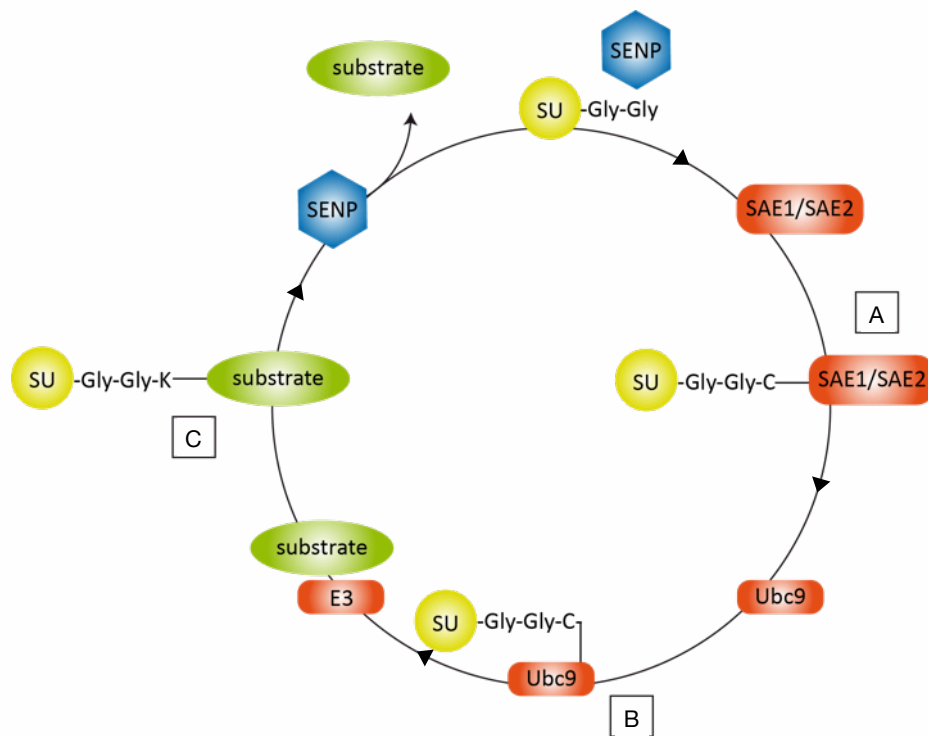


Fig. 5 Pathway of SUMO-conjugation. Three-step enzymatic cycle of SUMO-conjugation and de-conjugation. (A) SUMO binds to the active site cysteine of the E1 Activating enzyme (SAE1/SAE2). (B) SUMO is transferred to the E2 conjugating enzyme (Ubc9). (C) SUMO is transferred to the substrate, facilitated by E3 SUMO ligases. SUMO: small ubiquitin-like modifier; SAE1/2: SUMO activating enzymes 1 and 2; Ubc9: ubiquitin carrier protein 9; SENP: sentrin-specific protease. Adapted from [122].

1.2.3 Post-translational modification of viral pathogens

Since PTMs of proteins modulate so many different yet important cellular pathways, it is not surprising that viruses evolved mechanisms to take advantage of the cellular PTM machinery. They either mimic cellular proteins involved in PTM or are post-translationally modified themselves.

As described before, HAdV-C5 E1B-55K and E4orf6 form an E3-ubiquitin-ligase marking various cellular proteins for proteasomal degradation [61]. Similar to HAdV, K3 from Kaposi's sarcoma-associated herpesvirus (KSHV) acts as an E3-ubiquitin-ligase to degrade MHC I molecules. K3 promotes the ubiquitination of MHC I and ubiquitinated MHC I is then internalized from the cell surface and further targeted to the late endosome, where it is degraded [156]. The E6 protein from human papilloma virus (HPV) 16 and 18 forms a complex with the E6-associated protein (E6-AP) that targets p53 [157, 158]. E6 binds to E6-AP, thus enabling the binding and subsequent ubiquitination of p53 [159]. Interestingly, ICP0 (infected cell polypeptide 0) from herpes simplex virus 1

(HSV1) represents an E3-ubiquitin-ligase with SUMO-targeted ubiquitin ligase (STUbL) activity that is able to ubiquitinate poly-SUMOylated targets. It has been shown that ICP0 disrupts poly-SUMOylated PML by targeting it for proteasomal degradation [160].

Furthermore, viral proteins can act as SUMO-E3-ligases, as it has been described for HAdV-C5 E1B-55K that SUMOylates the tumor suppressor p53 [59, 60]. Recently, another adenoviral SUMO-E3-ligase has been detected. Sohn *et al.* described that E4orf3 is able to SUMOylate TIF-1 γ and furthermore promote SUMO-3 chain formation [161]. The transcriptional factor KSHV basic-leucine-zipper (K-bZIP) from KSHV is even able to SUMOylate itself as well as p53 and pRb. In contrast to HAdV-C5, where SUMOylation of p53 has been shown to repress p53 transactivation, K-bZIP is activating the tumor suppressor upon SUMOylation [162]. Intriguingly, SUMO-E3-ligase function is conserved among viral homologues of herpesviruses. EB2 from Epstein-Barr virus (EBV), ICP27 from HSV1 as well as UL69 from human cytomegalovirus (HCMV) increase the global SUMOylation in infected cells and have been shown to SUMOylate p53 *in vitro* [163].

As mentioned above, viral proteins are targets of PTMs, as well. Since the discovery of SUMO, more and more viral targets of the SUMO conjugation machinery have been discovered [164]. It has been shown that immediate early protein 2 (IE2) from HCMV and EB1 from EBV are both modified by SUMO-1 and SUMO-2/3, and that this modification regulates their transactivation capacity [165, 166]. SUMOylation of the 3C protease from enterovirus 71 (EV71) decreases its protease activity as well as stability [167]. The protein p6 from human immunodeficiency virus type 1 (HIV-1) even regulates virion infectivity [168]. Finally, also E1B-55K from HAdV-C5 is SUMOylated at the lysine on position 104 (K104), the consequences of which will be described in more detail in the next chapter of this work [75].

1.2.4 HAdV-C5 E1B-55K as a target of the cellular PTM machinery

HAdV-C5 E1B-55K is a substrate for different PTMs. It is SUMOylated at a conserved SCM around K104 and phosphorylated at the C-terminus [75, 80, 81]. In general, SUMOylation regulates many functions of the protein. E3-SUMO-ligase function of E1B-55K towards p53 as well as Sp100A are dependent on E1B-55K's own SUMOylation [59, 60, 97]. Remarkably, both

proteins are sequestered to the cytoplasm upon SUMO modification by HAdV-C5 E1B-55K [60, 97]. Moreover, SUMOylation of HAdV-C5 E1B-55K is a prerequisite for efficient repression of p53-stimulated transcription [75]. However, the E3-SUMO-ligase function of HAdV-C5 E1B-55K towards p53 is not required for maximal repression of p53 transactivation [59, 60]. Additionally, immunoprecipitation experiments showed that SUMOylation of E1B-55K is also necessary for binding to different PML isoforms [96]. The interaction with PML IV and V can occur in a SUMO-dependent and -independent manner, ultimately leading to the localization of E1B-55K to PML-NBs. In infection, other viral proteins regulate the binding of E1B-55K and PML, as well, indicating that a change between SUMOylation and deSUMOylation of E1B-55K regulates its targeting to PML and PML-NBs [96]. Interestingly, degradation of Daxx, the so far only cellular protein that is degraded independently of E4orf6, is also dependent on SUMOylation of HAdV-C5 E1B-55K [90]. Together, these studies provide further evidence that efficient transformation of pBRKs is highly reliant on the SUMOylation of E1B-55K [75]. Lastly, nuclear export as well as intranuclear targeting of HAdV-C5 E1B-55K is correlated to its PTM. SUMOylation of HAdV-C5 E1B-55K recruits the protein to viral RCs and inactivation of SUMO conjugation completely abrogates this co-localization [169, 170]. Furthermore, it has been suggested that SUMOylation interferes with nuclear export of the protein by obstructing the binding of CRM1 to the NES. However, HAdV-C5 E1B-55K evolved mechanisms to exit the nucleus in a CRM1-independent manner, although the exact method behind it remains to be elusive [169].

As described above, SUMOylation is an important regulator of HAdV-C5 E1B-55K function. Interestingly, SUMOylation of HAdV-C5 E1B-55K itself is regulated by several mechanisms. Wimmer *et al.* showed that depletion of the three phosphorylation sites S490, S491 and T495 leads to a markedly reduction of SUMOylation at K104 [170]. Besides phosphorylation, nuclear export is another mechanism to regulate HAdV-C5 E1B-55K SUMOylation. HAdV-C5 E1B-55K has a leucine-rich nuclear export signal (NES) that enables the protein to shuttle between the cytoplasm and the nucleus. On the one hand, inactivation of the NES abrogates CRM1-dependent shuttling, resulting in an exclusively nuclear localization accompanied by higher SUMOylation [74, 169]. On the other hand, inactivation of the SCM by K104R mutation inhibits the intracellular

shuttling of E1B-55K and the protein remains mainly cytoplasmic. Consequently, phosphorylation and nuclear export also regulate functions of HAdV-C5 E1B-55K that are induced by SUMOylation, such as p53 transactivation and SUMOylation, degradation of Daxx and ultimately the oncogenic potential of HAdV-C5 E1B-55K [75, 170, 171].

2 Material

2.1 Cells

2.1.1 Bacterial Strains

Strain	Genotype
DH5 α	<i>supE44, ΔlacU169, (ϕ80dlacZΔM5), <i>hsdR17, recA1, endA1, gyrA96, thi-1, relA1</i> [172].</i>

2.1.2 Mammalian cell lines

#	Cell line	Genotype	Reference
8	A549	Human lung carcinoma cell line expressing wild-type p53 [173].	DMSZ
7	H1299	Human lung carcinoma cell line, p53-negative [174].	ATCC
56	HeLa	Human cervix carcinoma cell line, p16-negative [175].	DMSZ
925	HeLa-SU1	HeLa cells stably expressing N-terminally 6-His-tagged SUMO-1 under puromycin selection (2 μ g/ml) [176].	R. Hay
926	HeLa-SU2	HeLa cells stably expressing N-terminally 6-His-tagged SUMO-2 under puromycin selection (2 μ g/ml) [176].	R. Hay
-	pBRK	Primary baby rat kidney cells, freshly isolated from 3-5-day old Sprague Dawley rats (Janvier, France).	Group database

2.2 Viruses

#	Adenovirus	Characteristics
100	H5pg4100	Wild-type HAdV-C5 carrying an 1863 bp deletion (nt 28602-30465) in the E3 reading frame [169].
101	H5pm4101	HAdV-C5 mutant containing three aa exchanges (L83/87/91A) in the NES of E1B-55K [169].
102	H5pm4102	HAdV-C5 mutant containing an aa exchange (K104R) in the SCM of E1B-55K [169].
245	H5pm4243	HAdV-C5 mutant containing an aa exchange (K101R) in the putative SCM of E1B-55K (group database).
246	H5pm4244	HAdV-C5 mutant containing two aa exchanges (K101/104R) in the SCM and the putative SCM of E1B-55K (group database)
273	H5hh4305	HAdV-C5 mutant containing an aa exchange (K101A) in the putative SCM of E1B-55K (group database).

2.3 Nucleic acids

2.3.1 Oligonucleotides

The following oligonucleotides were used for sequencing, PCR and site-directed mutagenesis. All nucleotides were ordered from Metabion and numbered according to the internal group *Filemaker Pro* database.

#	Name	Sequence	Purpose
64	E1B bp2043 fwd	5'-CGC GGG ATC CAT GGA GCG AAG AAA CCC ATC TGA GC-3'	Sequencing
366	cmv	5'-CCC ACT GCT TAC TGG C-3'	Sequencing
636	pcDNA3-rev	5'-GGC ACC TTC CAG GGT CAA G-3'	Sequencing

782	E1-Box fwd 2454 bp	5'-CAA GGA TAA TTG CGC TAA TGA GC-3'	Sequencing
1318	E1B-C-Terminus	5'-GGCCTCCGACTGTGGTTGCT TC-3'	Sequencing
592	HAdV-5 K104R fwd	5'-GGG CTA AAG GGG GTA AGG AGG GAG CGG GGG-3'	Site-directed mutagenesis
593	HAdV-5 K104R rev	5'-CCC CCG CTC CCT CCT TAC CCC CTT TAG CCC-3'	Site-directed mutagenesis
2787	HAdV-5 K101R fwd	5'- GGG CAG GGG CTA AGG GGG GTA AAG AGG G-3'	Site-directed mutagenesis
2788	HAdV-5 K101R rev	5'-CCC TCT TTA CCC CCC TTA GCC CCT GCC C-3'	Site-directed mutagenesis
3368	HAdV-4 K93R fwd	5'-CGA GTG GTC GGG AGA GGG GTA TTA GGC GGG AGA GGC-3'	Site-directed mutagenesis
3369	HAdV-4 K93R rev	5'-GCC TCT CCC GCC TAA TAC CCC TCT CCC GAC CAC TCG-3'	Site-directed mutagenesis
3339	HAdV-9 K103R fwd	5'-CAG GGG AGT TAG GAG GGA GAG-3'	Site-directed mutagenesis
3340	HAdV-9 K103R rev	5'-CTC TCC CTC CTA ACT CCC CTG-3'	Site-directed mutagenesis
3372	HAdV-12 K88R fwd	5'-GCG CAG ATG ATA GAG ATA GGC AGG-3'	Site-directed mutagenesis
3373	HAdV-12 K88R rev	5'-CCT GCC TAT CTC TAT CAT CTG CGC-3'	Site-directed mutagenesis
3161	HAdV-16 K101R fwd	5'-CAG GAC AGG GGC ATT CGG AGG GAA AGG AAT CC-3'	Site-directed mutagenesis
3162	HAdV-16 K101R rev	5'-GGA TTC CTT TCC CTC CGA ATG CCC CTG TCC TG-3'	Site-directed mutagenesis
3165	HAdV-34 K103R fwd	5'-GAT AGG GGC GTT CGG AGG GAG AGG GC-3'	Site-directed mutagenesis
3166	HAdV-34 K103R rev	5'-GCC CTC TCC CTC CGA ACG CCC CTA TC-3'	Site-directed mutagenesis

3329	HAdV-40 K90R fwd	5'-CAA AGG GGG ACA AGG AGA AAG ATG G-3'	Site-directed mutagenesis
3330	HAdV-40 K90R rev	5'-CCA TCT TTC TCC TTG TCC CCC TTT G-3'	Site-directed mutagenesis

2.3.2 Vector plasmids

The following vectors plasmids were used for sub-cloning or as transfection controls. They are numbered according to the internal group *Filemaker Pro* database.

#	Name	Purpose	Reference
136	pcDNA3	Expression vector for mammalian cells, CMV promoter	Invitrogen
196	pcDNA3-Flu	Expression vector for mammalian cells, CMV promoter, N-terminal HA-tag	Group database
138	pGL3 basic	<i>Firefly</i> -Luciferase-Assay	Promega
180	pRL-TK	<i>Renilla</i> -Luciferase-Assay	Promega

2.3.3 Recombinant plasmids

The following recombinant plasmids were used for cloning and transfection experiments. All plasmids are numbered according to the internal group *Filemaker Pro* database.

#	Name	Vector	Insert	Reference
608	pXC-15	pXC15	HAdV-C5 E1 region (1-5790)	Group database
737	pE1A	pML	HAdV-C5 E1A	Group database
1319	pcDNA-E1B-55K	pcDNA3	HAdV-C5 E1B-55K	Group database

1908	E1B-19K- E1B-55K	pPG-S3	HAdV-C5 E1-region, E1B-19K negative, E1B-55K	Group database
1022	E1B-55K-SCS	pcDNA3	HAdV-C5 E1B-55K K104R	Group database
1023	E1B-55K-NES	pcDNA3	HAdV-C5 E1B-55K L83/87/91A	Group database
2841	E1B-55K K101R	pcDNA3	HAdV-C5 E1B-55K K101R	Group database
2842	E1B-55K K101/104R	pcDNA3	HAdV-C5 E1B-55K K101/104R	Group database
2985	E1B-19K- E1B-55K K101A	pPG-S3	HAdV-C5 E1-region, E1B-19K negative, E1B-55K K101A	This work
2988	E1B K101A	pcDNA3	HAdV-C5 E1B-55K K101A	This work
2990	E1B-19K- E1B-55K K104R	pPG-S3	HAdV-C5 E1-region, E1B-19K negative, E1B-55K K104R	This work
2991	E1B-19K- E1B-55K K101R	pPG-S3	HAdV-C5 E1-region, E1B-19K negative, E1B-55K K101R	This work
2992	E1B-19K- E1B-55K NES	pPG-S3	HAdV-C5 E1-region, E1B-19K negative, E1B-55K NES	This work
2993	E1B-19K- E1B-55K K101/104R	pPG-S3	HAdV-C5 E1-region, E1B-19K negative, E1B-55K K101/104R	This work
3290	E1B-55K K138R	pcDNA3	HAdV-C5 E1B-55K K138R	This work
3291	E1B-55K K185R	pcDNA3	HAdV-C5 E1B-55K K185R	This work
2214	Ad4 HA55K pcDNA3	pcDNA3	HAdV-E4 E1B-55K wt	P. Blanchette

2215	Ad5 HA55K pcDNA3	pcDNA3	HAdV-C5 E1B-55K wt	P. Blanchette
2216	Ad9 HA55K pcDNA3	pcDNA3	HAdV-D9 E1B-55K wt	P. Blanchette
2217	Ad12 HA55K pcDNA3	pcDNA3	HAdV-A12 E1B-55K wt	P. Blanchette
2218	Ad16 HA55K pcDNA3	pcDNA3	HAdV-B16 E1B-55K wt	P. Blanchette
2219	Ad34 HA55K pcDNA3	pcDNA3	HAdV-B34 E1B-55K wt	P. Blanchette
2220	Ad40 HA55K pcDNA3	pcDNA3	HAdV-F40 E1B-55K wt	P. Blanchette
3226	Ad5 HA55K K101R	pcDNA3	HAdV-C5 E1B-55K K101R	L. Kieweg
3227	Ad5 HA55K K104R	pcDNA3	HAdV-C5 E1B-55K K104R	L. Kieweg
3229	Ad16 HA55K K101R	pcDNA3	HAdV-B16 E1B-55K K101R	L. Kieweg
3231	Ad34 HA55K K103R	pcDNA3	HAdV-B34 E1B-55K K103R	L. Kieweg
3255	Ad40 HA55K K90R	pcDNA3	HAdV-F40 E1B-55K K90R	L. Kieweg
3260	Ad9 HA55K K103R	pcDNA3	HAdV-D9 E1B-55K K103R	L. Kieweg
3292	Ad12 HA55K K88R	pcDNA3	HAdV-A12 E1B-55K K88R	This work
3395	Ad4 HA55K K93R	pcDNA3	HAdV-E4 E1B-55K K93R	This work

2.4 Antibodies

2.4.1 Primary antibodies

#	Name	Properties
1	2A6	Monoclonal mouse ab against the N-terminus of HAdV-C5 E1B-55K [177].
369	4E8	Monoclonal rat ab against the central region of HAdV-C5 E1B-55K [178].
113	B6-8	Monoclonal mouse ab against HAdV-C5 E2A [179].
88	β -actin (AC-15)	Monoclonal mouse ab against β -actin (Sigma-Aldrich, A5441).
551	6-His	Monoclonal mouse ab against 6xHis-tag (Clontech, 631212).
62	DO-1	Monoclonal mouse ab against the N-terminal aa 11-25 of human p53 (Santa Cruz, sc-126) [180].
54	FL-393	Polyclonal rabbit ab against human and rat p53 (Santa Cruz, sc-6243).
588/629	3F10	Monoclonal rat ab against the HA-epitope (Roche, 11867423001).
412	SUMO-2/-3	Monoclonal mouse ab against SUMO-2/-3 (MoBiTec, M114-3).

2.4.2 Secondary antibodies

2.4.2.1 Antibodies for Western Blotting

Name	Properties
HRP-anti-mouse IgG	Polyclonal horseradish peroxidase (HRP) conjugated antibody against mouse IgG (H+L, F(ab') ₂ fragment), raised in goat (Jackson, 115-036-003).

HRP-anti-rat IgG	Polyclonal HRP conjugated antibody against rat IgG (H+L, F(ab') ₂ fragment), raised in goat (Jackson, 112-036-003).
HRP-anti-rabbit IgG	Polyclonal HRP conjugated antibody against rabbit IgG (H+L, F(ab') ₂ fragment), raised in goat (Jackson, 111-036-003).
HRP-anti-mouse IgG (light chain specific)	Polyclonal HRP conjugated antibody against the light chain of mouse IgG, raised in goat (Jackson, 115-035-174).
HRP-anti-rabbit IgG (light chain specific)	Polyclonal HRP conjugated antibody against the light chain of rabbit IgG, raised in mouse (Jackson, 211-032-171).

2.4.2.2 Antibodies for Immunofluorescence

Name	Properties
Alexa Fluor™ 488 anti-mouse	Polyclonal Alexa™488 conjugated antibody against mouse IgG (H+L, F(ab') ₂ fragment), raised in goat (Invitrogen, A-11001).
Alexa Fluor™ 488 anti-rabbit	Polyclonal Alexa™488 conjugated antibody against rabbit IgG (H+L, F(ab') ₂ fragment), raised in goat (Invitrogen, A-11008).
Cy3 anti-rat	Polyclonal Cy3 conjugated antibody against rat IgG (H+L, F(ab') ₂ fragment), raised in goat (Dianova, 712-166-153).

2.5 Standards and markers

Product	Company
1 kb and 100 bp DNA ladder	NEB
Page Ruler™ Prestained Protein Ladder	Thermo Scientific

2.6 Commercial systems

Product	Company
Dual-Luciferase Reporter Assay System	Promega
Plasmid Purification Mini, Midi und Maxi Kit	Qiagen
Protein Assay	BioRad
SuperSignal™ West Pico Chemiluminescent Substrate	Thermo Scientific
SuperSignal™ West Femto Maximum Sensitivity Substrate	Thermo Scientific
ProFection® Mammalian Transfection System	Promega
QIAquick Gel Extraction Kit	Qiagen

2.7 Chemicals, enzymes, reagents, equipment

All chemicals, enzymes and reagents used in this work were obtained from AppliChem, Biomol, Invitrogen, Merck, New England Biolabs, Promega, Qiagen, Roche, Sigma Aldrich, Stratagene and ThermoFisher Scientific. Cell culture materials, general plastic material and other equipment were supplied by BioRad, Biozym, Brand, Engelbrecht, Eppendorf GmbH, Falcon, Gibco BRL, Greiner, Hartenstein, Hellma, Ibidi, Nunc, Pan, Sarstedt, Protean, Schleicher&Schuell, VWR and Whatman.

2.8 Software and databases

Software	Purpose	Reference
Acrobat 9 Pro	PDF data processing	Adobe
CLC Main Workbench 7	Sequence data processing	CLC bio
Filemaker Pro 14	Database management	Filemaker, Inc.

Illustrator CS6	Layout processing	Adobe
Photoshop CS6	Layout processing	Adobe
Word 2011/365	Text processing	Microsoft
PowerPoint 2011/365	Layout processing	Microsoft
PubMed	Literature database, open sequence analysis	Open software (provided by NCBI)
Fiji	Image processing	[181]
Prism 5	Data graphing, statistical analysis	GraphPad
NIS-Elements	Imaging of confocal fluorescence images	Nikon
NIS-Elements Viewer 4.20	Imaging software	Nikon
Gene tools	Imaging of agarose gels and transformation assays	GBox-Systems (Syngene)
GPS-SUMO	Prediction of SUMOylation sites	[182, 183]
Mendeley Desktop 1.17.13	Reference management	Mendeley Ltd.

3 Methods

3.1 Bacteria

3.1.1 Culture and storage

Liquid cultures of bacteria (*E. coli*) were inoculated with a single bacteria colony and grown in sterile LB-media containing 100 $\mu\text{g}/\text{ml}$ ampicillin. Cultures were then incubated over night at 30 °C/37 °C at 200 rpm in an *Inova 4000 Incubator* (New Brunswick). Single bacteria colonies were grown on LB-Agar plates containing 15 g/l agar and 100 $\mu\text{g}/\text{ml}$ ampicillin.

Agar plate cultures can be stored at 4 °C for several weeks. For long-term storage, liquid cultures were centrifuged at 4000 rpm for 5 min at RT (Multifuge 3 S-R; Heraeus), the pellet was resuspended in 1 ml LB medium supplemented with 50 % sterile glycerol, transferred into *CryoTubes* (Nunc) and stored at -80 °C.

LB-Medium		10 g/l Trypton
		5 g/l Yeast extract
		5 g/l NaCl (Autoclaved)

Antibiotic solution		100 mg/ml Ampicillin (Sterile filtered; stored at -20 °C)
----------------------------	--	-----------------------------------------------------------

3.1.2 Chemical transformation of *E. coli*

For transformation of *E. coli* 100 μl of chemical competent bacterial cells (DH5 α) were thawed on ice were transferred to a pre-cooled 15 ml Falcon containing approx. 100 ng of plasmid DNA. After incubation on ice for 30 min, a heat shock was performed at 42 °C for 45 sec. Cells were immediately chilled on ice for 2 min, then 1 ml of LB medium without antibiotics was added followed by incubation for 1 h at 30/37 °C and 220 rpm in an *Inova 4000 Incubator* (New Brunswick). Finally, 100 μl of bacterial suspension was plated on an LB agar plate containing appropriate antibiotics (100 $\mu\text{g}/\text{ml}$ ampicillin). The rest of the suspension was pelleted (4000 rpm, 2 min; *Megafuge 1.0*, Heraeus), resuspended

in 100 μ l LB medium and as well plated on LB agar. LB agar plates were incubated over night at 30/37 °C.

3.2 Mammalian cells

3.2.1 Cultivation and passaging

Adherent cells were grown in monolayers on polystyrene cell culture dishes (6-well, 12-well, 100 mm, 150 mm tissue culture dish; Sarstedt/Falcon). They were cultivated in *Dulbecco's Modified Eagle Medium* (DMEM; Sigma) containing 0.11 g/l sodium pyruvate, 10 % FBS (Pan) and 1 % penicillin/streptomycin solution (1,000 U/ml penicillin and 10 mg/ml streptomycin in 0.9 % NaCl; Pan). Culture medium for human cervix carcinoma cell lines (HeLa) stably overexpressing 6-His-tagged SUMO-1 or SUMO-2 was additionally supplemented with 1 μ g/ml puromycin. All cells were incubated at 37 °C and 5 % CO₂ atmosphere (*CO₂ incubator BBD 6220*; Heraeus).

In order to split confluent cells, the medium was removed, and cells were washed once with sterile PBS. Cells were then incubated with 0.5 % trypsin/EDTA (Pan) for 2-5 min at 37 °C. Trypsin was inactivated by adding culture medium (1:1 v/v) and the cell suspension was transferred to a 50 ml falcon followed by centrifugation at 2000 rpm for 3 min (*Multifuge 3S-R*; Heraeus). The supernatant was removed, and cells were resuspended in medium. Depending on the experimental conditions, cells were either split in an appropriate ratio (1:2-1:20) or counted prior to seeding using a hemocytometer (*Neubauer cell counter*; Carl Roth). Therefore, the cell suspension was mixed with Trypan blue solution (1:1 v/v) and pipetted onto the counting chamber. The mean number of cells in 16 small squares was determined using a *Leica DMIL* light microscope and the number of viable cells was calculated using the following formula:

$$\text{cell number/ml} = \text{counted cells} \times 2 \text{ (dilution factor)} \times 10^4$$

PBS	140 mM	NaCl
	3 mM	KCl
	5 mM	Na ₂ HPO ₄
	1.5 mM	KH ₂ PO ₄ in H ₂ O
	→ autoclave	
Trypan Blue Solution	0.15 %	Trypan Blue
	0.85 %	NaCl

3.2.2 Storage

For long-term storage, subconfluent cultures were trypsinized and pelleted as described above (see 3.2.1). Cells were resuspended in FBS containing 10 % DMSO, transferred to *CryoTubes* (Nunc) and slowly frozen using a freezing container (*Mr. Frosty*; Nalgene Labware). Frozen cells were stored in liquid nitrogen.

For re-cultivation of cells, they were rapidly thawed in a water bath at 37 °C and resuspended in pre-warmed culture medium. To remove the DMSO, cells were centrifuged once at 2000 rpm for 3 min. Finally, cells were resuspended in 1 ml culture medium, seeded on an appropriate cell culture dish and incubated as described before (see 3.2.1).

3.2.3 Transfection of mammalian cells

3.2.3.1 Transfection with Polyethylenimine (PEI)

Transfection of mammalian cells was in general performed using Polyethylenimine (PEI). PEI was dissolved in ddH₂O (1 mg/ml), neutralized to pH 7.2 by 0.1 M HCl, sterile filtered (pore size 0.22 μm; VWR), aliquoted and stored at -80 °C. 24 h before transfection, cells were seeded on 6-well or 100 mm cell culture dishes. Plasmid DNA was mixed with 600 μl pre-warmed DMEM without supplements and PEI was added in a ratio of 10:1 (DMEM:PEI, v/v). The transfection solution was shortly vortexed and incubated at RT for 10 min before it was added drop wise to the cells in fresh DMEM without supplements. After incubation for 4-5 h at standard conditions, the transfection solution was

replaced by standard culture medium, since PEI is toxic to the cells. Transfected cells were harvested 24-72 h post transfection (p.t.).

3.2.3.2 Transfection with calcium phosphate (ProFection® Mammalian Transfection System)

This method of transfection was used for transformation assays of pBRK cells (see 3.2.5). The protocol has been modified from the manufacturer's protocol of the *ProFection® Mammalian Transfection System* Kit (Promega). 48 h prior to transfection, pBRK cells were freshly isolated and seeded on 100 mm cell culture dishes. Plasmid DNA was diluted with sterile deionized H₂O to a volume of 437.5 μ l and mixed gently before 62.5 μ l 0.2 M CaCl₂ were added. In parallel, 500 μ l sterile 2x HBS were prepared in a 15 ml falcon. The DNA solution was then added drop wise to the HBS while it was continuously vortexed. After incubation for 30-60 min at RT, the transfection solution was added drop wise to the cells in standard culture medium. 6-8 h after transfection, the medium was changed once again.

3.2.4 Cell harvesting

Transfected or infected cells were harvested with cell scrapers and collected in 15/50 ml falcons followed by centrifugation at 2000 rpm for 3 min. Cells were washed once in sterile PBS and stored at -20 °C for later experiments.

3.2.5 Transformation of pBRK cells

pBRK cells were transfected as described above (see 3.2.3.2). The cells were grown for approximately 3 weeks and medium was changed twice a week. After that time, most non-transfected cells died, whereas cells transfected with adenoviral gene products were considered transformed, resulting in multilayered cell colonies (*foci*). These *foci* were stained with a crystal violet solution and counted for statistical analysis. The number of *foci* represents the efficiency of cellular and viral oncogenes to initiate the transformation process.

Crystal Violet	1 % (w/v)	Crystal Violet
Staining Solution	25 % (v/v)	Methanol (in ddH ₂ O)

3.3 Adenovirus

3.3.1 Infection of mammalian cells

Cells were seeded as described before (see 3.2.1) and infected at a confluency of 50-70 %. Prior to infection, the culture medium was removed and replaced by medium without supplements. Virus dilutions were prepared using the following formula:

$$\text{volume virus stock solution } (\mu\text{l}) = \frac{\text{multiplicity of infection (MOI)} \times \text{total cell number}}{\text{virus titer (fluorescence forming units (ffu)/}\mu\text{l)}}$$

The virus was then diluted in an appropriate amount of medium without supplements and added to the cells. After 2 h incubation at standard conditions, the medium was replaced with complete culture medium. Infected cells were harvested at desired time points according to the experimental setup.

3.3.2 Propagation and storage of high-titer virus stocks

Propagation of high-titer virus stocks was performed in A549 cells. Therefore, cells were infected as described above (see 3.3.1) at a MOI of 15 *ffu*/cell. After 3-5 days, cells were harvested followed by centrifugation at 2000 rpm for 3 min. Cells were washed once in PBS and resuspended in an appropriate amount of medium without supplements. In order to release viral particles into the medium, cells were broken up by freezing in liquid nitrogen and rapid thawing in a water bath at 37 °C. Freeze and thaw cycles were repeated three times. The cell debris was then pelleted at 4500 rpm for 10 min and the supernatant was mixed with sterile glycerol to a concentration of 10 % (v/v). Virus stocks were kept at -80 °C for long-term and -20 °C for short-term storage.

3.3.3 Titration of virus stocks

Determination of virus titers is based on the number of fluorescence forming units (*ffu*) after immunofluorescence staining of the adenoviral DNA binding protein (DBP/E2A). Each virus stock was diluted by a factor of 10^0 - 10^{-5} to infect 3×10^5 A549 cells per 6-well with each dilution. 24 h p.i., cells were fixed with ice-cold methanol for 20 min at -20 °C. Afterwards, the methanol was removed, and cells were air-dried at RT. To block unspecific binding sites, cells were

incubated with TBS-BG (1x) for 1 h at RT. Each well was incubated with primary antibody against DBP/E2A (B6-8; 1:10 dilution in TBS-BG 1x) for 2 h at RT followed by three washing steps with TBS-BG (1x). *Alexa Fluor 488* coupled secondary antibody was incubated for 2 h at RT, cells were washed three times with TBS-BG and overlaid with 1 ml TBS-BG. Finally, cells were counted using a fluorescence microscope (*DMIL*, Leica). To analyze virus titers, fluorescent cells of four different visual fields were counted and the average was calculated. The total number of infectious particles was then calculated, taking into account the number of infected cells, the virus dilutions and the microscope magnification used.

TBS-BG	Tris/HCl, pH 7.6	20 mM
	NaCl	137 mM
	KCl	3 mM
	MgCl ₂	1.5 mM
	Tween-20	0.05 % (v/v)
	Sodium-azide	0.05 % (w/v)
	Glycine	5 % (w/v)
	BSA	5 % (w/v)

3.4 DNA techniques

3.4.1 Preparation of plasmid DNA from *E. coli*

To isolate plasmid DNA from *E. coli* cultures, 500 ml of LB medium were inoculated with 200-500 μ l of a pre-culture derived from a single bacteria colony. After incubation for 16-20 h at 30/37 °C (*Inova 4000 Incubator*; New Brunswick), bacteria were pelleted at 6000 rpm for 10 min at 4 °C (*Avanti J-E*; Beckman & Coulter). Afterwards, plasmid DNA was extracted according to the manufacturer's protocol using a *MaxiKit* (Qiagen).

For analysis of newly generated plasmids, bacteria from 1 ml cultures were pelleted at 6000 rpm for 3 min at 4 °C (*Zentrifuge 5417 R*; Eppendorf GmbH). The pelleted bacteria were resuspended in 300 μ l *resuspension buffer P1* (Qiagen), lysed by adding 300 μ l *lysis buffer P2* (Qiagen) and incubated for 5 min at RT. After adding 300 μ l *neutralization buffer P3* (Qiagen) and incubation for another 5 min at -20 °C, salts and cellular debris were pelleted by centrifugation at

13000 rpm for 5 min and 4 °C. The supernatant was transferred into a new 1.5 ml Eppendorf tube and 1 volume of isopropanol as well as 0.1 volume of 3 M NaAc was added. DNA was precipitated by centrifugation at 13000 rpm for 30 min at 4 °C. Pelleted DNA was washed once with 1 ml 70 % (v/v) ethanol, centrifuged for 5 min at 13000 rpm and 4 °C, air dried and rehydrated in 20-50 μ l ddH₂O.

3.4.2 Quantitative determination of nucleic acid concentrations

DNA/RNA concentrations were determined with a *NanoDrop* spectrophotometer (Peachlab) at a wavelength of 260 nm. An OD of 1.0 corresponds to a concentration of 50 μ g/ml for dsDNA, 33 μ g/ml for ssDNA and 40 μ g/ml for RNA, respectively. DNA purity was assessed by calculation of the OD₂₆₀/OD₂₈₀ ratio. For highly pure DNA this ratio should be located at 1.8, for highly pure RNA at 2.0.

3.4.3 Agarose gel electrophoresis

Analytical and preparative gels were prepared by dissolving agarose (*Seakem® LE agarose*; Biozym) in 1x TBE buffer to a final concentration of 0.8-1.2 % (w/v). Agarose was dissolved in a microwave (Siemens) and supplemented with 50 ng/ml ethidium bromide. The solution was then poured into an appropriate gel tray. DNA samples were mixed with 6x loading dye, loaded onto the agarose gel and separated at 5-10 V/cm gel length in 1x TBE. DNA was visualized by applying UV light at 312 nm using the *G:BOX transilluminator system* (SynGene).

To elute DNA from agarose gels, bands of interest were cut out the gel and isolated using the *QIAquick Gel Extraction Kit* (Qiagen) according to the manufacturer's protocol.

5x TBE	450 mM Tris/HCl, pH 8.0
	450 mM Boric acid
	10 mM EDTA
	→ pH 7.8

6x loading	0.25 % (w/v)	Bromophenol blue
buffer	0.25 % (w/v)	Xylene cyanol
	50 % (v/v)	Glycerol
	2 % (v/v)	50x Tris acetate (TAE)

3.4.4 Polymerase Chain Reaction (PCR)

To amplify a DNA template, 50-100 ng DNA template, 0.2 μ M forward primer, 0.2 μ M reverse primer, 1 μ l dNTP mixture (dATP, dTTP, dCTP, dGTP; 1 mM each; New England Biolabs), 5 μ l 10x PCR reaction buffer (Omnilab) and 5 U Taq-Polymerase (Roche) were prepared in a 0.2 ml PCR tube. PCR was performed in a thermocycler (*Flexcycler*; Analytic Jena) using the following programme:

DNA denaturation	1 min	95 °C
Primer annealing	45 s	55-70 °C
Extension	1 min/kb	72 °C (20-30 cycles)
Final extension	10 min	72 °C
Storage	∞	4 °C

To determine PCR efficiency, 5 μ l PCR reaction was analyzed on an agarose gel (see 3.4.3). Fragment size and yield was examined under UV light with the *G:Box transilluminator system* (SynGene).

3.4.5 Site-directed mutagenesis

Site-directed point mutations were inserted into plasmid DNA by PCR. Primers (forward and reverse) were designed with the desired mutations and ordered from Metabion (Munich). PCR was performed using the following programme:

DNA denaturation	1 min	95 °C
Primer annealing	45 s	55 °C
Extension	45 s/kb	68 °C (12-16 cycles)
Final extension	10 min	68 °C
Storage	∞	4 °C

PCR efficiency was determined by analyzing 10 μ l PCR reaction on an agarose gel (see 3.4.3). The remaining 40 μ l were incubated with 1 μ l restriction enzyme *DpnI* (New England Biolabs) for 2 h at 37 °C to remove methylated template DNA. 10 μ l of the digest were transformed into chemical competent DH5 α (see 3.1.2). The next day, single colonies were picked and cultured overnight in LB medium (see 3.1.1). Plasmid DNA was prepared and analyzed by agarose gel electrophoresis (see 3.4.3) and sequencing (see 3.4.6).

3.4.6 DNA sequencing

For sequencing of purified DNA, 1-1.2 μ g of DNA were mixed with 30 pmol of the appropriate primer and adjusted to 15 μ l with ddH₂O. Sequencing was performed by SeqLab (Göttingen).

3.5 Protein techniques

3.5.1 Preparation of total cell lysates

In order to prepare total cell lysates, cells were harvested as described above (see 3.2.4). Depending on the pellet size, cells were resuspended in 100-500 μ l of ice-cold RIPA buffer, freshly supplemented with 1 mM PMSF, 10 U/ml aprotinin, 1 μ g/ml leupeptin and 1 μ g/ml pepstatin. This highly stringent buffer ensured proper solubilisation of matrix associated proteins, such as E1B-55K. Cells were then incubated on ice for 30 min and shortly vortexed every 10 min to allow efficient cell disruption. Afterwards, lysates were sonified for 30 s at 4 °C (output 0.8, 0.8 impulse/s; *Branson Sonifier 450*) to shear genomic DNA. If not indicated otherwise, cell debris as well as insoluble components were pelleted (11000 rpm, 3 min, 4 °C; *Zentrifuge 5417R*; Eppendorf GmbH) and the protein concentration of the supernatant was determined by spectrophotometry (see 3.5.2). Finally, all lysates were adjusted to the same concentrations by adding pre-cooled ddH₂O. Lysates were then denatured by adding the required volume of 5x SDS sample buffer (Laemmli buffer) and boiling at 95 °C for 5 min. Protein lysates were stored at -20 °C.

RIPA lysis buffer	50 mM	Tris/HCl (pH 8)
	150 mM	NaCl
	5 mM	EDTA
	1 % (v/v)	Nonidet P-40
	0.1 % (w/v)	SDS
	0.5 % (v/v)	Sodium desoxycholate
5x SDS sample buffer	100 mM	Tris/HCl (pH 6.8)
	200 mM	DTT
	10 % (w/v)	SDS
	0.2 % (w/v)	Bromophenol blue

3.5.2 Quantitative determination of protein concentrations

Protein concentrations of total cell lysates were determined using the Bradford-based BioRad Protein-Assay by measuring the absorption of protein-bound chromogenic substrate at 595 nm [184]. Therefore, 1 μ l of each sample was mixed with 800 μ l ddH₂O and 200 μ l *Bradford Reagent* (BioRad) and incubated for 5 min at RT. Samples were measured in a *SmartSpec Plus* spectrophotometer (BioRad) at 595 nm against a blank, and protein concentrations were determined by interpolation from a standard curve with BSA (concentrations of 1-16 μ g/ μ l; New England Biolabs).

3.5.3 SDS polyacrylamide gel electrophoresis (SDS-PAGE)

Protein samples were separated according to their molecular weight by SDS-PAGE. The negatively charged SDS compensates for the positive charge of the proteins by accumulating on them at constant weight ratios. Thus, proteins can be separated only by their molecular weight. Protein separation is further increased by using a discontinuous stacking gel with lower pH (6.8). Proteins concentrate in this gel before migrating into the separating gel [185]. Polyacrylamide gels were made using 30 % acrylamide/bisacrylamide solution (37,5:1 *Rotiphorese Gel 30*; Roth), diluted to a final concentration of 10-15 % with ddH₂O. All gels were run in TGS-buffer at 15-20 mA/gel. The *PageRuler™ Prestained Protein Ladder Plus* (Thermofisher) was used for protein weight comparison.

Acrylamide Stock Solution (30 %)	29 % (w/v) Acrylamide N
	1 % (w/v) N'Methylenbisacrylamide
Stacking gel (5 %)	17 % (v/v) Acrylamide stock solution
	120 mM Tris/HCl (pH 6.8)
	0.1 % (w/v) SDS
	0.1 % (w/v) APS
	0.1 % (v/v) Temed
Separating Gel (10 %)	34 % Acrylamide stock solution
	250 mM Tris/HCl (pH 8.8)
	0.1 % (w/v) SDS
	0.1 % (w/v) APS
	0.04 % (v/v) Temed
Separating Gel (15 %)	50 % Acrylamide stock solution
	250 mM Tris/HCl (pH 8.8)
	0.1 % (w/v) SDS
	0.1 % (w/v) APS
	0.6 % (v/v) Temed
TGS buffer	25 mM Tris
	200 mM Glycine
	0.1 % (w/v) SDS

3.5.4 Western Blot analysis

Separated proteins from SDS-PAGE (see 3.5.3) were transferred onto nitrocellulose membranes (pore size $\varnothing=0.45\ \mu\text{m}$; GE Healthcare) using the *TransBlot Electrophoretic Transfer Cell System* (BioRad). Briefly, gels and membranes were soaked in *Towbin* buffer and placed between two blotting papers (Whatman) and two blotting pads, also soaked in *Towbin* buffer, in a plastic grid. Protein transfer was performed in a blotting tank filled with *Towbin* buffer at 400 mA for 90 min. Afterwards, membranes were incubated in 5 % non-fat dry milk (w/v in PBS-Tween; Frema) overnight at 4 °C on an orbital shaker (GFL) to saturate non-specific antibody binding sites. The blocking

solution was discarded and membranes were washed 3x with PBS-Tween for 10 min each followed by incubation with the respective primary antibody for 3 h at 4 °C. Antibody dilutions were established for each individual antibody. Afterwards, membranes were washed again as indicated above and incubated with the suitable HRP-coupled secondary antibody (Amersham) for 2 h at 4 °C. Secondary antibodies were diluted 1:10,000 in 3 % non-fat dry milk (w/v in PBS-Tween; Frema). After three final washing steps in PBS-Tween for 10 min each, protein bands were visualized by enhanced chemiluminescence using *SuperSignal™ West Pico Chemiluminescent Substrate* (ThermoFisher) according to the manufacturer's instructions. For very weak protein expression, the *SuperSignal™ West Femto Maximum Sensitivity Substrate* (ThermoFisher) was used. Finally, protein bands were detected by X-ray films (*RP New Medical X-Ray Film*; CEA) using a *GBX Developer* (Kodak). X-ray films were scanned, cropped using *Photoshop CS6* (Adobe) and figures were prepared using *PowerPoint* (Microsoft) and *Illustrator CS6* (Adobe).

Towbin buffer	25 mM	Tris/HCl (pH 8.3)
	200 mM	Glycine
	0.05 % (w/v)	SDS
	20 % (v/v)	Methanol
PBS-Tween	0.1 % (v/v)	Tween20 in 1x PBS

3.5.5 Denaturing purification and analysis of SUMO-conjugates

HeLa cells stably overexpressing 6-His-tagged SUMO-1 or SUMO-2 were infected or transfected as described before (see 3.3.1 and 3.2.3.1). After 48 h, cells were harvested, washed once with 1x PBS and lysed in 5 ml Guanidinium hydrochloride (GuHCl) lysis buffer, freshly supplemented with 1 mM PMSF, 10 U/ml aprotinin, 1 µg/ml leupeptin and 1 µg/ml pepstatin. 10 % of the cells were lysed in RIPA buffer for analysis of total cell lysates (see 3.5.1). The lysates in GuHCl lysis buffer were incubated overnight at 4 °C on a rotator (GFL) with 50 µl Ni-NTA agarose (Thermo Scientific), prewashed 3x with 1 ml lysis buffer. Afterwards, the agarose beads were washed once with lysis buffer and once with each wash buffer (pH 8.0 and pH 6.3), freshly supplemented with 1 mM

PMSF, 10 U/ml aprotinin, 1 $\mu\text{g}/\text{ml}$ leupeptin and 1 $\mu\text{g}/\text{ml}$ pepstatin. Elution of 6-His-tagged SUMO-conjugates was done in 60 μl elution buffer followed by boiling at 95 °C for 5 min. Eluted samples were stored at -20 °C until analyzed by SDS-PAGE and Western Blot (see 3.5.3 and 3.5.4).

GuHCl lysis buffer	6 M GuHCl
	100 mM Na_2HPO_4
	100 mM NaH_2PO_4
	10 mM Tris/HCl, pH 8.0
	20 mM Imidazol
	5 mM β -mercaptoethanol
Wash buffer, pH 8.0	8 mM Urea
	100 mM Na_2HPO_4
	100 mM NaH_2PO_4
	10 mM Tris/HCl, pH 8.0
	20 mM Imidazol
	5 mM β -mercaptoethanol
Wash buffer, pH 6.3	8 mM Urea
	100 mM Na_2HPO_4
	100 mM NaH_2PO_4
	10 mM Tris/HCl, pH 6.3
	20 mM Imidazol
	5 mM β -mercaptoethanol
Elution buffer	200 mM Imidazol
	0.1 % (w/v) SDS
	150 mM Tris/HCl, pH 6.3
	30 % (v/v) Glycerol
	720 mM β -mercaptoethanol
	0.01 % (w/v) Bromophenol blue

3.5.6 Indirect immunofluorescence

Cells were grown on glass coverslips in 6-well plates and infected or transfected as described before (see 3.3.1 or 3.2.3.1). For some experiments, cells were treated with leptomycin B (LMB) prior to fixation. Therefore, 20 nM/ μ l LMB in EtOH was added to the cells 28 h p.t. Control cells were treated with EtOH only. All cells were fixed 24 h p.t. with 4 % PFA for 20 min at 4 °C. Cells were permeabilized with PBS containing 0.5 % Triton X-100 for 10 min at RT followed by 30 min blocking in TBS-BG buffer. The coverslips were incubated with primary antibody, diluted in PBS, for 1 h at RT. After three washing steps with TBS-BG, the coverslips were incubated with the corresponding Alexa488- (Invitrogen) or Cy3-conjugated (Dianova) secondary antibody for 30 min at RT. Secondary antibody was diluted in PBS with DAPI (1:5000). Finally, cells were washed 3x with TBS-BG and 1x with PBS and mounted in *glow medium*. Digital images were acquired with a confocal spinning-disk microscope (Nikon Eclipse Ti-E stand; Yokagawa CSU-W1 spinning disk; 2x Andor888 EM-CCD camera; Nikon 100x NA 1.49 objective). Images were analyzed and cropped using *Fiji* and assembled with *Illustrator CS6* (Adobe).

PBS-Triton	0.5 M Triton X-100 in 1x PBS
------------	---------------------------------

3.5.7 Reporter gene assay

For quantitative determination of promoter activity, the *Dual-Luciferase Reporter Assay System* (Promega) was used according to the manufacturer's instructions. Promoter activity was determined by expression of *firefly* luciferase (*Photinus pyralis*) under the control of the investigated promoter. For normalization, and as an internal transfection control, *renilla* luciferase (*Renilla reniformis*) expression was measured, which is under the control of the herpes simplex virus thymidine kinase (HSV-TK) promoter. Cells were grown on 12-well plates and transfected as described before (see 3.2.3.1). After 24 h, cells were washed once with 1x PBS and 100 μ l/well *passive lysis buffer* (Promega) were added. Plates were incubated on an orbital shaker (GFL) for 10 min with vigorous shaking. 10 μ l of the lysate were mixed with 20 μ l of the *firefly* luciferase substrate and the *firefly* emission was measured immediately in a *Lumat LB 9507 luminometer* (Berthold Technologies). The reaction was then stopped by addition of 20 μ l *Stop&Glow*

substrate, which additionally is converted by the *renilla* luciferase and this emission was measured again.

4 Results

4.1 K101 affects SUMOylation of HAdV-C5 E1B-55K

4.1.1 HAdV-C5 E1B-55K K101R is highly SUMOylated in transient transfection and during infection

HAdV-C5 E1B-55K is an early protein that evolved several mechanisms contributing to its oncogenic potential. Previously, E1B-55K has been shown to be a substrate of the SUMO conjugation machinery and that many of its functions are regulated by PTMs [59, 96, 97, 111]. Furthermore, our group identified a link between the different PTMs of E1B-55K and showed that phosphorylation at its C-terminus regulates SUMOylation at lysine 104 (K104) [170]. A site-specific SUMO-proteome, performed by members of our group in cooperation with Ron Hay from the University of Dundee revealed several lysines on E1B-55K, which are possibly involved in SUMOylation [186]. Amongst them was a lysine at position 101 (K101), which is in close proximity to the main SCM of E1B-55K at K104. Therefore, we assumed that this site could also play a role in the regulation of E1B-55K SUMOylation. It has been shown before for other proteins, that two adjacent lysines are regulating each other regarding their PTMs [137]. In addition, many proteins are modified by multiple PTMs, already indicating that they might be linked to one another. It is known that PML is ubiquitinated, SUMOylated, phosphorylated as well as acetylated (reviewed in [187]). Further, it has been described for PML that inactivation of acetylation at K487 results in a loss of SUMOylation at K490 [137].

Thus, in a first experiment we generated mutations of the putatively SUMOylated lysines revealed by the SUMO-proteome on E1B-55K by site-directed mutagenesis. Afterwards, SUMOylation of E1B-55K was analyzed by a Ni-NTA pulldown of transfected HeLa cells constitutively overexpressing 6-His-SUMO-1 or 6-His-SUMO-2 (Fig. 6). This experiment allows the detection of SUMOylated proteins, as they are migrating slower in the SDS-PAGE with a SUMO attached to them. By exchanging the lysine with an arginine (K to R), putative SUMOylation at this site is inhibited, while biochemical properties of the residue are preserved. A lysine to alanine (K to A) exchange however,

results in a much smaller and hydrophobic residue. For the sake of simplicity, HAdV-C5 E1B-55K wt is referred to as E1B-55K in the following. Additionally, all mutants are termed according to the site of their mutation.

Remarkably, immunoblotting of Ni-NTA purified 6-His-SUMO-1 and 6-His-SUMO-2 conjugates with E1B-55K specific antibody revealed that the K101R mutant is SUMOylated more than the wt-protein (Fig. 6 A; lanes 11 and 12 + Fig. 6 B; lanes 11 and 12). For the latter, we detected only a very faint slower migrating band in the SUMO-1 conjugated protein (Fig. 6 B; lane 11). In general, E1B-55K was much less conjugated to SUMO-1, since this isoform is bound to substrates as a monomer. As already published, inactivation of the main SCM (K104R) showed no SUMOylation with SUMO-1 or SUMO-2, suggesting that the lysine K101 is not SUMOylated (Fig. 6 A; lane 13 + Fig. 6 B; lane 13) [75]. The fact that no SUMO conjugates were found in the double mutant E1B-55K K101/104R further suggests that K104 is the main SUMOylation site in the K101R mutant (Fig. 6 A; lane 14 + Fig. 6 B; lane 14). As it has been observed before, inactivation of the NES led to a higher SUMOylation compared to the wt (Fig. 6 A; lane 15 + Fig. 6 B; lane 15) [169]. However, the pattern of SUMOylation appeared to be different from E1B-55K K101R as there is a band missing in the SUMO-2 conjugated protein (Fig. 6 A; indicated by white arrows). Additionally, the NES mutant is much higher SUMOylated by SUMO-1 than E1B-55K K101R (Fig. 6 B; lanes 12 and 15). Here, we even observed multiple slower migrating bands, indicating that SUMO-1 is incorporated into chains (Fig. 6 B; lane 15). In contrast to E1B-55K K101R, the K101A mutant was remarkably less SUMOylated by both SUMO isoforms (Fig. 6 A; lane 16 + Fig. 6 B; lane 16). Interestingly, in this mutant even the SUMO-2 conjugated protein seems to be modified by a monomer, since we detected only one slower migrating band in the immunoblot (Fig. 6 A; lane 16). To exclude that K to R mutation of any lysine led to a similar increase in SUMOylation as seen for E1B-55K K101R, we also tested the K138R and K185R mutants. These mutants showed comparable SUMOylation patterns to the wt-protein with SUMO-1 and SUMO-2 (Fig. 6 A; lanes 17 and 18 + Fig. 6 B; lanes 17 and 18). No SUMOylation was detectable in the controls comprising HeLa parental cells or cells transfected with an empty vector (Fig. 6 A; lanes 1-10 + Fig. 6 B; lanes 1-10). Similar results were obtained in H1299 cells co-transfected

with the respective mutants and His-tagged SUMO-1 or SUMO-2 (data not shown).

In summary, we identified that SUMOylation of E1B-55K with SUMO-1 and SUMO-2 at the SCM around K104 is strongly affected by the lysine K101 nearby.

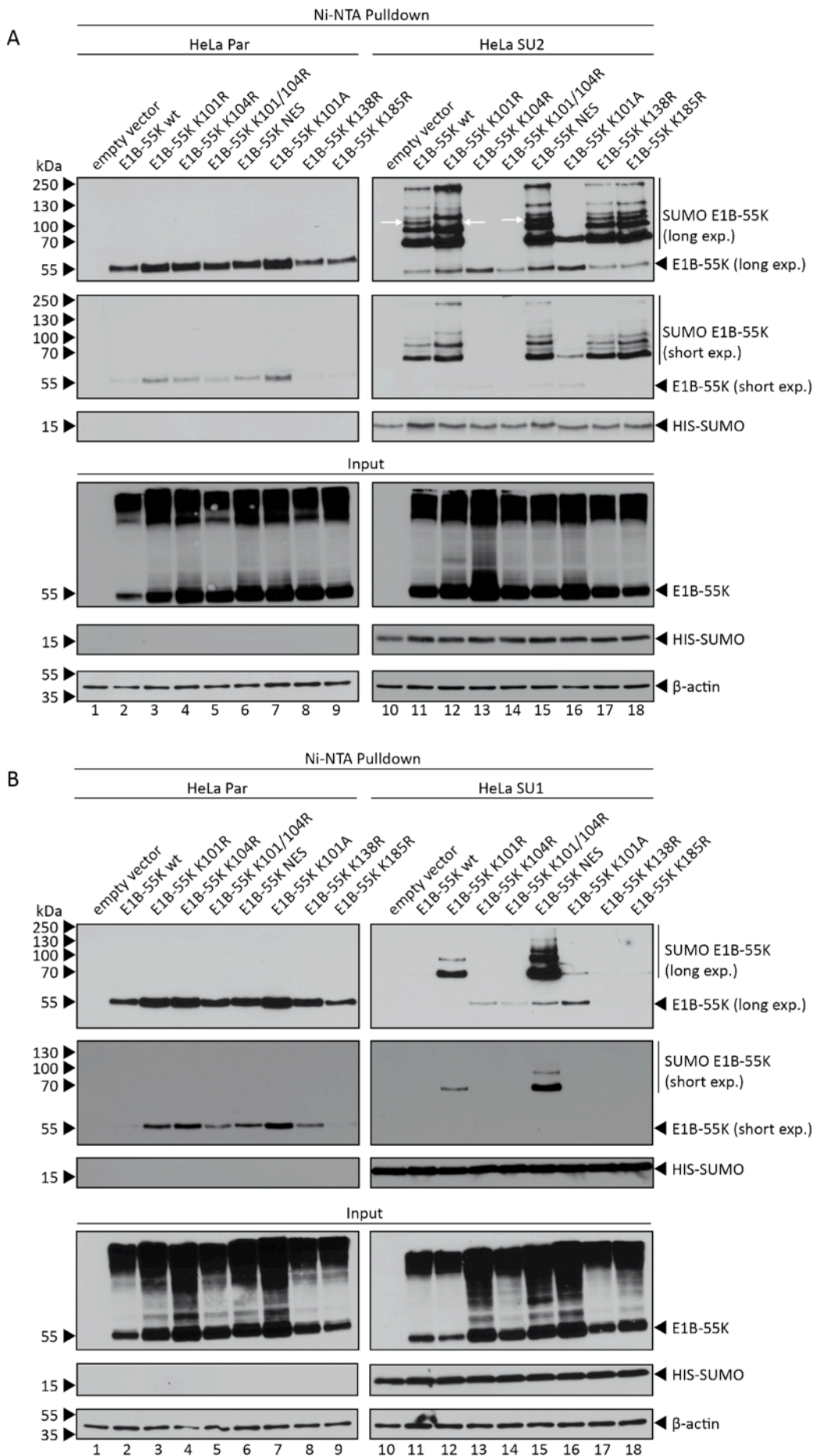


Fig. 6: SUMO conjugation is increased in E1B-55K K101R in transfection (A) HeLa parental cells and HeLa cells stably overexpressing 6-His-tagged SUMO-2 or (B) HeLa parental cells and HeLa cells stably overexpressing 6-His-tagged SUMO-1 were transfected with an empty vector control or E1B-55K wt, K101R, K104R, K101/104R, NES, K101A, K138R or K185R. Cells were harvested 48 h p.t. and Ni-NTA purification of 6-His-SUMO conjugates was performed. Proteins were separated by SDS-PAGE and subjected to immunoblotting. Protein levels of input and Ni-NTA purified proteins were detected using mAb AC-15 (β -actin), mAb 2A6 (E1B-55K) and mAb 6-His (His). Molecular weights in kDa are indicated on the left, detected proteins on the right. The blots represent the result of several repeated experiments.

Given that the SUMOylation of E1B-55K K101R was strongly increased in transient transfection experiments, we also tested the mutant in the context of viral infection. Thereby, we wanted to see, if we can still detect higher SUMOylation in the presence of other viral proteins. HeLa cells stably expressing 6-His-SUMO-2 were infected with HAdV-C5 E1B-55K wt and mutants according to the transfection experiment (Fig. 6). Then, His-SUMO conjugates were purified by Ni-NTA pulldown (Fig. 7). As expected, SUMOylation of E1B-55K was neither observed in the mock-infected samples nor in infected HeLa parental cells (Fig. 7; lanes 1-7). Consistent with our observations in transient transfection, E1B-55K of the K101R virus mutant was higher SUMOylated than E1B-55K of the wt-virus (Fig. 7; lanes 8 and 9). Infection with E1B-55K K104R resulted in a loss SUMOylation, which has been already observed after transfection (Fig. 7; lane 10) [169]. Similarly, the K101/104R virus revealed no SUMOylation of E1B-55K (Fig. 7; lane 11). Finally, infection with E1B-55K NES led to the highest SUMOylation of E1B-55K (Fig. 7; lane 12).

Taken together, we saw that K101 affects SUMOylation of E1B-55K with SUMO-2 in both transfection and infection.

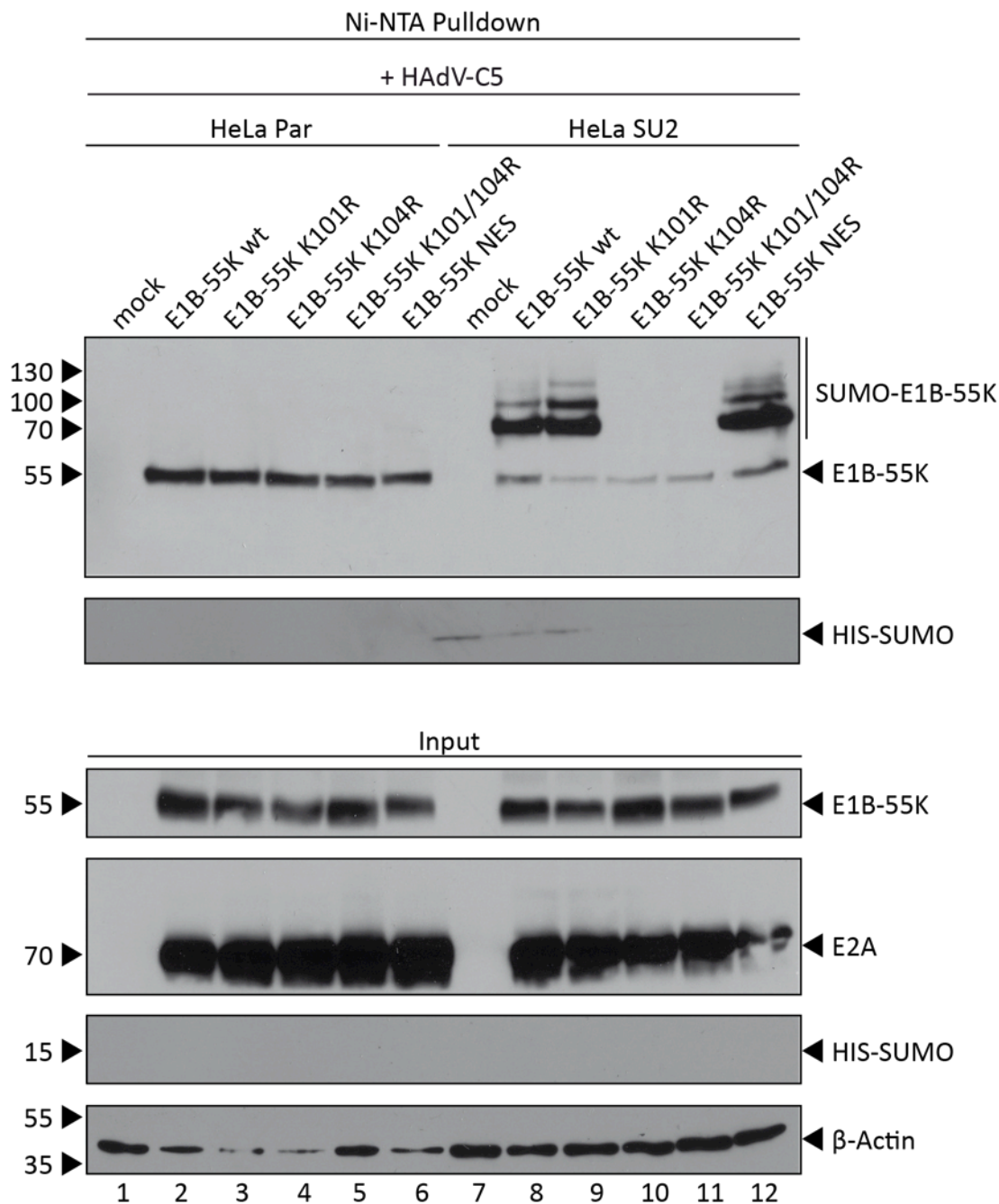


Fig. 7: SUMO-2 conjugation of E1B-55K is increased in HAdV-C5 E1B-55K K101R during infection. HeLa parental cells or HeLa cells stably overexpressing SUMO-2 were infected with HAdV-C5 wt virus (H5pg4100), HAdV-C5 E1B-55K K101R (H5pm4243), HAdV-C5 E1B-55K K104R (H5pm4102), HAdV-C5 E1B-55K K101/104R (H5pm4244) or HAdV-C5 E1B-55K NES (H5pm4101) at a MOI of 15. Cells were harvested 48 h p.i. and Ni-NTA purification of 6-His-SUMO conjugates was performed. Proteins were separated by SDS-PAGE and subjected to immunoblotting. Protein levels of input and Ni-NTA purified proteins were detected using mAb AC-15 (β -actin), mAb B6-8 (E2A), mAb 2A6 (E1B-55K) and mAb 6-His (His). Molecular weights in kDa are indicated on the left, detected proteins on the right. The blot represents the result of several repeated experiments.

4.1.2 HAAdV-C5 E1B-55K K101R localizes to the nucleus in transient transfection

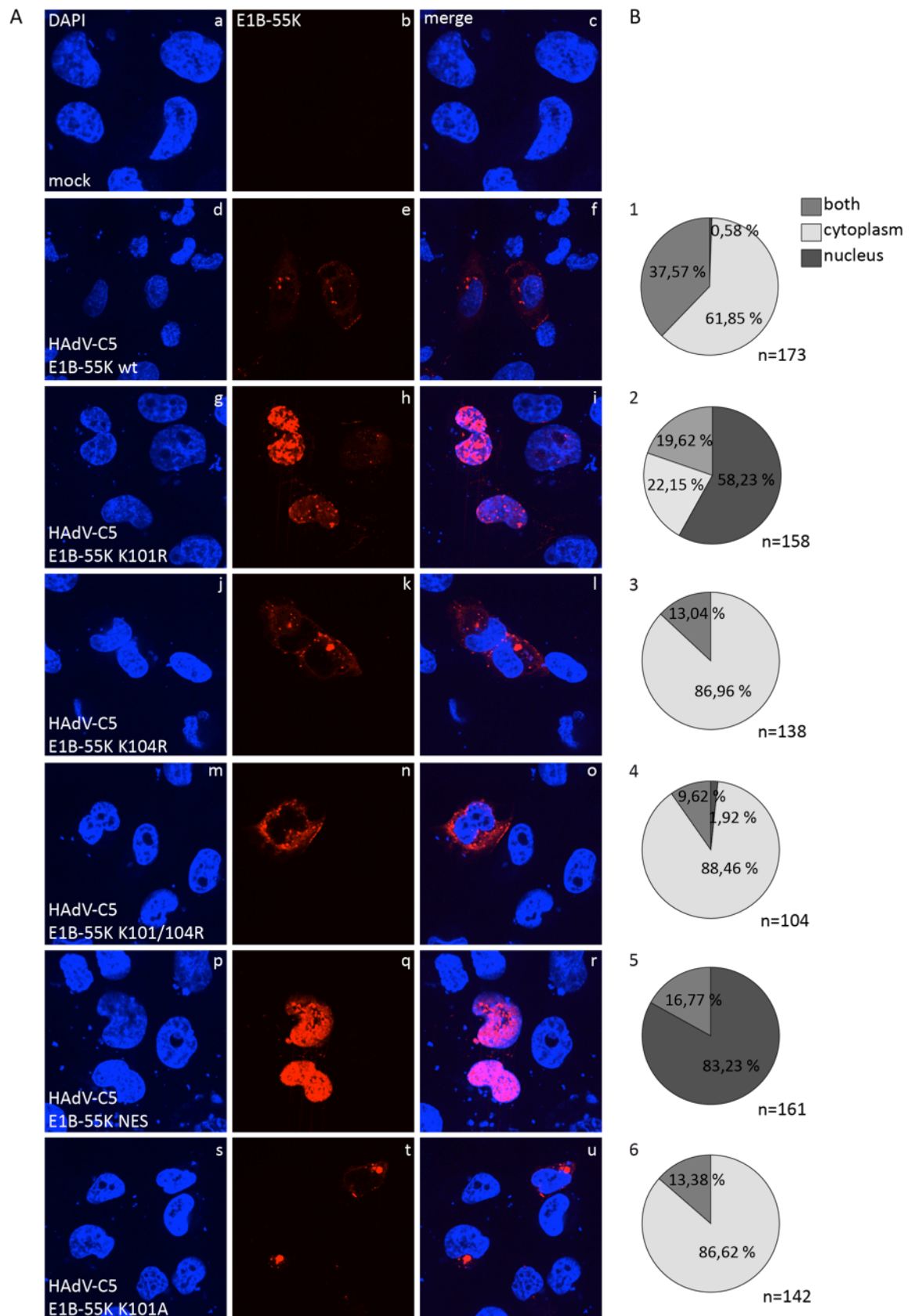
SUMOylation of a protein is closely linked to its subcellular localization. For example, it has been shown that SUMO conjugation to RanGAP greatly facilitates its nuclear localization [138, 139]. Likewise, this observation was made for E1B-55K. Here, it was shown that inactivation of the SUMOylation prevents the protein from efficiently entering the nucleus [75, 169]. Moreover, E1B-55K actively shuttles between the nucleus and cytoplasm and shuttling is important for the protein to fulfill its functions [74, 188]. To assess the localization of the differently SUMOylated E1B-55K mutants, we performed immunofluorescence experiments in H1299 cells transfected with plasmids encoding for E1B-55K wt and the respective SUMO mutants (Fig. 8). To see, whether the mutants are still able to enter the nucleus and thus shuttle, we additionally treated the cells with the CRM1 inhibitor leptomycin B (LMB) prior to fixation (Fig. 8 C). All control cells that were not treated with LMB were treated with the solvent EtOH instead (Fig. 8 A). To better compare the different phenotypes observed in this experiment, cells were counted according to the E1B-55K localization (nuclear, cytoplasmic or both) and the quantitative distribution was calculated (Fig. 8 B + D).

No E1B-55K was detected in cells transfected with an empty vector (Fig. 8 A; Ab and Ac). Transfection with E1B-55K wt led to a mainly cytoplasmic localization of the protein in 61.85% of the cells (Fig. 8 A; Ae and Af + Fig. 8 B; B1). In contrast, the highly SUMOylated E1B-55K K101R was present in the nucleus in 58.23% of the cells (Fig. 8 A; Ah and Ai + Fig. 8 B; B2). Similar to this observation, the NES mutant revealed a nuclear localization of the protein in even 83.23% of the cells (Fig. 8 A; Aq and Ar + Fig. 8 B; B5). As observed before, E1B-55K K104R was almost exclusively found in the cytoplasm, namely in 86.96% of the cells (Fig. 8 A; Ak and Al + Fig. 8 B; B3). Interestingly, both E1B-55K K101/104R and K101A were detected in the cytoplasm in 88.46% and 86.62% of the cells, respectively (Fig. 8 A; An and Ao, At and Au; + Fig. 8 B; B4, B6). Since these mutants were also less SUMOylated or not SUMOylated at all (Fig. 6 and Fig. 7), these results further support a correlation between SUMOylation and subcellular localization.

Treating the cells with LMB did not alter the localization of the already nuclear E1B-55K mutants K101R and NES (data not shown). However, localization of

E1B-55K wt changed to a mainly nuclear localization in 63.87% of the cells (Fig. 8 C; Ce and Cf + Fig. 8 D; D1). In contrast to this, the largest fractions of E1B-55K K104R and K101A were visible in both cellular compartments (59.59% and 65.79%) (Fig. 8 C; Ch and Ci, Ck and Cl + Fig. 8 D; D2, D3). An exclusively cytoplasmic localization was detectable in 40.41% of cells transfected with E1B-55K K104R and 33.33% of cells transfected with E1B-55K K101A in contrast to only 1.05% of cells transfected with the wt-protein (Fig. 8 D; D1, D2, D3).

Taken together, these results further indicate that SUMOylation of E1B-55K is a prerequisite to enter the nucleus [169]. Additionally, the position K101 seems to be involved in the shuttling of E1B-55K by either increasing the import or reducing the export of the protein.



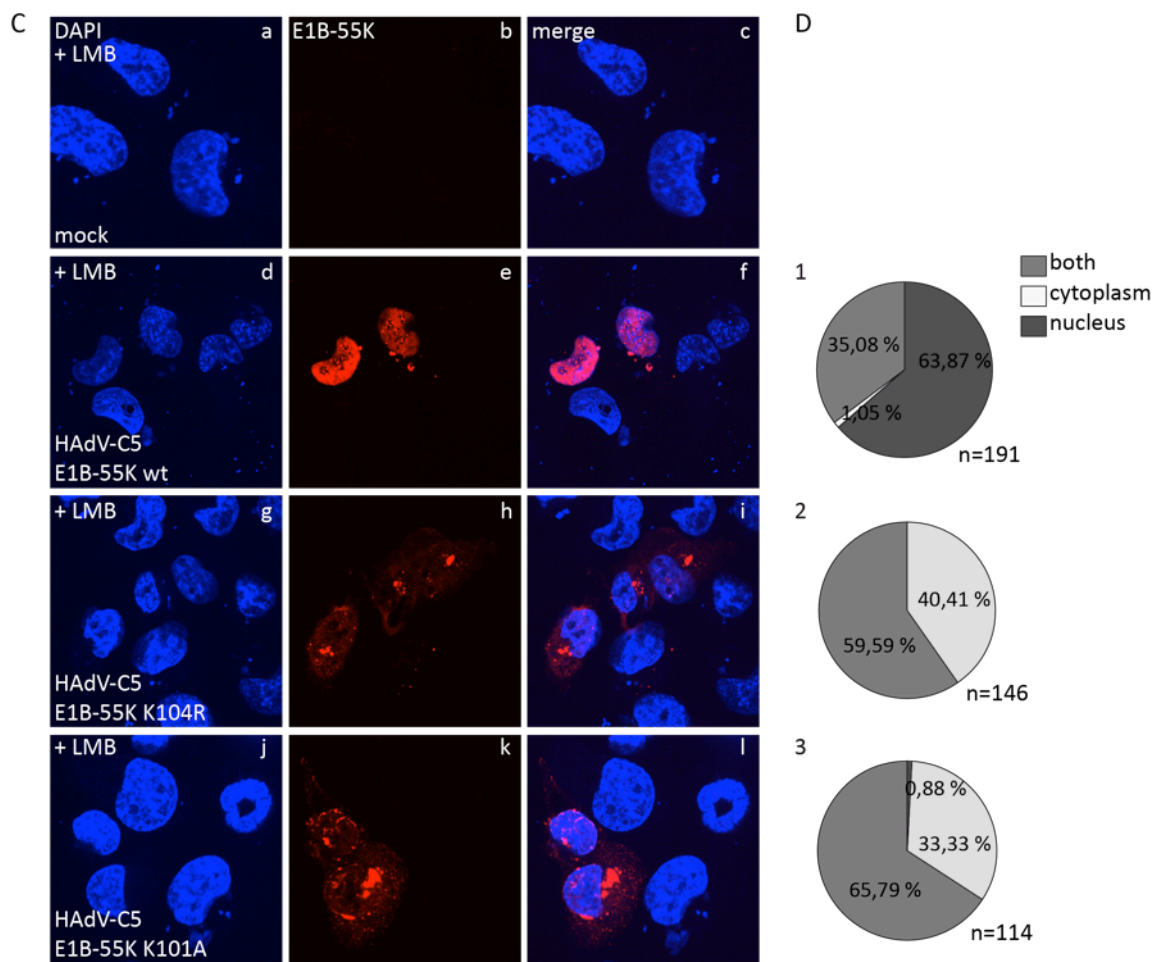


Fig. 8: K101 regulates subcellular localization and shuttling of HAAdV-C5 E1B-55K. (A) H1299 cells were transfected with an empty vector control or 1.5 μg of plasmid encoding for HAAdV-C5 E1B-55K wt, K101R, K104R, K101/104R, NES or K101A. As a control for the LMB treatment, cells were treated with 2 μl EtOH for 4 h at 20 h p.t. Cells were fixed 24 h p.t. with 4% PFA and labeled with rat mAb 4E8 (E1B-55K), detected with Cy3-conjugated secondary antibody (red channel). Nuclei were labeled with DAPI. α -E1B-55K (red; Ab, Ae, Ah, Ak, An, Aq, At), DAPI (blue; Aa, Ad, Ag, Aj, Am, Ap, As) and overlay of the single images (merge; Ac, Af, Ai, Al, Ao, Ar, Au) are shown. (B) Statistical analysis of the captured phenotypes (n). The phenotype that represents the majority of analyzed cells is shown in A. (C) H1299 cells were transfected with an empty vector control or 1.5 μg of plasmid encoding for HAAdV-C5 E1B-55K wt, K104R or K101A. Cells were treated with 20 nM/ μl LMB for 4 h at 20 h p.t. Cells were fixed 24 h p.t. with 4% PFA and labeled with rat mAb 4E8 (E1B-55K), detected with Cy3-conjugated secondary antibody (red channel). Nuclei were labeled with DAPI. α -E1B-55K (red; Cb, Ce, Ch, Ck), DAPI (blue; Ca, Cd, Cg, Cj) and overlay of the single images (merge; Cc, Cf, Ci, Cl) are shown. (D) Statistical analysis of the captured phenotypes (n). The phenotype that represents the majority of analyzed cells is shown in C.

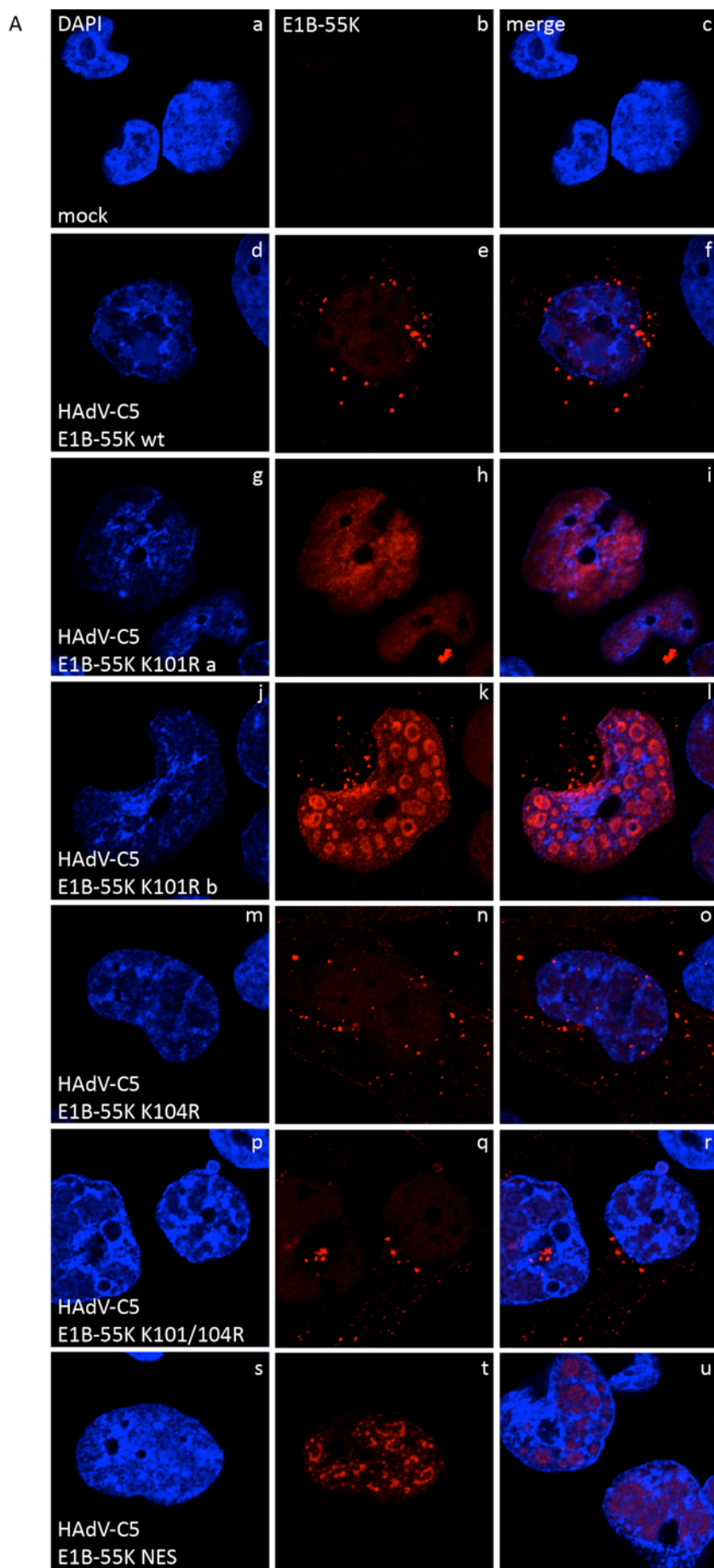
4.1.3 HAAdV-C5 E1B-55K K101R localizes to structures resembling viral replication center (VRC) during infection

To confirm the results obtained in transiently transfected cells and to investigate the localization of E1B-55K K101R in presence of other viral proteins, we performed immunofluorescence experiments in infection. Therefore, H1299 cells were infected with E1B-55K wt as well as the different E1B-55K virus mutants

(Fig. 9 A). Both, the E1B-55K localization and its ability to shuttle were analyzed with LMB, comparable to the transfection experiments (Fig. 9 B).

In mock-infected cells, no unspecific signal for E1B-55K was detected (Fig. 9 A; Ab and Ac + Fig. 9 B; Bb and Bc). Upon infection with the wt virus, E1B-55K was mainly found diffusely in the nucleus or in cytoplasmic aggregates (Fig. 9 A; Ae and Af). Treatment with LMB completely relocalized E1B-55K wt into the nucleus, similar to previous publications showing that E1B-55K is exported in a CRM1-dependent manner (Fig. 9 B; Be and Bf) [74]. Furthermore, the protein was co-localizing with structures most likely resembling viral replication center (VRC), as it has been described before that E1B-55K co-localizes with VRCs in infection (Fig. 9 B; Be and Bf) [169, 189]. Relocalization of E1B-55K to these structures was also seen in LMB untreated cells infected with the higher SUMOylated virus mutants K101R and NES (Fig. 9 A; Ah, Ai, Ak, Al, At, Au). In these mutants, treatment with LMB did not alter the localization of E1B-55K (data not shown). Interestingly, the less SUMOylated virus mutants E1B-55K K104R and K101/104R revealed a largely cytoplasmic localization and even treatment of the cells with LMB did not trap the E1B-55K mutants in the nucleus (Fig. 9 A; An, Ao, Aq, Ar + Fig. 9 B; Bh, Bi, Bk, Bl).

Here, we could show that K101R influences the subcellular localization of E1B-55K even in the context of viral infection, as E1B-55K K101R seems to facilitate the recruitment of E1B-55K to nuclear structures, most likely VRCs.



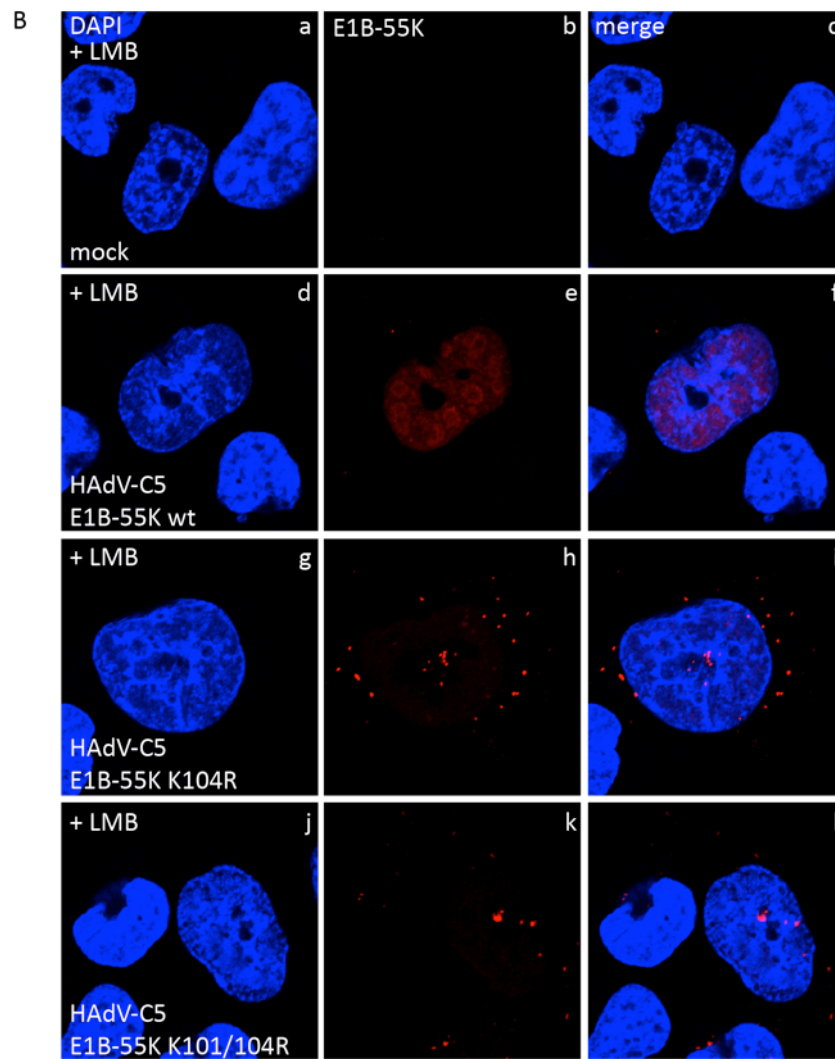


Fig. 9: HAdV-C5 E1B-55K K101R localizes to the nucleus in infection. (A) H1299 cells were infected with HAdV-C5 wt virus (H5pg4100), HAdV-C5 E1B-55K K101R (H5pm4243), HAdV-C5 E1B-55K K104R (H5pm4102), HAdV-C5 E1B-55K K101/104R (H5pm4244) or HAdV-C5 E1B-55K NES (H5pm4101) at a MOI of 15. As a control for the LMB treatment, cells were treated with 2 μ l EtOH for 4 h at 20 h p.t. Cells were fixed 24 h p.i. with 4% PFA and labeled with rat mAb 4E8 (E1B-55K), detected with Cy3-conjugated secondary antibody (red channel). Nuclei were labeled with DAPI. α -E1B-55K (red; Ab, Ae, Ah, Ak, An, Aq, At), DAPI (blue; Aa, Ad, Ag, Aj, Am, Ap, As) and overlay of the single images (merge; Ac, Af, Ai, Al, Ao, Ar, Au) are shown. (B) H1299 cells were infected with HAdV-C5 wt virus (H5pg4100), HAdV-C5 E1B-55K K104R (H5pm4102) or HAdV-C5 E1B-55K K101/104R (H5pm4244) at a MOI of 15. 20 h p.i. cells were treated with 20 nM/ μ l LMB for 4 h. Cells were fixed with 4% PFA 24 h p.i. and labeled with rat mAb 4E8 (E1B-55K), detected with Cy3-conjugated secondary antibody (red channel). Nuclei were labeled with DAPI. α -E1B-55K (red; Bb, Be, Bh, Bk), DAPI (blue; Ba, Bd, Bg, Bj) and overlay of the single images (merge; Bc, Bf, Bi, Bl) are shown.

4.2 HAdV-C5 E1B-55K K101R leads to a “gain-of-function” in transiently transfected cells

4.2.1 HAdV-C5 E1B-55K K101R shows increased repression of p53-stimulated transcription

Several publications have shown before that the multiple functions of E1B-55K are dependent on its SUMOylation [59, 96, 97, 111]. Thus, in a next step we investigated if the higher SUMOylation of E1B-55K K101R affects known functions of E1B-55K.

Repression of the tumor suppressor and transcription factor p53 is one of the main functions of E1B-55K [85]. It has been shown that the acidic amino terminus of p53 is responsible for its function as a transcriptional activator and E1B-55K binds to p53 specifically at this site, inhibiting p53-dependent transcription [76, 190].

To find out whether the K101R mutation alters the functions of E1B-55K on p53, we first investigated the repression of p53-stimulated transcription. Therefore, we performed a dual luciferase assay with p53-negative H1299 cells. We transfected a plasmid encoding the *firefly* luciferase under a CMV promoter downstream of five p53 binding sites and co-transfected it with a plasmid expressing p53 and the different E1B-55K mutant plasmids (Fig. 10).

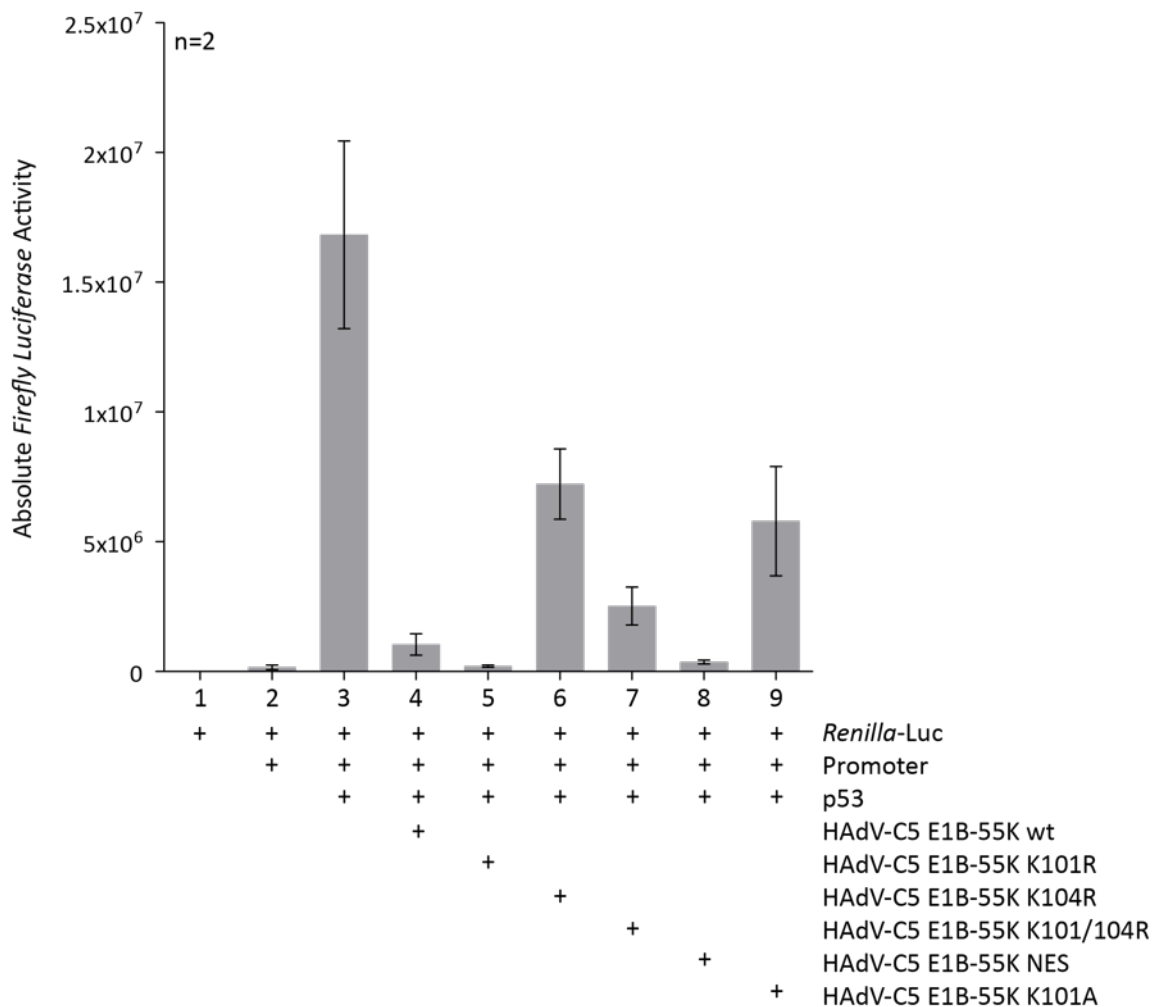


Fig. 10: Repression of p53-stimulated transcription is increased in HAdV-C5 E1B-55K K101R. H1299 cells were transfected with 0.5 μg of HAdV-C5 E1B-55K wt, K101R, K104R, K101/104R, NES or K101A in combination with 0.0015 μg p53, 0.5 μg of a plasmid expressing the *firefly* luciferase gene under control of a CMV promoter downstream of five p53-binding sites and 0.5 μg of a plasmid expressing the *renilla* luciferase. Transfection and measurements were done in triplicates. The activities of both luciferases were measured in a dual luciferase assay 24 h p.t. The mean values with the corresponding SEM of two independent experiments are shown. SEM: standard error of the mean.

As seen in Fig. 10, the p53-induced *firefly* luciferase activity was highly reduced in the presence of E1B-55K wt when compared to the promoter activity only in the presence of p53 (Fig. 10; lanes 3 and 4). Interestingly, E1B-55K K101R was able to repress p53-stimulated transcription even more than the wt protein (Fig. 10; lane 5). This effect is probably due to the high SUMOylation of the E1B-55K K101R mutant, as the also highly SUMOylated NES mutant led as well to a higher repression of promoter activity compared to the wt protein (Fig. 10; lane 8). However, we observed the lowest *firefly* luciferase activity in the presence of E1B-55K K101R (Fig. 10; lane 5). Furthermore, E1B-55K mutants that revealed less or no SUMOylation (E1B-55K K104R, K101/104R and K101A) also

showed a lower repression of p53-stimulated transcription (Fig. 10; lanes 6, 7 and 9).

Taken together, these results further confirm a strong correlation between the SUMOylation of E1B-55K on the repression of p53 transcriptional activity. Moreover, our results support the idea that K101 might be a regulator for E1B-55K SUMOylation at K104, since inactivation of K101 leads to a “gain-of-function”.

4.2.2 HAΔV-C5 E1B-55K K101R leads to enhanced focus formation in pBRK cells

In 1992, it was published that repression of p53-stimulated transcription is a prerequisite for transformation of pBRK cells by the adenoviral oncogenes E1A and E1B-55K [190]. Because we detected an increased inhibition of p53 promoter activity with E1B-55K K101R in section 4.2.1, we wondered if the transformation efficiency was also increased in this mutant. Hence, we performed a transformation assay by transfecting pBRKs with plasmids encoding the E1-Box, comprising E1A and E1B-55K wt or the respective mutants of E1B-55K (Fig. 11). As expected, co-transfection with E1B-55K K101R resulted in an almost 2-fold increase in *focus* formation compared to E1B-55K wt (Fig. 11 A; lanes 3 and 4 + Fig. 11 B; B3 and B4). As expected, loss of SUMOylation in E1B-55K K104R and K101/104R led to a vast reduction of *foci* formation (Fig. 11 A; lanes 5 and 6 + Fig. 11 B; B5 and B6). In contrast, cells transfected with E1B-55K NES produced almost similar amounts of *foci* as the wt, although the protein is highly SUMOylated (Fig. 11 A; lanes 3 and 7 + Fig. 11 B; B3 and B7). Finally, *focus* formation of E1B-55K K101A was also reduced compared to the wt-protein (Fig. 11 A; lane 8 + Fig. 11 B; B8).

Taken together, we showed that the high SUMOylation of E1B-55K K101R is linked to a “gain-of-function” with increased repression of p53-stimulated transcription (4.2.1) and thus increased focus formation in pBRKs.

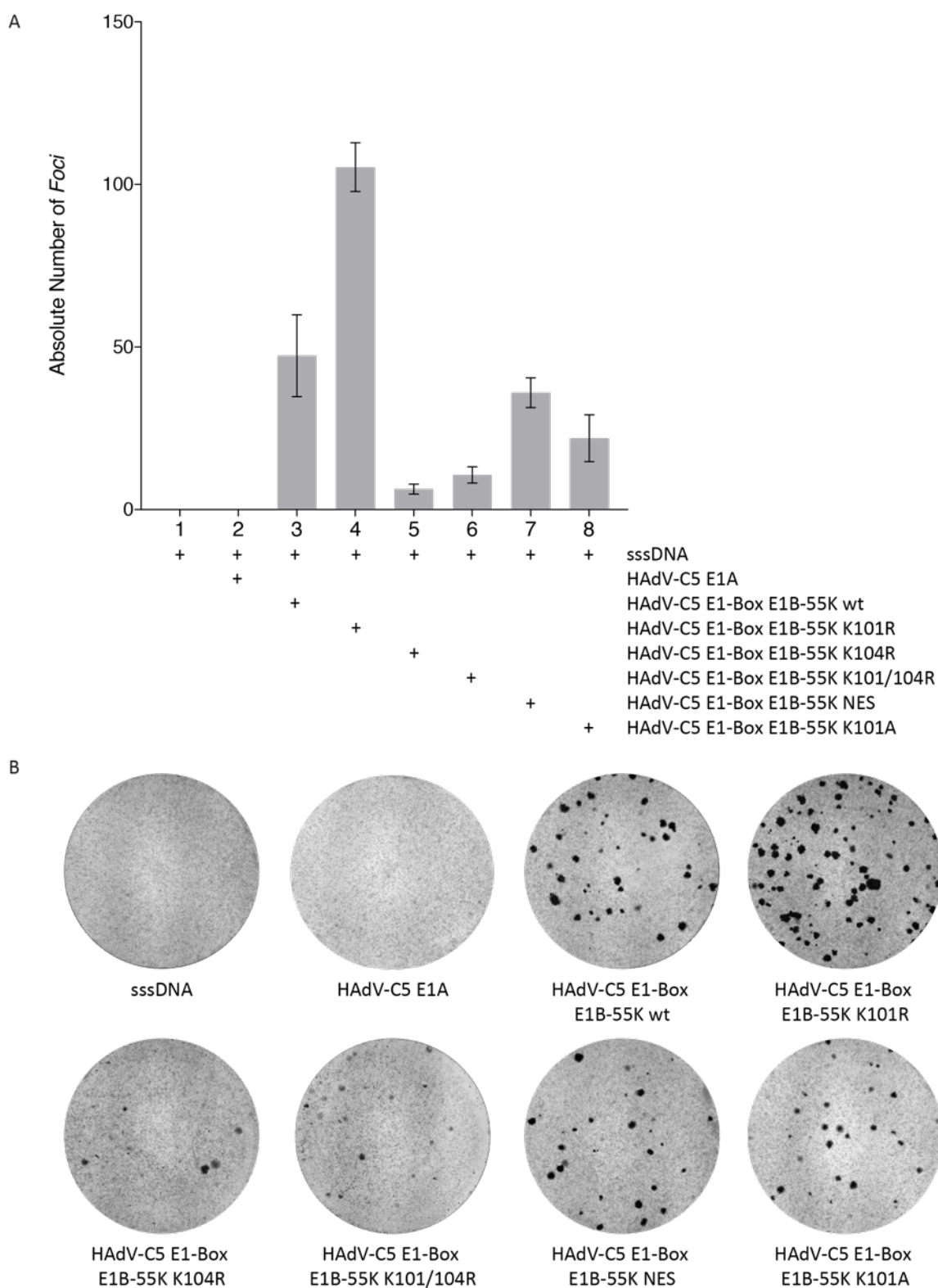


Fig. 11: Focus formation of HAdV-C5 E1B-55K K101R in pBRKs is increased. Primary BRK cells were transfected with 16 μ g of plasmids encoding the E1-Box with HAdV-C5 E1A and HAdV-C5 E1B-55K wt, K101R, K104R, K101/104R, NES or K101A as well as 8 μ g of sssDNA. The experiment was performed in quadruplicates and each transfected 100 mm plate was split into four 100 mm plates at 48 h p.t. The cells were kept in culture for six weeks and afterwards, three plates were fixed with a crystal violet solution (25% MeOH and 1% crystal violet in H₂O). Visible foci were counted. Foci were picked from the fourth plate in order to establish stable cell

lines (data not shown). (A) Mean number of *foci* with SEM from triplicates. (B) Example of a culture plate with *foci*. A representative plate is shown. The results show a representative of three independent experiments. sssDNA: sheared salmon sperm DNA; SEM: standard error of the mean.

4.2.3 Acetylation of HAdV-C5 K101 might downregulate SUMOylation at K104

PTM of proteins often occur at lysine residues. In order to examine whether a protein is indeed modified at a specific lysine, single lysines are often conservatively exchanged to an arginine and subjected to immunoprecipitation experiments. We did the same in HAdV-C5 E1B-55K K101R and surprisingly observed an increase of SUMOylation, while HAdV-C5 E1B-55K K101A led to a reduction of it (4.1.1). Interestingly, PML SUMOylation is regulated through acetylation of a lysine nearby [137]. Furthermore, mutation of a lysine to an arginine (K to R) blocks acetylation, while replacement of a lysine with an alanine or glutamine (K to A or K to Q) mimics acetylation [137, 191]. Therefore, it is conceivable that K101 might affect SUMOylation of E1B-55K via acetylation. To address this question, we exchanged lysine 101 to glutamine (K101Q), and performed a Ni-NTA pulldown assay (Fig. 12). Remarkably, we observed that E1B-55K K101Q is less SUMOylated than the wt protein (Fig. 12; lanes 2 and 6). As shown before we could detect a very high SUMOylation in the K101R mutant and SUMOylation was abrogated in E1B-55K K104R and K101/104R (Fig. 12; lanes 3-5). Finally, no SUMOylation was seen with the empty vector (Fig. 12; lane 1).

The lower SUMOylation of HAdV-C5 E1B-55K K101Q might indicate that K101 is negatively affecting E1B-55K SUMOylation through acetylation. However, further experiments using mass spectrometry as well as antibodies detecting acetylated lysines need to be performed to further validate this preliminary result.

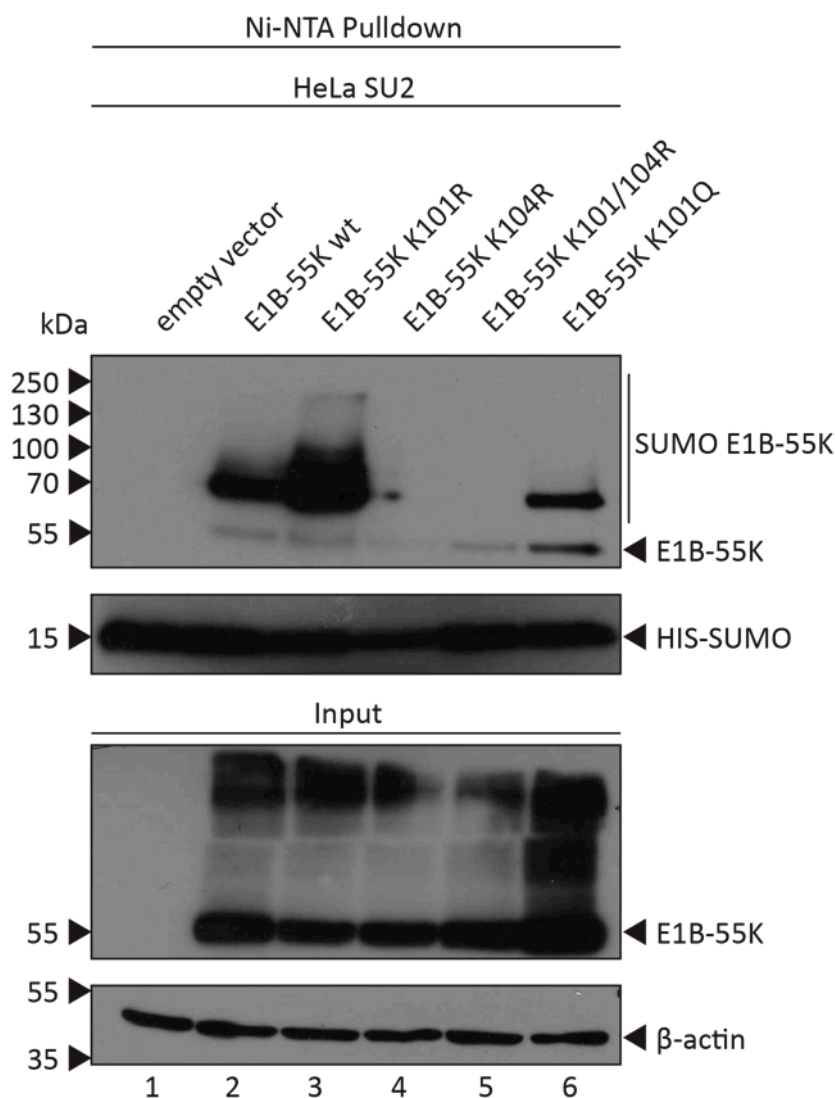


Fig. 12: SUMOylation of HAdV-C5 E1B-55K K101Q is decreased. HeLa cells stably overexpressing 6-His-tagged SUMO-2 were transfected with HAdV-C5 E1B-55K wt, K101R, K104R, K101/104R or K101Q. Cells were harvested 48 h p.t and Ni-NTA purification of 6-His SUMO conjugates was performed. Proteins were separated by SDS-PAGE and subjected to immunoblotting. Protein levels of input and Ni-NTA purified proteins were detected using mAb AC-15 (β -actin), mAb 2A6 (E1B-55K) and mAb 6-His (His). Molecular weights in kDa are indicated on the left, detected proteins on the right.

4.3 SUMOylation of E1B-55K is conserved amongst HAdV species

4.3.1 K101 is specific for E1B-55K of species C HAdV

Most studies on E1B-55K were performed with HAdV-C5. However, in the last years more and more studies have been published that focused on the large E1B-proteins from other HAdV species. They all have a molecular mass of about 55 kDa and for the sake of simplicity will be referred to as E1B-55K. Amongst

others, it has been shown that the E3-Ubiquitin-ligase complex of E1B-55K and E4orf6 is highly conserved between different HAdV species, but that they differ in their target specificity [100, 101]. In contrast, aggresome formation of E1B-55K is not conserved [103]. Although it has been shown in many publications and in this work that SUMOylation is an important regulator of HAdV-C5 E1B-55K functions, no study ever focused on the SUMOylation of E1B-55K from other HAdV species. Since it is known that proteins are mainly SUMOylated at a consensus motif, we first aligned one representative E1B-55K protein from each species A-F and compared them with the HAdV-C5 E1B-55K (Fig. 13).

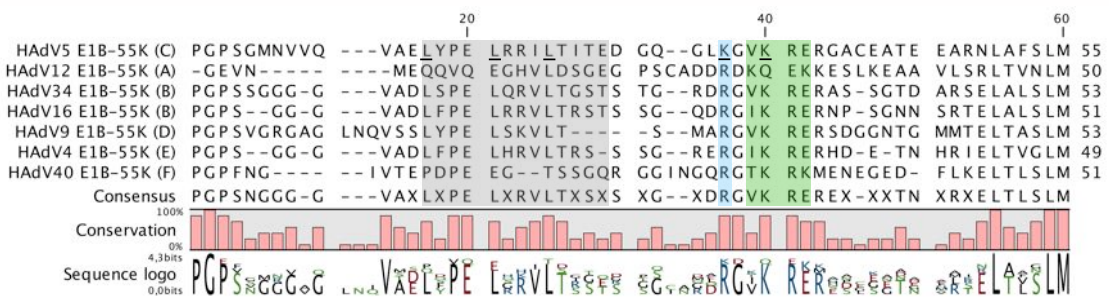


Fig. 13: Alignment of large E1B proteins from different HAdV species. Amino acid (aa) alignment of E1B-55K proteins with one representative from each species A-F. Types and species are indicated on the left. HAdV-C5 is shown on the top row and aa marking the functional sites are underlined. The sequences aligning with the SCM of HAdV-C5 are boxed in green, aa aligning with K101 are boxed in blue and the sites aligning to HAdV-C5 NES are boxed in gray. SCM: SUMO conjugation motif; NES: nuclear export signal.

As seen in Fig. 13, the classic SCM ($PKx E/D$) found in species C was highly conserved among the different HAdV species (Fig. 13; green box). Only HAdV-A12 E1B-55K and HAdV-F40 did not possess a consensus SCM at this specific site (Fig. 13; green box, second row and last row). Surprisingly, the K101 we identified in HAdV-C5 E1B-55K was only present in species C and all the other species revealed an arginine at the corresponding position (Fig. 13; blue box). Finally, the leucine-rich NES of HAdV-C5 E1B-55K was also only present in this species. All of the other species except HAdV-A12 and HAdV-F40 had conserved leucines at positions 83, 87 and 91. However, all of them were missing the isoleucines at positions 90 and 93, decreasing the score for a putative NES motif (Fig. 13; grey box). We additionally performed an *in-silico* analysis of all the E1B proteins using the algorithm *GPS-SUMO* to look for other SCM in the different E1B-55K [182, 183]. In this analysis, we did not find any other consensus SCM in E1B-55K from HAdV-C5, -B34, -B16 and -E4. HAdV-D9 revealed two SCMs, the one we highlighted in Fig. 13 and another one around

lysine 296. For HAdV-F40, several non-consensus SCMs were found (data not shown).

4.3.2 E1B-55K from different HAdV species are highly SUMOylated at a conserved SCM

Discovering that E1B-55K from almost all species possess a SCM and moreover that K101 is unique to HAdV-C, we decided to analyze the SUMOylation of the putative E1B-55K SCM in the other species. Therefore, we generated mutants of the lysine in the putative SCM by replacing it with an arginine. These constructs were transfected in HeLa cells either stably overexpressing 6-His SUMO-1 or 6-His SUMO-2 and the SUMOylation of the different E1B-55K proteins was detected by a Ni-NTA pulldown assay (Fig. 14 and Fig. 15).

As seen in Fig. 14, SUMOylation by SUMO-2 is highly conserved between HAdV species. No SUMOylation of E1B-55K was detected in the HeLa parental cell line or in the empty vector controls (Fig. 14 A; lanes 1-16 + Fig. 14 B; lane 1). Remarkably, almost all E1B proteins were highly SUMOylated and we observed very high SUMO-2 conjugation in HAdV-C5 E1B-55K K101R, HAdV-D9 E1B-55K wt, HAdV-B16 E1B-55K wt, HAdV-B34 E1B-55K wt and HAdV-F40 E1B-55K wt (Fig. 14 B; lanes 6, 7, 11, 13 and 15). SUMOylation of HAdV-E4 E1B-55K wt was similar to HAdV-C5 E1B-55K wt (Fig. 14 B; lanes 2 and 4). Moreover, SUMOylation of HAdV-A12 E1B-55K wt was very low and mutation of the lysine did not alter the SUMOylation of the protein (Fig. 14 B; lanes 9 and 10). This observation was expected since HAdV-A12 E1B-55K wt does not contain a SCM. In contrast, we could detect the lysine in HAdV-F40 E1B-55K as the main SUMOylation site of the protein, although it does not belong to a consensus SCM (Fig. 14 B; lanes 16). For this and all the other HAdV species, inactivation of the SCM led to a loss of SUMOylation (Fig. 14 B; lanes 3, 5, 12, 14 and 16), indicating that the mutated amino acids in the SCM are responsible for the SUMOylation of E1B-55K in the different species assayed. Interestingly, only reduced SUMOylated protein could be detected in HAdV-D9 E1B-55K K103R, which can be explained by the second SCM we found in the *in-silico* analysis. However, the strong reduction in SUMOylation of the K103R mutant suggests that the main SCM is around this lysine (Fig. 14 B; lanes 7 and 8).

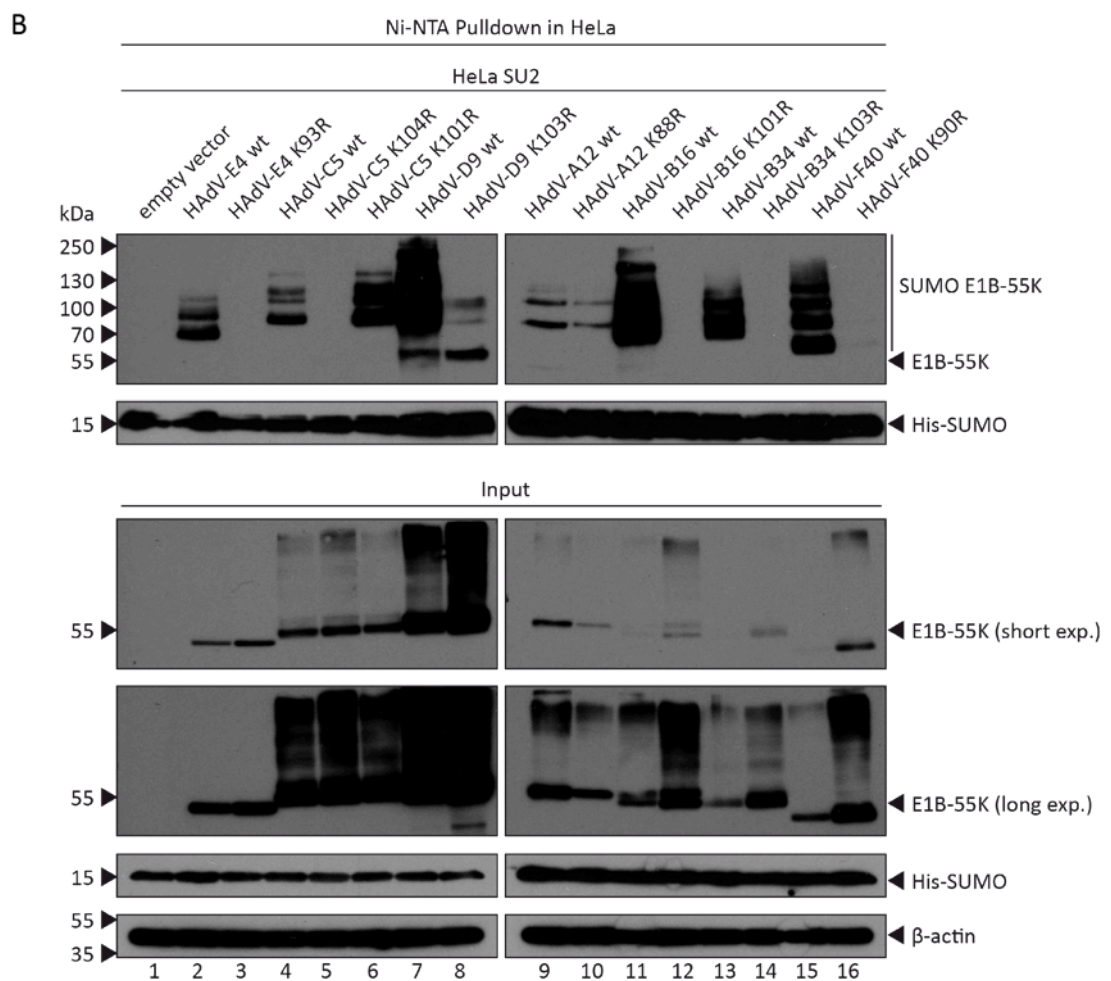
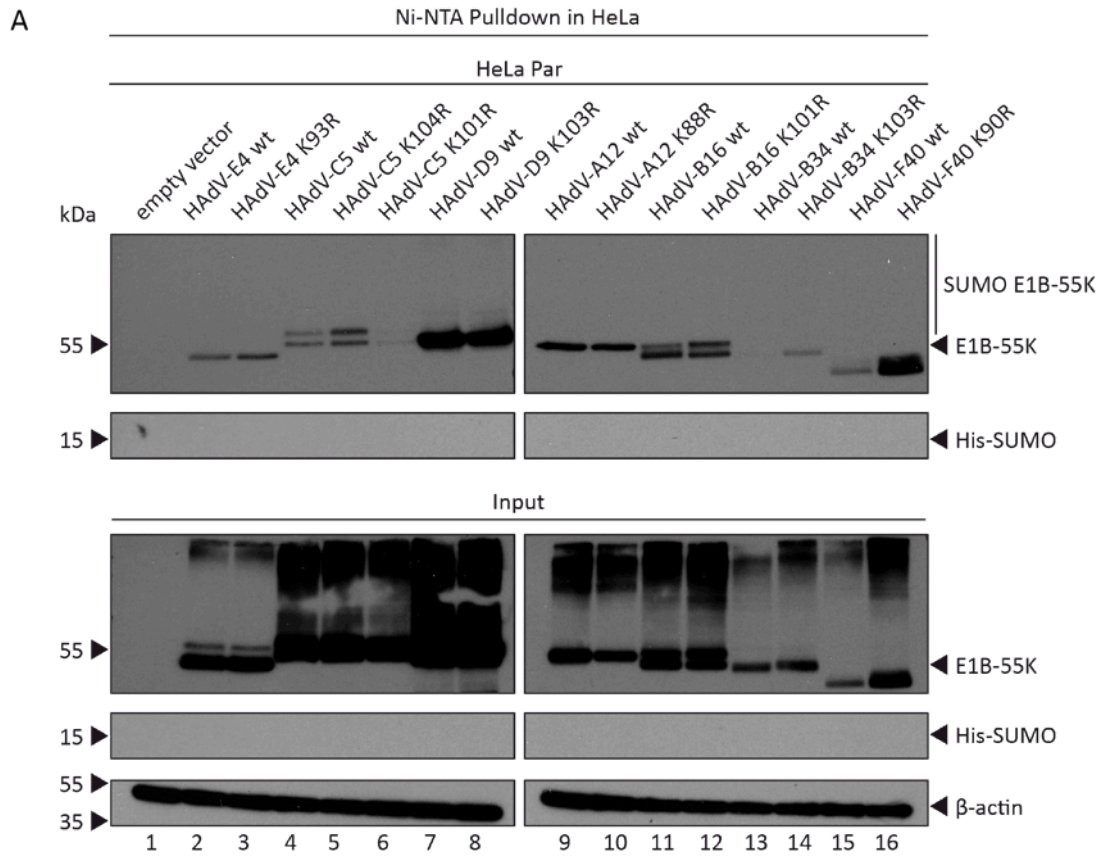


Fig. 14: SUMO-2 conjugation of E1B-55K is highly conserved among most HAdV species (A) HeLa parental cells and (B) HeLa cells stably overexpressing 6-His-tagged SUMO-2 were transfected with HAdV-E4 E1B-55K wt and K93R, HAdV-C5 E1B-55K wt, K104R and K101R, HAdV-D9 E1B-55K wt and K103R, HAdV-A12 E1B-55K wt and K88R, HAdV-B16 E1B-55K wt and K101R, HAdV-B34 E1B-55K wt and K103R or HAdV-F40 E1B-55K wt and K90R. Cells were harvested 48 h p.t. and Ni-NTA purification of 6-His SUMO conjugates was performed. Proteins were separated by SDS-PAGE and subjected to immunoblotting. Protein levels of input and Ni-NTA purified proteins were detected using mAb AC-15 (β -actin), mAb 3F10 (HA/E1B-55K) and mAb 6-His (His). Molecular weights in kDa are indicated on the left, detected proteins on the right. The blot represents the result of several repeated experiments.

In contrast, analysis of Ni-NTA purified His-SUMO-1-conjugates revealed that SUMOylation with this isoform is not conserved among the different HAdV species tested in this work. No SUMOylation of E1B-55K was detected in the HeLa parental cell line or in the empty vector controls (Fig. 15 A; lanes 1-16 + Fig. 15 B; lane 1). As shown before, SUMOylation of HAdV-C5 E1B-55K K101R was increased, while it was completely abolished in the K104R mutant (Fig. 15 B; lanes 5 and 6). Only the E1B-55K wt proteins from HAdV-E4, HAdV-B34, HAdV-D9, and HAdV-B16 were found SUMOylated by SUMO-1, the last two being the ones that presented the highest His-SUMO-1 conjugation level (Fig. 15 B; lanes 2, 7, 11 and 13). Accordingly, their respective SCM mutants presented no SUMOylation by SUMO-1 (Fig. 15 B; lanes 3, 5, 8, 12, 14). The E1B-55K proteins from HAdV-A12 and HAdV-F40, as well as their corresponding SCM mutants, however, were not SUMOylated by SUMO-1 (Fig. 15 B; lanes 9 and 10, 15 and 16). SUMOylation of HAdV-C5 E1B-55K wt by SUMO-1 was not detected in our experimental settings, probably due to different cell lines and assays, although it has been shown to be SUMOylated by SUMO-1 [75] (Fig. 15 B; lane 4).

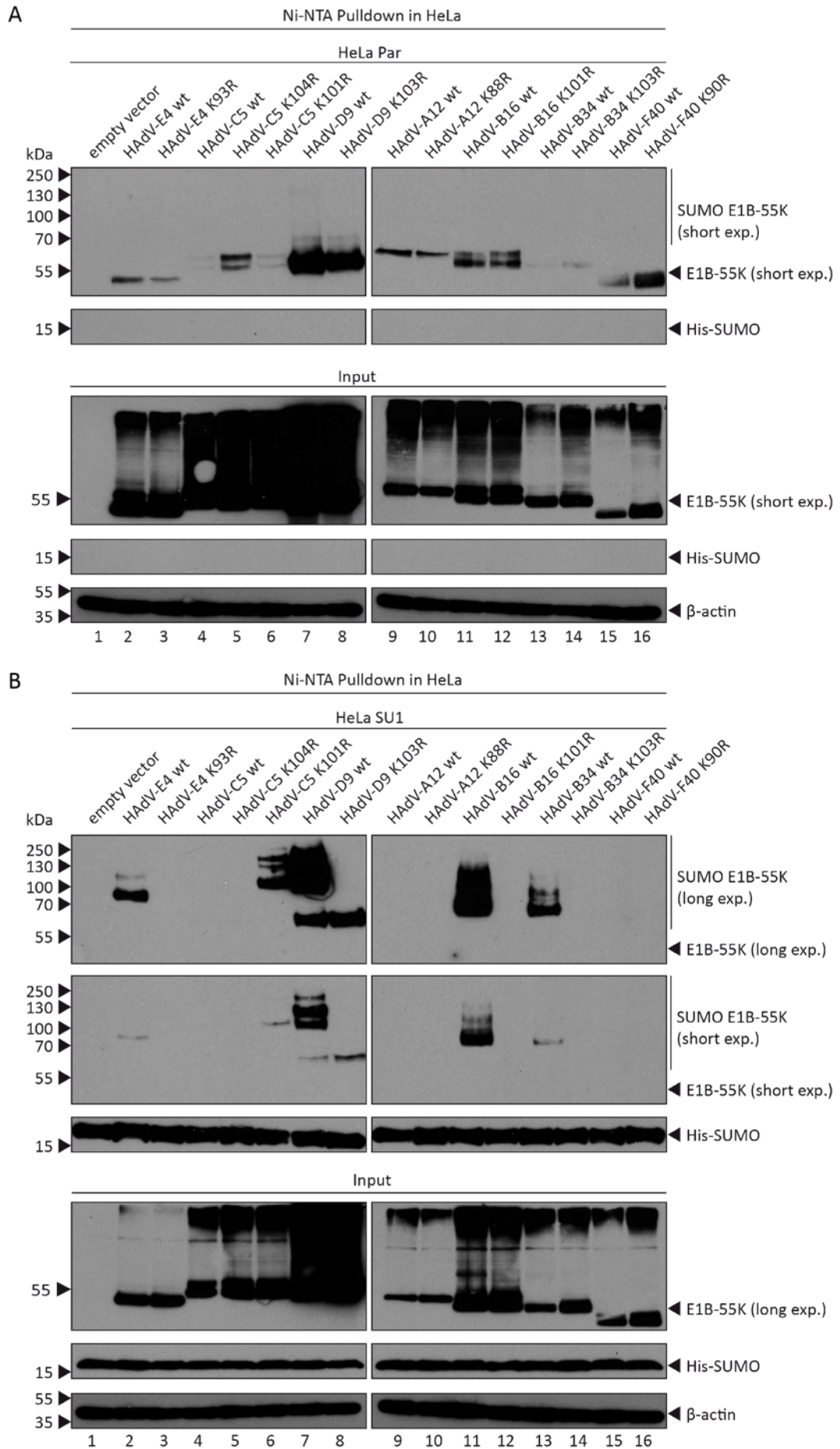


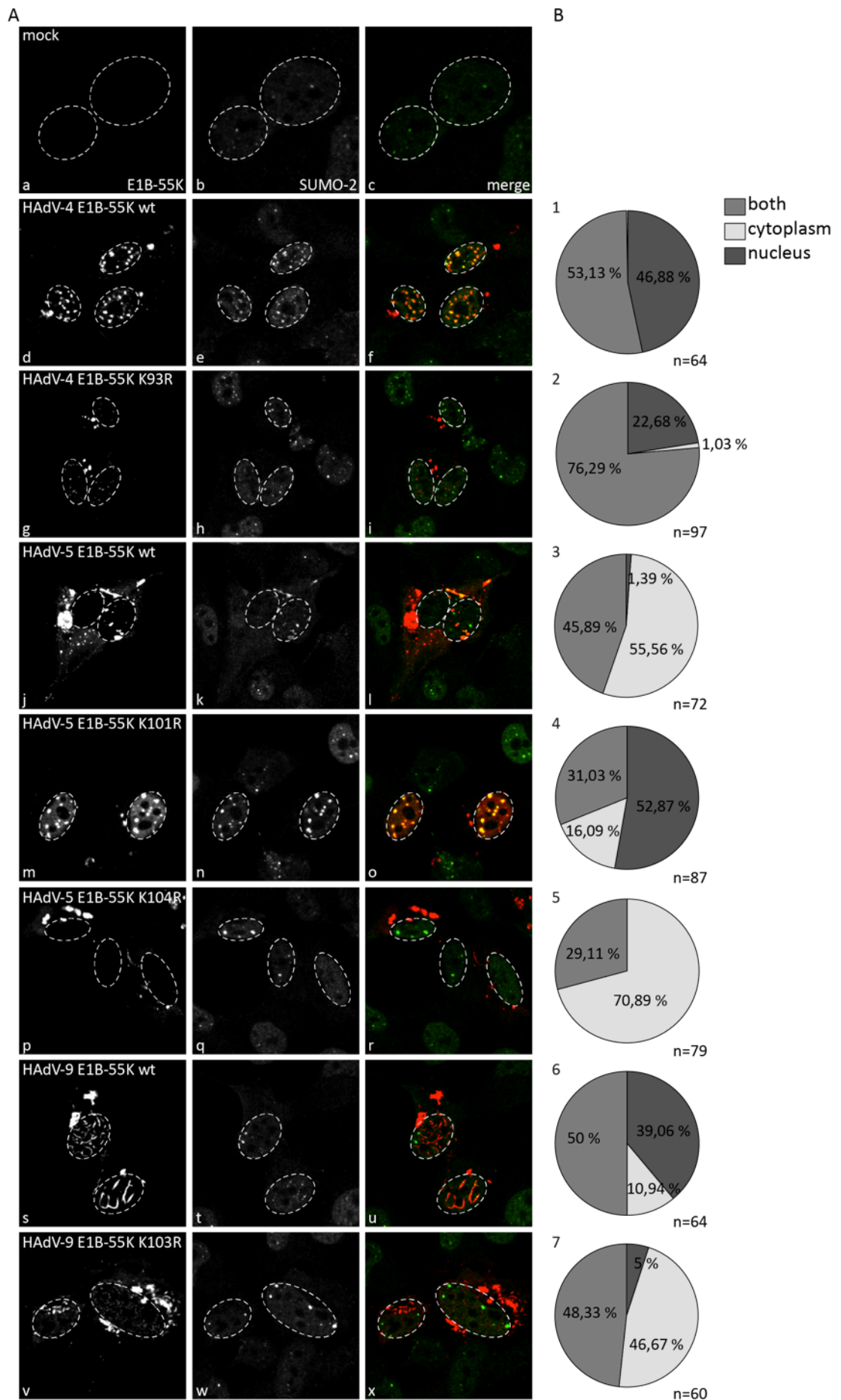
Fig. 15: SUMO-1 conjugation of E1B-55K is not conserved among HAdV species (A) HeLa parental cells and (B) HeLa cells stably overexpressing 6-His-tagged SUMO-1 were transfected with HAdV-E4 E1B-55K wt and K93R, HAdV-C5 E1B-55K wt, K104R and K101R, HAdV-D9 E1B-55K wt and K103R, HAdV-A12 E1B-55K wt and K88R, HAdV-B16 E1B-55K wt and K101R, HAdV-B34 E1B-55K wt and K103R or HAdV-F40 E1B-55K wt and K90R. Cells were harvested 48 h p.t. and Ni-NTA purification of 6-His SUMO conjugates was performed. Proteins were separated by SDS-PAGE and subjected to immunoblotting. Protein levels of input and Ni-NTA purified proteins were detected using mAb AC-15 (β -actin), mAb 3F10 (HA/E1B-55K) and mAb 6-His (His). Molecular weights in kDa are indicated on the left, detected proteins on the right. The blot represents the result of several repeated experiments.

Next, we wanted to further investigate the regulatory role of K101 in HAdV-C5 E1B-55K. Therefore, we mutated the arginine to a lysine in the other HAdV species, which corresponds to the K101 residue in HAdV-C5 E1B-55K. We again performed a Ni-NTA pulldown to see whether SUMOylation of these mutants is decreased. Surprisingly, this mutation did not alter the SUMOylation of E1B-55K from the other HAdV species (data not shown).

Taken together, we identified a conserved SCM of E1B-55K in almost all HAdV-species and could show that these proteins are highly SUMOylated specifically in this motif. Furthermore, we could show that K101 and its regulatory functions are specific for HAdV-C5 E1B-55K.

4.3.3 Nuclear localization of E1B-55K from different HAdV species is dependent on SUMOylation

As described in 4.1.2, we observed a mainly nuclear localization of HAdV-C5 E1B-55K in cells transfected with the highly SUMOylated K101R mutant when compared to the wt-protein, indicating that SUMOylation regulates the subcellular localization of E1B-55K. Since almost all E1B proteins from other HAdV species are highly SUMOylated as well, we analyzed their localization by immunofluorescence experiments. Therefore, we transfected H1299 cells with HA-tagged E1B-55K from different HAdV species as well as their respective SUMO mutants (Fig. 16). We not only stained the cells for E1B-55K but also for SUMO-2 to further analyze the co-localization of SUMOylated proteins.



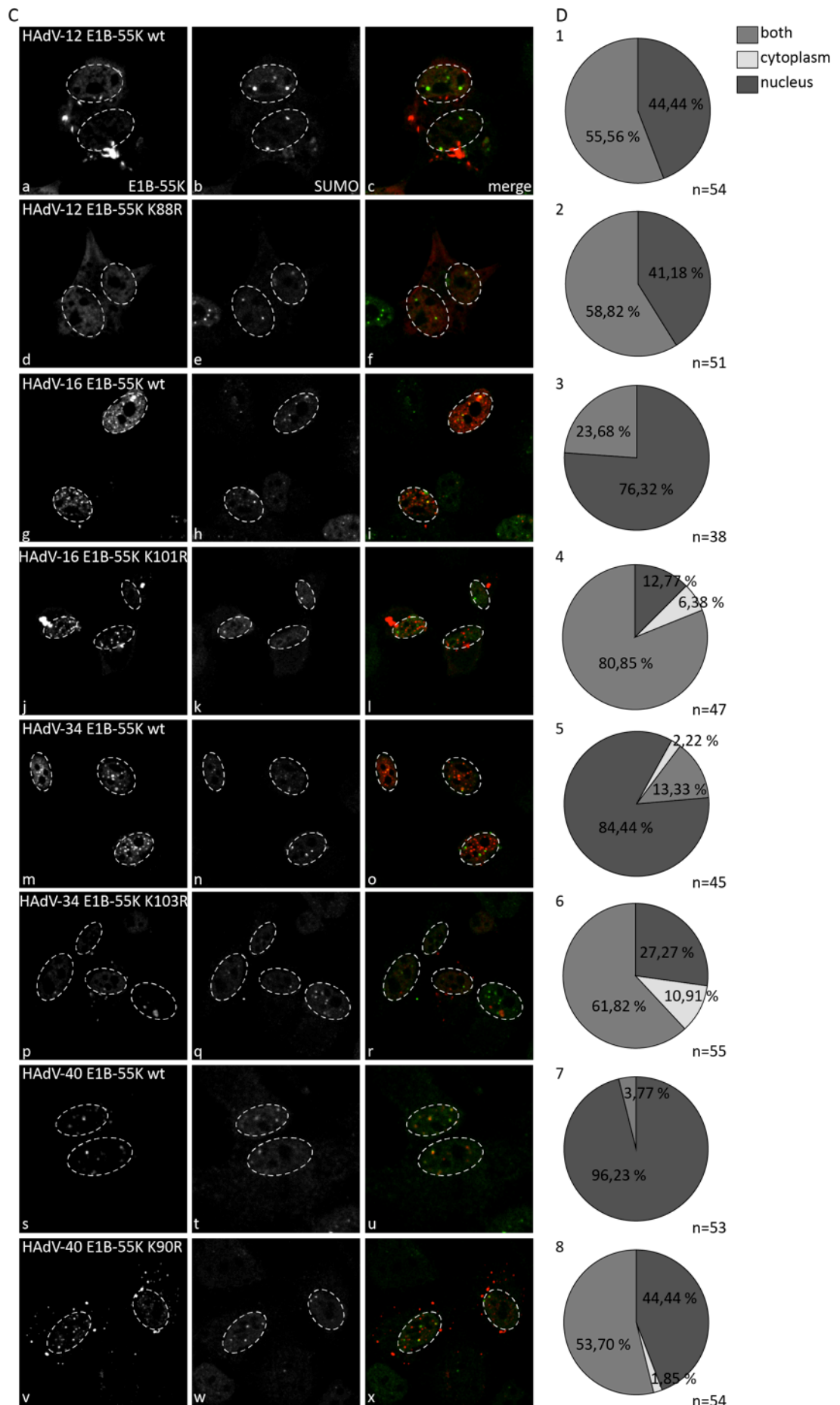


Fig. 16: E1B-55K from different HAdV species localizes mainly in the nucleus. (A+C) H1299 cells were transfected with plasmids encoding HAdV-E4 E1B-55K wt and K93R, HAdV-C5 E1B-55K wt, K104R and K101R, HAdV-D9 E1B-55K wt and K103R, HAdV-A12 E1B-55K wt and K88R, HAdV-B16 E1B-55K wt and K101R, HAdV-B34 E1B-55K wt and K103R or HAdV-F40 E1B-55K wt and K90R. 24 h p.t. cells were fixed with 4% PFA and labeled with rat mAb 3F10 (HA/E1B-55K), detected with Cy3-conjugated secondary antibody (red channel) and rabbit pAb SUMO-2/3 (SUMO-2), detected with Alexa488-conjugated secondary antibody (green channel). Nuclei are indicated by the dotted lines. α -HA (red; Aa, Ad, Ag, Aj, Am, Ap, As, Av, Ca, Cd, Cg, Cj, Cm, Cp, Cs, Cv), α -SUMO-2 (green; Ab, Ae, Ah, Ak, An, Aq, At, Aw, Cb, Ce, Ch, Ck, Cn, Cq, Ct, Cw) and overlay of the single images (merge; Ac, Af, Ai, Al, Ao, Ar, Au, Ax, Cc, Cf, Ci, Cl, Co, Cr, Cu, Cx) are shown. (B+D) Statistical analysis of the captured phenotypes (n). The phenotype that represents the majority of analyzed cells is shown in (A+C).

As seen in Fig. 16, no E1B-55K was detected in the mock control (Fig. 16 A; Aa). As previously shown, HAdV-C5 E1B-55K wt was seen mainly in the cytoplasm in 55.56 % of the cells and the SUMO mutant HAdV-C5 E1B-55K K104R was detected in the cytoplasm even in 70.89 % of the cells (Fig. 16 A; Aj, Al, Ap and Ar + Fig. 16 B; B3 and B5). Again, HAdV-C5 E1B-55K K101R was mainly detected in the nucleus in 52.87 % of the cells and only 16.09 % revealed a cytoplasmic localization of the protein (Fig. 16 A; Am and Ao + Fig. 16 B; B4). In cells transfected with HAdV-E4 E1B-55K wt, the protein was found in both cellular compartments in 53.13 % of the cells, with the largest fraction of the protein present in the nucleus (nuclear > cytoplasm) (Fig. 16 A; Ad and Af + Fig. 16 B; B1). HAdV-E4 E1B-55K wt was even detected exclusively in the nucleus in 46.88 % of the analyzed cells (Fig. 16 B; B1). In contrast, HAdV-E4 E1B-55K K93R was found in both cellular compartments in 76.29 % of the cells, but the largest fraction of the protein was detected in the cytoplasm (nuclear < cytoplasm) (Fig. 16 A; Ag and Ai + Fig. 16 B; B2). Here, restricted nuclear localization was only observed in 22.68 % of the cells (Fig. 16 B; B2). HAdV-D9 E1B-55K was observed in both cellular compartments in the wt protein (50 %) as well as in the K103R mutant (48.33 %) (Fig. 16 A; As, Au, Av and Ax + Fig. 16 B; B6 and B7). However, the largest fractions of the protein were found in the nucleus in HAdV-D9 E1B-55K wt (nuclear > cytoplasm) and 39.06 % of the cells revealed a solely nuclear localization (Fig. 16 A; As + Fig. 16 B; B6). Conversely, HAdV-D9 E1B-55K K103R was merely detected in the cytoplasm in 46.67 % of the cells (Fig. 16 A; Av + Fig. 16 B; B7). Interestingly, HAdV-D9 E1B-55K wt formed track-like structures in the nucleus that were not observed in HAdV-D9 E1B-55K K103R or in any other E1B protein from other HAdV species (Fig. 16 A; As and Au). Different from all the other HAdV species, HAdV-A12 E1B-55K revealed the same nucleo-cytoplasmic localization of the protein in cells

transfected with the wt protein (55.56 %) and the K88R mutant (58.82 %) (Fig. 16 C; Ca, Cc, Cd and Cf + Fig. 16 D; D1 and D2). This is in concordance with the fact that HAdV-A12 E1B-55K does not contain a SCM and the protein is only SUMOylated to a very low extent. Transfection with HAdV-B16 E1B-55K wt led to a nuclear localization of the protein in 76.32 % of the cells (Fig. 16 C; Cg and Ci + Fig. 16 D; D3). However, HAdV-B16 E1B-55K K101R was present in the nucleus only in 12.77 % of the cells and the protein was rather found in both cellular compartments (80.85 %) (Fig. 16 C; Cj and Cl + Fig. 16 D; D4). Similar results were obtained for HAdV-B34 and HAdV-F40. Here, E1B-55K wt was almost exclusively detected in the nucleus in 84.44 % and 96.23 % of the cells, respectively (Fig. 16 C; Cm, Co, Cs and Cu + Fig. 16 D; D5 and D7). Mutation of the SCM led to a shift of the protein into the cytoplasm and HAdV-B34 E1B-55K K103R as well as HAdV-F40 E1B-55K K90R were then seen in both cellular compartments (61.82 % and 53.70 %, respectively) (Fig. 16 C; Cp, Cr, Cv and Cx + Fig. 16 D; D6 and D8).

In summary, these results show that highly SUMOylated E1B-55K from several HAdV species mainly localize in the nucleus similar to the observations made for HAdV-C5 E1B-55K K101R. In this line and in agreement with previous results of this work, loss of SUMOylation shifted these E1B-55K proteins into the cytoplasm. Taken together, these results suggest that SUMOylation is an important regulator of E1B-55K subcellular localization not only in HAdV-C5 but also in other HAdV species.

After we have observed a change of E1B-55K subcellular localization from almost all HAdV species upon inactivation of the SCM, we examined their co-localization with SUMO-2. Thus, we counted the number of cells that revealed a clear co-localization of E1B-55K and SUMO-2 (Fig. 16). Only cells that showed no co-localization of E1B-55K and SUMO-2 at all were counted as negative. Hence, cells with a partial co-localization signal between E1B-55K and SUMO-2 were counted as positive. The results of the analysis are displayed in Fig. 17.

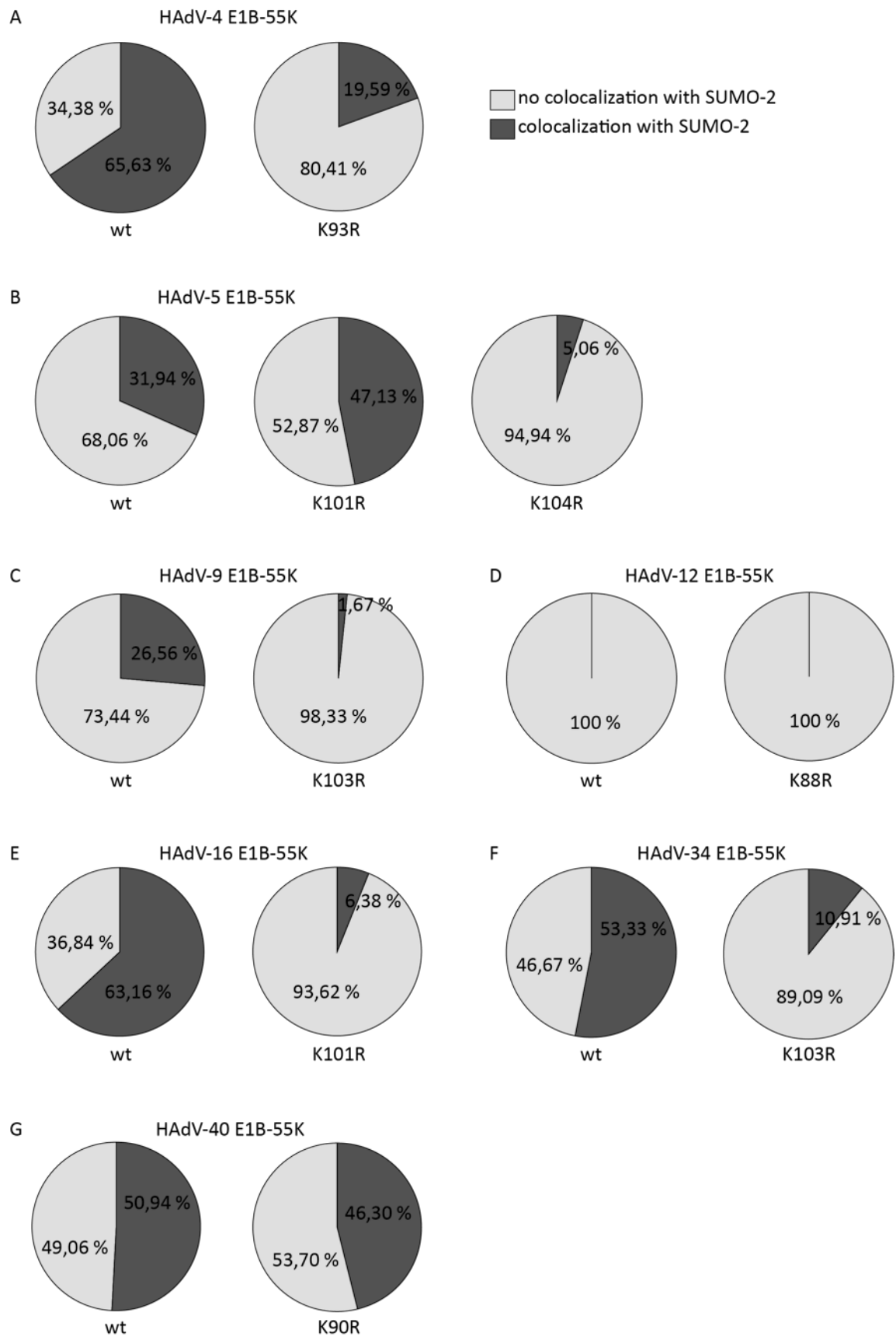


Fig. 17 E1B-55K of HAdV species co-localize with SUMO-2. Transfected cells from 4.3.3 (Fig. 16; n) were counted according to the co-localization of E1B-55K and SUMO-2 signals. The percentage of positive and negative cells was calculated. Cells that showed partial or complete co-localization of E1B-55K with SUMO-2 were counted as positive. Remaining cells were

counted as negative. The pie charts represent the distribution of cells with (dark grey) and without (light grey) co-localization of E1B-55K and SUMO-2. (A) HAdV-E4 E1B-55K wt and K93R (B) HAdV-C5 E1B-55K wt, K101R and K104R (C) HAdV-D9 E1B-55K wt and K103R (D) HAdV-A12 E1B-55K wt and K88R (E) HAdV-B16 E1B-55K wt and K101R (F) HAdV-B34 E1B-55K wt and K103R (G) HAdV-F40 E1B-55K wt and K90R.

Co-localization of transfected SUMO-2 and HAdV-C5 E1B-55K was detected in 31.94% of the cells in case of the wt-protein and even in 47.13% after K101R mutant transfection (Fig. 17 B). In contrast, only 5.06 % of the cells revealed a co-localization of E1B-55K and SUMO-2 in HAdV-C5 E1B-55K K104R (Fig. 17 B). For HAdV-E4 E1B-55K wt a co-localization with SUMO-2 was observed in 65.63 % of the cells, whereas for the HAdV-E4 E1B-55K K93R mutant this was only seen in 19.59 % of the cells (Fig. 17 A). Similar results were obtained for HAdV-D9 E1B-55K where co-localization was seen in 26.56 % of the cells with the wt protein and only in 1.67 % with the K103R mutant (Fig. 17 C). Both HAdV-B16 and HAdV-B34 E1B-55K revealed a strong co-localization with SUMO-2 in cells transfected with the wt protein, namely 63.16 % and 53.33 %, respectively (Fig. 17 E and F). Additionally, inactivation of the SCM led to a vast reduction of co-localization to 6.38 % for HAdV-B16 E1B-55K K101R and 10.91 % for HAdV-B34 K103R (Fig. 17 E and F). Interestingly, co-localization of E1B-55K and SUMO-2 was almost similar in HAdV-F40 E1B-55K wt with 50.94 % and HAdV-F40 E1B-55K K90R with 46.30 % (Fig. 17 G). As expected, no co-localization of E1B-55K and SUMO-2 was observed in HAdV-A12, neither with HAdV-A12 E1B-55K wt nor with HAdV-A12 E1B-55K K88R (Fig. 17 D).

These results showed a markedly reduction of the co-localization between E1B-55K from several HAdV species and SUMO-2 upon SCM inactivation, which is in line with the results obtained from pulldown experiments (4.3.2). Taken together, these results further confirmed that E1B-55K proteins from most HAdV species are SUMOylated at a highly conserved SCM as mutation of this site leads to loss of SUMOylation accompanied by subcellular relocalization of these proteins.

4.3.4 Several E1B-55K proteins from HAdV species are able to repress p53- stimulated transcription in a SUMO-dependent manner

We have observed earlier in this work that high SUMOylation of HAdV-C5 E1B-55K K101R led to a “gain-of-function” regarding the repression of

p53-activated transcription, showing that this function of E1B-55K on p53 is strongly regulated by SUMOylation (4.2.1). Besides, it has been shown before that repression of p53 by E1B-55K is highly conserved among the different HAdV species. Cheng *et al.* could show that all E1B proteins, except HAdV-E4 E1B-55K, were able to repress p53-stimulated transcription [101]. Thus, we wanted to investigate whether SUMOylation of E1B-55K from other HAdV species is also able to regulate E1B-55K repression of p53-activated transcription. Therefore, we performed a dual luciferase assay as described in 4.2.1 but with E1B-55K wt and the respective SUMO mutants from different HAdV species.

In Fig. 18, the absolute *firefly* luciferase activity (= promoter activity) is shown. No promoter activity was observed with *renilla* luciferase or the promoter alone (Fig. 18 A; left and middle lane). In the presence of p53, we observed a strong promoter activity, serving as a positive control (Fig. 18 A; right lane). As shown in previous experiments, HAdV-C5 E1B-55K wt was able to reduce p53-dependent promoter activity, which was even greater when the K101R mutant was transfected (Fig. 18 B; left and right lane). As described before, HAdV-C5 E1B-55K K104R was not able to repress p53-stimulated transcription (Fig. 18 B; middle lane). Regarding the other HAdV species, similar results were obtained for HAdV-B16 and HAdV-F40 E1B-55K. Here, a strong reduction of promoter activity was seen for the wt proteins (Fig. 18 F and H; left lanes). Mutation of their SCM prevented inhibition of p53 transactivation shown by higher promoter activity compared to their wt proteins (Fig. 18 F and H; right lanes). However, HAdV-D9 E1B-55K wt strongly repressed the promoter activity, which was only slightly decreased in HAdV-D9 E1B-55K K103R (Fig. 18 D). For HAdV-E4 E1B-55K wt we observed a weaker repression of p53-stimulated transcription compared to HAdV-C5 and there was a slight difference between the wt protein and the SCM mutant (HAdV-E4 E1B-55K K93R) (Fig. 18 C). Moreover, both HAdV-A12 E1B-55K wt and its SCM mutant (K88R) showed rather low repression of p53-stimulated transcription (Fig. 18 E). Interestingly, we detected a strong repression of promoter activity for both the HAdV-B34 E1B-55K wt and its SCM mutant (K103R), although the mutant is not SUMOylated anymore and showed a different localization (Fig. 18 G). This might suggest that HAdV-B34 E1B-55K uses a SUMO-independent mechanism to repress p53-stimulated transcription.

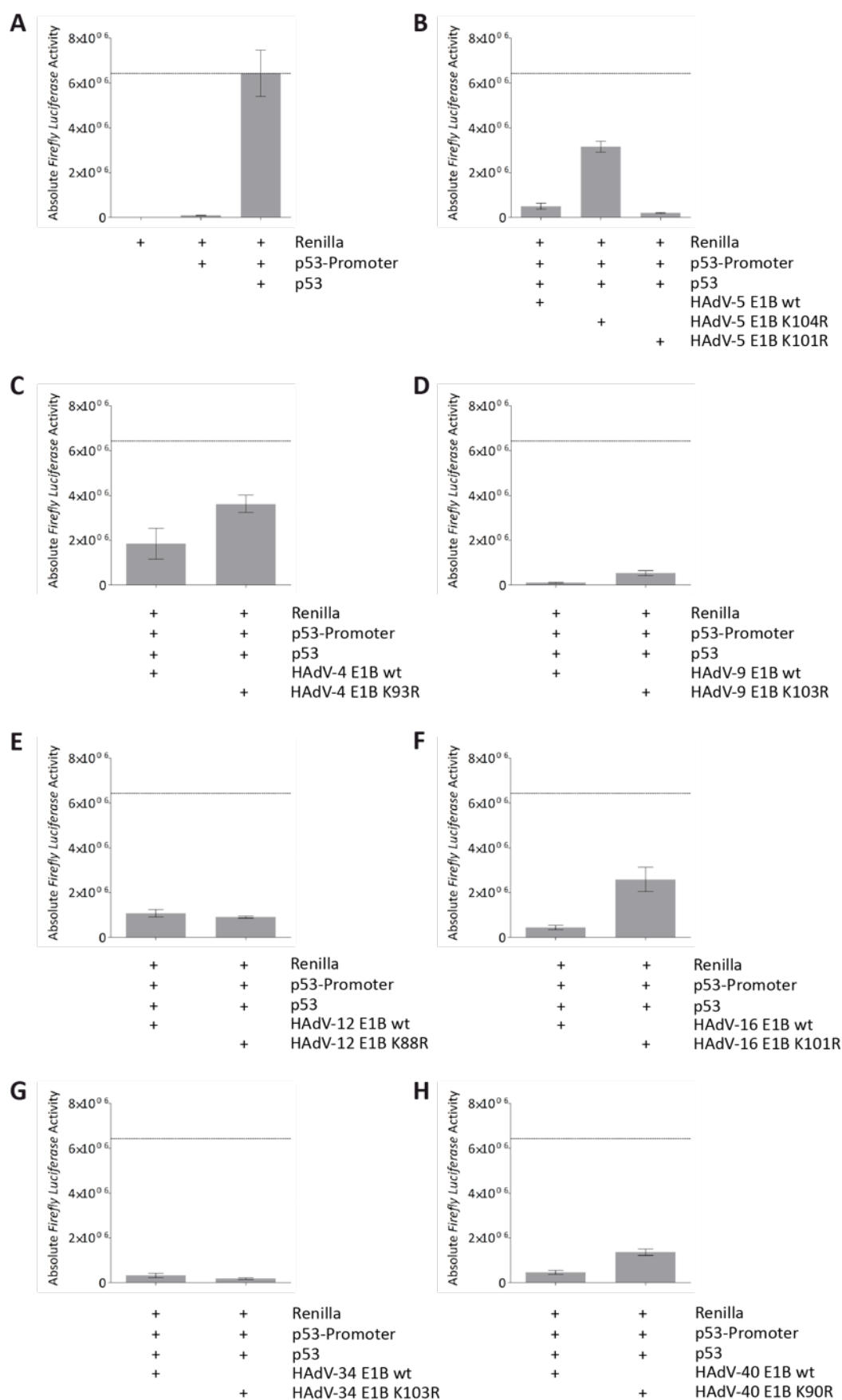


Fig. 18 Repression of p53-stimulated transcription is mainly dependent on SUMOylation. H1299 cells were transfected with 0.5 μ g of HAAdV-E4 E1B-55K wt and K93R, HAAdV-C5 E1B-55K wt, K104R and K101R, HAAdV-D9 E1B-55K wt and K103R, HAAdV-A12 E1B-55K wt and

K88R, HAdV-B16 E1B-55K wt and K101R, HAdV-B34 E1B-55K wt and K103R or HAdV-F40 E1B-55K wt and K90R in combination with 0.0015 μg p53, 0.5 μg of a plasmid expressing the *firefly* luciferase gene under control of a CMV promoter downstream of five p53-binding sites and 0.5 μg of a plasmid expressing the *renilla* luciferase. Transfection and measurements were done in triplicates. The activities of both luciferases were measured in a dual luciferase assay 24 h p.t. The graphs correspond to one representative experiment and show the mean values with SEM. The dashed line represents the value of the positive control shown in (A). SEM: standard error of the mean.

In summary, we could confirm that repression of p53-stimulated transcription by E1B-55K is mainly conserved among HAdV species. Remarkably, E1B-55K from some HAdV species seem to have evolved another SUMO-independent mechanism to repress p53 promoter activity. Further experiments need to be done to elucidate these mechanisms in detail.

4.3.5 E3-SUMO-ligase function of HAdV E1B-55K is not conserved throughout different species

We detected that E1B-55K from different HAdV species were highly SUMOylated. It is well known that HAdV-C5 E1B-55K SUMOylation regulates E1B-55K mediated repression of p53-stimulated transcription (4.3.4). Furthermore, HAdV-C5 E1B-55K is able to SUMOylate p53 with SUMO-1, thereby acting as an E3-SUMO-ligase itself [59, 60]. Since this function is also regulated by E1B-55K SUMOylation, we decided to investigate the E3-SUMO-ligase function of the highly SUMOylated E1B-55K proteins from other HAdV species [59]. The multiple ways of HAdV-C5 E1B-55K to inhibit p53 all contribute to the oncogenic potential of the protein. Another mechanism of E1B-55K from other species to inactivate p53 similar to HAdV-C5 could provide further insights into the transformation efficiency of these proteins. So far, *focus* formation has been observed only with E1A from HAdV-C5 [101]. Here, we transfected H1299 cells with p53, 6-His-tagged SUMO-1 as well as E1B-55K from the different HAdV species or their respective SUMO mutants and performed a Ni-NTA pulldown (Fig. 19).

Immunoblotting of the 6-His-SUMO-1-conjugates revealed that E1B-55K wt from HAdV-E4, HAdV-C5, HAdV-B16, HAdV-B34 and HAdV-F40 induced SUMOylation of p53 with SUMO-1 (Fig. 19; lanes 3, 5, 12, 14, 16). Remarkably, HAdV-B34 E1B-55K wt induced the highest SUMOylation of p53 (Fig. 19; lane 14). For HAdV-E4 E1B-55K, we did not see any change in SUMOylated p53 upon inactivation of the SCM (Fig. 19; lanes 3 and 4). SUMOylation of p53 by HAdV-C5 E1B-55K appeared to be very weak in this experiment (Fig. 19; lane

5). However, we could confirm previous results by showing that SUMOylation of p53 is abrogated in HAdV-C5 E1B-55K K104R (Fig. 19; lane 6). Interestingly, HAdV-C5 E1B-55K K101R revealed a higher SUMOylation of p53, most probably due to the enhanced SUMOylation of HAdV-C5 E1B-55K K101R (Fig. 19; lane 7), which is known to regulate its E3 ligase function [59]. Inactivation of the SCM in HAdV-B16 E1B-55K K101R and HAdV-B34 K103R led to a clear reduction of SUMOylated p53 (Fig. 19; lanes 13 and 15). In HAdV-F40 E1B-55K K90R SUMOylation of p53 was completely abrogated (Fig. 19; lane 17). Furthermore, neither HAdV-D9 wt nor its SCM mutant (K103R) was able to SUMOylate p53 (Fig. 19; lanes 8 and 9). Interestingly, although no SUMOylation of p53 was induced by HAdV-A12 E1B-55K wt, a very faint band corresponding to SUMOylated p53 could be detected when transfecting its SCM mutant (K88R) (Fig. 19; lane 11). Finally, no SUMOylation of p53 was observed in the empty controls, where p53 and 6-His-SUMO-1 were transfected without E1B-55K (Fig. 19; lanes 1 and 2).

Taken together, we have shown that the E3-SUMO-ligase function of E1B-55K is only conserved in some HAdV species, indicating that HAdV species might have evolved different mechanisms to counteract p53. Moreover, E1B-55K SUMOylation might not necessarily regulate SUMOylation of p53 in other species, as it has been shown for species C. The results described here provide hints from a single experiment that needs to be repeated in order to confirm the outcome.

5 Discussion

5.1 K101 is a novel regulator of HAdV-C5 E1B-55K SUMOylation

E1B-55K is an early adenoviral protein with multiple functions. Its roles in regulation of gene expression, cell cycle control, apoptosis, DDR and innate immunity render it an important viral factor throughout the whole life cycle of HAdVs [68, 97–99, 192, 193]. Furthermore, E1B-55K possesses an oncogenic potential through its anti-apoptotic functions, especially repression and depletion of p53 but also proteasomal degradation of other cellular factors involved in DDR, such as Mre11 or SPOC-1 [61, 62, 68, 69, 84, 85]. Soon after the discovery of SUMO, E1B-55K has been shown to be modified by SUMO-1 at a consensus motif around K104 [75]. SUMOylation is an enzymatic process during which the SUMO protein is covalently bound to a target protein and can have several effects on the modified proteins. It might alter protein-protein interactions as well as protein stability, localization or activation [194]. In fact, SUMOylation of E1B-55K is required for many functions of the protein. Inactivation of SUMOylation in E1B-55K K104R leads to impaired intranuclear shuttling and cytoplasmic localization of the protein [169]. Furthermore, E3-SUMO-ligase functions towards p53 and Sp100A as well as degradation of Daxx are highly dependent on SUMOylated E1B-55K [59, 90, 97]. Finally, SUMOylation regulates repression of p53-stimulated transcription by E1B-55K [75].

Aim of this work is the analysis of a lysine at position 101 (K101) and its role on the PTMs of E1B-55K. Remarkably, we detect a higher SUMOylation of E1B-55K upon K101R mutation (Fig. 6 + Fig. 7). However, when transfecting with the K101A mutant, we observe a much lower SUMOylation of the protein (Fig. 6). This observation, together with the fact that no SUMOylation was observed in the E1B-55K K101/104R double mutant reveals that K104 is the main SCM in E1B-55K and that SUMOylation at this site is highly affected by K101. We could specify the regulation through K101, since inactivation of other lysines present in E1B-55K (K138R and K185R) did not alter the SUMOylation of the protein (Fig. 6). One hypothesis for the increase in E1B-55K SUMOylation might be a structural change of E1B-55K upon K101 mutation. Up to date, the exact

structure of E1B-55K is still unknown. However, it has been shown that the N-terminal part of E1B-55K is intrinsically disordered. Furthermore, prediction tools assume that the central part of E1B-55K is ordered, while the C-terminal part is intrinsically disordered again [195]. Structural changes of proteins upon single amino acid mutations have been reported before. Single nucleotide polymorphisms (SNPs) of the protein kinase Pim-1 (proviral insertion site in moloney murine leukemia-virus) are found in many cancer tissues and it has been shown that these SNPs result in a local change of the tertiary protein structure [196]. The K101R mutation might change the structure of E1B-55K, which leads to a higher exposure of the SCM to SUMO. K101A on the other site might be masking the SCM, resulting in a lower SUMOylation of E1B-55K.

On a different note, higher SUMOylation of HAdV-C5 E1B-55K K101R might be explained by an increased import of the protein into the nucleus. A similar mechanism has been observed for Mdm2, which is another cellular protein that is only nuclear when it is modified by SUMO. Moreover, RanBP2 and PIAS have been identified as E3-SUMO-ligases for Mdm2. Since RanBP2 is located at the nuclear pores, it is suggested that Mdm2 is SUMOylated upon entering the nucleus. Inside the nucleus, the protein is further SUMOylated by PIAS [197]. It is possible that the K101R-mutation of the protein increases its interaction with cellular factors promoting the nuclear import of the protein. Because SUMOylation mainly occurs in the nucleus, higher import into the nucleus might consequently increase SUMOylation of HAdV-C5 E1B-55K K101R. Up to now, the E3-SUMO-ligase of HAdV-C5 E1B-55K has not been identified. Additional experiments need to be performed to further investigate this hypothesis.

HAdV-C5 E1B-55K encodes a nuclear export signal (NES) close to the main SCM and the newly discovered K101 (Fig. 4) [74]. Proteins that harbor a NES are transported out of the nucleus through binding of the nuclear transport receptor CRM1. Kindsmüller *et al.* previously modeled an interplay between HAdV-C5 E1B-55K SUMOylation, nuclear export and intranuclear targeting [169]. They state that, while SUMOylation of HAdV-C5 E1B-55K restricts CRM1 binding, it enables the protein to migrate to viral RCs, where it interacts with cellular factors. At the RCs, the protein is deSUMOylated again and can enter CRM1-dependent export pathways [169]. Interestingly, Kindsmüller *et al.* presume another, CRM1-independent pathway for nuclear export of HAdV-C5

E1B-55K. This is supported by the observation that a double mutant virus, HAdV-C5 E1B-55K NES K104R, is still able to exit the nucleus [169]. There are several examples in the literature showing that SUMOylation of a protein enhances its nuclear retention, especially when a NES is nearby. It is suggested that SUMOylation is covering the NES, thereby blocking its function [198, 199]. SUMOylation of Krüppel-like factor 5 (KLF5) greatly enhances its nuclear localization by inhibiting the upstream NES [198]. Furthermore, mutations in the SCM of CREB (cAMP-response element-binding protein) and CtBP1 (C-terminal binding protein of adenovirus E1A) abrogate the nuclear localization of these proteins [200, 201]. Du *et al.* further reveal that these two proteins contain a putative NES close to their SCM as well [198]. Comparably, we observe here that exchange of the lysine to an arginine (K101R) leads to a change in the protein's subcellular localization in transient transfection and infection (Fig. 8 + Fig. 9). Thus, highly SUMOylated HAdV-C5 E1B-55K K101R might enhance nuclear localization by masking the NES at leucines 83, 87 and 91 (L83/87/91), as well. In immunofluorescence experiments we still observe approximately 20 % of the K101R mutant in the cytoplasm. On the one hand, this result further supports the model by Kindsmüller *et al.* of a CRM1-independent export (Fig. 8) [169]. On the other hand, the remaining cytoplasmic localization of HAdV-C5 E1B-55K K101R could be explained by a different observation. It has been reported that only a small portion the protein population is SUMOylated and that this fraction is sufficient to maintain the effects of SUMOylation [120, 124]. Thus, only a small fraction of HAdV-C5 E1B-55K wt might be SUMOylated, leaving enough unSUMOylated protein for its cytoplasmic functions. In contrast, the K101R mutation might result in a larger fraction of SUMOylated E1B-55K, leaving only a minor amount of cytoplasmic protein.

Furthermore, we observe a localization of HAdV-C5 E1B-55K K101R to nuclear structures strongly resembling the viral RCs in infection experiments (Fig. 9). It has been described before that HAdV-C5 E1B-55K localizes to viral RCs during infection, at the same time supposedly removing cellular factors involved in cellular mRNA export [189]. Moreover, localization to viral RCs is increased when the NES is inactivated and the protein is more strongly SUMOylated [169]. Therefore, HAdV-C5 E1B-55K K101R, which is more SUMOylated than

the NES mutant, might facilitate the recruitment of HAdV-C5 E1B-55K to viral RCs explaining the strong localization to these nuclear structures.

Besides, this work shows that high SUMOylation of E1B-55K K101R results in a “gain-of-function” with increased repression of p53-stimulated transcription and augmented *focus* formation (Fig. 10 + Fig. 11). Inhibition of p53 transactivation by E1B-55K is necessary for its oncogenic potential [190]. However, particular mutants of E1B-55K that are still able to repress p53-stimulated transcription fail to transform pBRKs. Thus, there are p53-repression independent mechanisms involved in the transformation process [78]. Investigations on the cellular protein Daxx (death domain-associated protein) have shown that E1B-55K mutants defective for Daxx degradation are less effective in transforming pBRKs [111]. Daxx is associated with PML-NBs and plays a role in the intrinsic antiviral immune response and transcriptional repression. Furthermore, it has been shown to negatively regulate HAdV-C5 infection [90, 202, 203]. Interactions with both p53 and Daxx, which are crucial for pBRK transformation, are known to be regulated by SUMO conjugation of E1B-55K [75, 111]. Therefore, it is most likely that the “gain-of-function” we have observed in the K101R mutant regarding oncogenic transformation is a logical consequence of its higher SUMOylation.

It has been shown before that HAdV-C5 E1B-55K is targeted by different PTMs, which regulate each other. On the one hand, it has been revealed that phosphorylation at its C-terminus is a positive regulator for efficient SUMOylation of HAdV-C5 E1B-55K at K104 [170]. On the other hand, we detect K101 as a negative regulator for HAdV-C5 E1B-55K SUMOylation (Fig. 6 + Fig. 7). Cross-talk of PTMs has already been described for other proteins. Investigating the PTMs of PML, Guan *et al.* detected an acetylation site at K487 as well as a SUMOylation site at K490. Furthermore, they showed that inactivation of acetylation by a K487R mutation led to an increase in SUMOylation, while the SUMO mutant of PML IV (K490R) was highly acetylated [137]. Therefore, we were especially interested in K101 and its role regarding PTMs of HAdV-C5 E1B-55K, because the lysine residue is in very close proximity to the main SCM of HAdV-C5 E1B-55K around K104. Of note, HAdV-C5 E1B-55K K101R reveals higher SUMOylation, whereas HAdV-C5 E1B-55K K101A and K101Q are less SUMOylated compared to the wt-protein (Fig. 12). Exchange of a lysine with an arginine (K to R) preserves the electric

charge of this site but blocks its acetylation, while mutation of lysine to glutamine (K to Q) neutralizes electric charges and mimics acetylation [137, 191, 204]. It is conceivable that mutation of HAdV-C5 E1B-55K K101R blocks acetylation of the protein while simultaneously promoting its SUMOylation at K104. HAdV-C5 E1B-55K K101A might mimic acetylation of E1B-55K, thereby partly blocking the SUMOylation of the protein, similar to the observations made for PML [137]. This hypothesis is further strengthened by the fact that HAdV-C5 E1B-55K K101Q, mimicking a constitutively acetylated form of the protein, is less SUMOylated (Fig. 12). This result indicates that acetylation of HAdV-C5 E1B-55K is negatively affecting SUMOylation of the protein. However, additional studies, including mass spectrometry analysis, have to be performed to verify this result.

It is also conceivable that K101 is modified by different PTMs that compete with each other. Acetylation of the tumor suppressor p53 at K320 inhibits ubiquitination by Mdm2 at the same site [135]. Usually, Mdm2 ubiquitinates p53, marking it for proteasomal degradation [205–207]. A switch to acetylation of p53, however, reduces degradation of the protein by occupying the ubiquitination site [135, 208]. HAdV-C5 E1B-55K K101 could be a target for different PTMs, like SUMOylation, ubiquitination or acetylation, and a switch between these PTMs might regulate its function or stability.

In summary, SUMOylation is essential for HAdV-C5 E1B-55K functions. Phosphorylation of the protein positively regulates its SUMOylation, and SUMOylation in turn negatively regulates nuclear export via a leucine-rich NES. Furthermore, we have identified for the first time that SUMOylation of HAdV-C5 E1B-55K is affected by a lysine at position 101. Several studies have shown a complex interplay between phosphorylation, SUMOylation and nuclear export and a crucial role for these in the protein's multiple functions, both in the nucleus and cytoplasm. In our model, we propose that K101 might diminish the E1B-55K SUMOylation at K104, therefore enabling the protein to efficiently shuttle between the nucleus and the cytoplasm. Upon K101R mutation, nuclear import of HAdV-C5 E1B-55K is increased while nuclear export is inhibited. Once in the nucleus, HAdV-C5 E1B-55K K101R might be further SUMOylated, simultaneously masking the NES close by. Furthermore, we propose that acetylation of K101 might be the reason for reduced SUMOylation of HAdV-C5 E1B-55K wt (Fig. 12). However, it is also possible

that K101 is modified by other PTMs, such as ubiquitination or SUMOylation. Yet, the exact mechanism behind the regulation of HAdV-C5 E1B-55K SUMOylation remains elusive (Fig. 20).

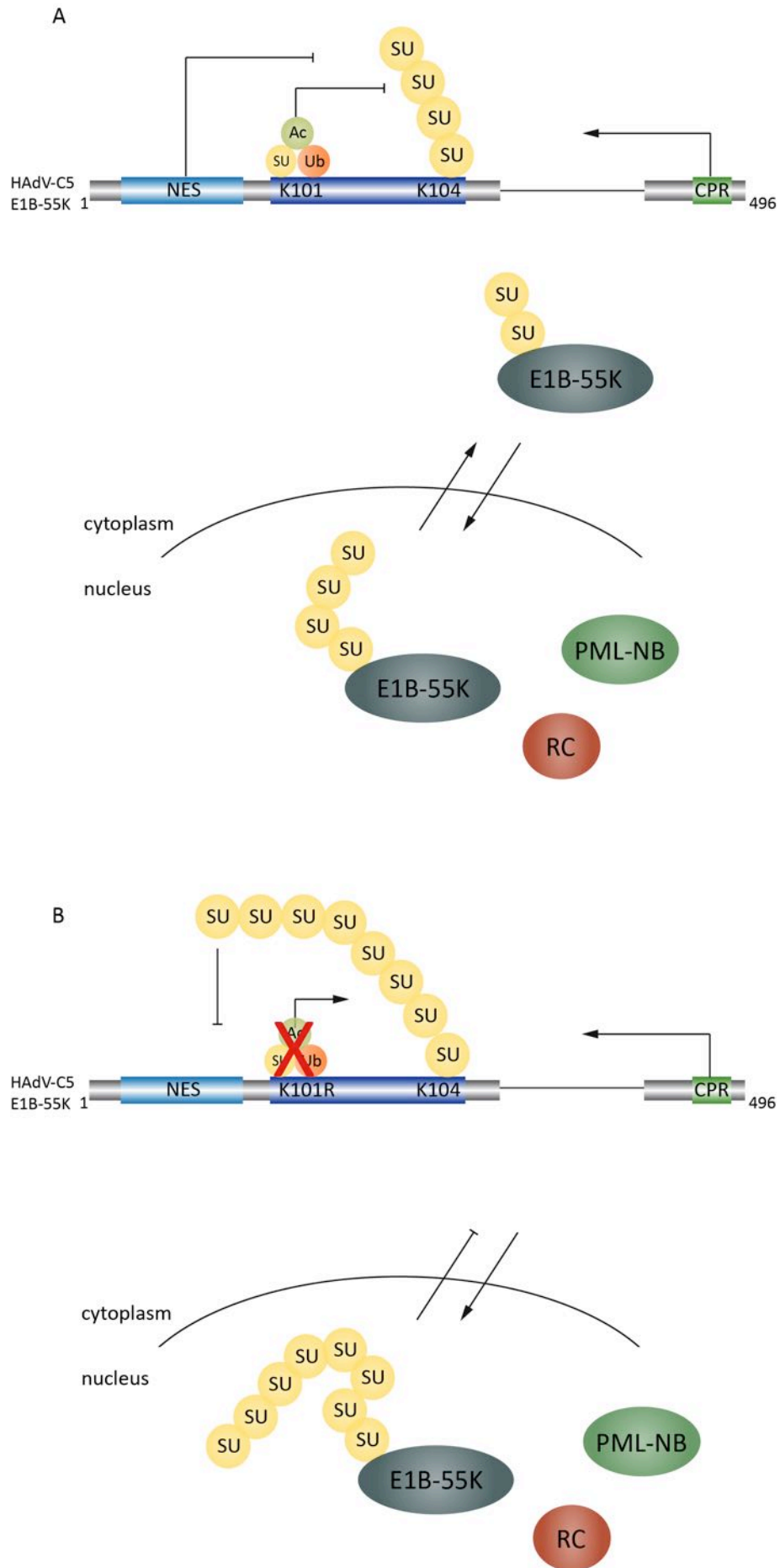


Fig. 20: Model for the regulation of HAdV-C5 E1B-55K SUMOylation by K101. (A) Regulation in E1B-55K wt: PTM of K101 further regulates SUMOylation at K104 and nucleo-cytoplasmic shuttling of the protein is promoted. SUMOylation of E1B-55K directs the protein to PML-NBs and RCs and deSUMOylation results in nuclear export via the NES. (B) Regulation in E1B-55K K101R: PTM of K101 is inhibited, resulting in an increased SUMOylation at K104. SUMOylated E1B-55K is directed to the nucleus, where it interacts with PML-NBs and RCs. High SUMOylation blocks both deSUMOylation and the NES and nucleo-cytoplasmic shuttling is impaired. PTM: post translational modification, PML-NB: PML nuclear bodies, RC: replication center, NES: nuclear export signal.

5.2 SUMOylation of E1B-55K is conserved among HAdV species

For a long time, observations from HAdV-C were applied to all HAdVs. Accordingly, most of the studies on E1B-55K were performed in HAdVs from species C. Recently, studies have concentrated on other HAdV species, revealing conserved functions but also differences among species [100–103]. Surprisingly, although SUMOylation has a major influence on HAdV-C5 E1B-55K, no studies have examined the impact of PTMs on E1B-55K functions.

In this work, we have identified a conserved SCM in E1B-55K from all species except HAdV-A12 and HAdV-F40 (Fig. 13). We show that all E1B-55K proteins, except HAdV-A12, are highly SUMOylated at this conserved SCM and even though HAdV-F40 E1B-55K does not possess a consensus motif, the protein is a target of the SUMO conjugation machinery (Fig. 14). SUMOylation of a protein on a lysine lacking the surrounding consensus motif has been observed before for other proteins such as Mdm2 or CREB [120, 197, 200]. Thus, HAdV-F40 E1B-55K is another protein that is modified by SUMO in spite of a missing SCM. Remarkably, PTM of HAdV-F40 occurs in the same region of E1B-55K where the other species SCM are located (Fig. 13). Our findings indicate that SUMOylation at the N-terminal region is conserved and therefore an important PTM of E1B-55K from most species, similar to HAdV-C. In contrast to the conserved SCM, the leucine-rich NES of HAdV-C5 E1B-55K is not conserved. Comparable to the SCM, HAdV-A12 as well as HAdV-F40 are lacking the complete motif (Fig. 13). However, we see a SUMO-dependent localization of E1B-55K in almost all species. Only HAdV-A12 did not change its localization (Fig. 16). Since the protein does not contain a SCM and the very weak SUMOylation is not altered upon mutation of the lysine residue, this observation is not surprising (Fig. 14). In fact, it further underlines the correlation between SUMOylation and intracellular localization. Comparable to HAdV-C5 E1B-55K, highly SUMOylated E1B-55K proteins from other species are mainly found in the nucleus and co-localized with SUMO-2. Upon SCM depletion, these proteins are

shifted to the cytoplasm and for most of them co-localization with SUMO-2 is abrogated (Fig. 16 + Fig. 17). It is therefore reasonable to assume that shuttling of E1B-55K in most of the HAdV species is regulated through a complex interplay between SUMOylation and intranuclear targeting. Similar to HAdV-C5, SUMOylated E1B-55K in other HAdV species is present in the nucleus. DeSUMOylation could then induce the export of the protein into the cytoplasm. While HAdV-C5 E1B-55K exits the nucleus via its NES, E1B-55K proteins from other species are lacking this site and presumably exit the nucleus via a CRM1-independent pathway. CRM1 is part of the importin- β superfamily and is involved in the nuclear export of most shuttling proteins [209]. However, there are other members of the importin- β superfamily that have been described to mediate nuclear export. Amongst them are CAS for the export of importin α and exportin-t for the export of tRNA [210, 211]. Thus, E1B-55K from other HAdV species might use one of the above-mentioned transport receptors to exit the nucleus. As described above, Kindsmüller *et al.* already suggested a second, CRM1-independent mechanism for shuttling of HAdV-C5 E1B-55K, as well [169]. Therefore, HAdV-C5 E1B-55K might have evolved an additional CRM1-dependent export via its NES to further facilitate the transfer to the cytoplasm. However, the exact mechanism behind remains elusive.

It has been shown before that some E1B-55K functions are conserved among the different species. Nevertheless, they differ in some important aspects. For example, the E3-ubiquitin-ligase that is formed by E1B-55K and E4orf6 together with the cellular factors Elongin B and C, Cullin and Rbx1 is highly conserved [61, 67, 100]. This ligase complex ubiquitinates cellular proteins and marks them for proteasomal degradation. However, the ligase complex from different HAdV species has been shown to incorporate different members of the Cullin family, either Cul2, Cul5 or even both [100]. Moreover, DNA-ligase IV is the only target that is degraded by all HAdV species [100, 102]. Mre11 and p53 are only degraded by E1B-55K from HAdV-A12, HAdV-C5, HAdV-F40 and HAdV-E4, although just in the context of infection for HAdV-E4 E1B-55K [101, 102]. However, E1B-55K evolved multiple mechanisms to inactivate p53. We and others have shown that E1B-55K from all species, except HAdV-E4, efficiently repress p53-stimulated transcription (Fig. 18) [101]. Moreover, we have shown here for the first time that E1B-55K from HAdV-E4, HAdV-B16, HAdV-B34 and HAdV-F40 are E3-SUMO-1-ligases for p53, similar to HAdV-C5

E1B-55K (Fig. 19). Pennella *et al.* showed that HAdV-C5 E1B-55K tethers p53 to PML-NBs and SUMOylates p53, thereby facilitating its nuclear export [60]. Therefore, it is possible that E1B-55K from the other HAdV species have evolved similar mechanisms. It has been described that E1B-55K from all other species bind to PML and that HAdV-A12, HAdV-B16 and HAdV-E4 relocalize p53 to the aggresome, similar to HAdV-C5 E1B-55K [101, 103]. Still, no study has concentrated on the correlation between E1B-55K induced relocalization to PML-NBs and SUMOylation of p53 followed by nuclear export in the other HAdV species. Remarkably, the interactions we observed with p53 are dependent on E1B-55K SUMOylation from the species HAdV-C5, HAdV-B16, HAdV-F40 and HAdV-B34 (Fig. 18 + Fig. 19). Interestingly however, the latter is able to repress p53 transactivation independent of SUMOylation (Fig. 18). E1B-55K from the remaining species HAdV-E4, HAdV-D9 and HAdV-A12 interact with p53 in a SUMO-independent fashion (Fig. 18 + Fig. 19). When trying to group E1B-55K from different HAdV species according to their p53 interactions or SUMO dependency, it soon becomes clear that this is not possible. We and others show that the mechanisms HAdV-C5 E1B-55K evolved to counteract p53 are not absolutely applicable to the other HAdV species [100–102]. Although all of them evolved antiapoptotic functions with regard to p53, none of the E1B-55K proteins examined in this work are entirely comparable to HAdV-C5 E1B-55K. Inhibition of p53 is critical to counteract the stabilization of the protein by E1A in HAdV-C5 [108, 109]. The differences of E1B-55K from other HAdV species to counteract p53 might be due to differences in p53 stabilization of the respective E1A protein. It is possible that less stabilization of p53 by E1A results in reduced antiapoptotic functions of E1B-55K and vice versa. So far, stabilization of p53 by E1A from other HAdV species has not been investigated and might be an interesting objective for future analyses.

Significantly, we detect K101 as a novel regulator for E1B-55K SUMOylation that is exclusively present in HAdV-C (4.3.1). SUMOylation is described to be a molecular switch between lytic and latent infections in viruses. For instance, the latency-associated nuclear antigen (LANA) is involved in the maintenance of KSHV latency through repression of lytic genes (reviewed in [212]). Furthermore, LANA possesses a SUMO interacting motif (SIM) and is highly SUMOylated [213]. It is suggested that LANA creates a SUMO-rich milieu favoring chromatin condensation and thus silencing of lytic genes [214].

Therefore, SUMOylation as well as SUMO-SIM interaction of LANA are important to inhibit the onset of a lytic infection [213]. Another example is the BZLF1 protein from EBV. BZLF1 is a transcriptional activator that is involved in the switch between latent and lytic infection [215]. SUMOylation of BZLF1 promotes viral latency whereas deSUMOylation by the EBV BGLF4-encoded protein kinase (EBV-PK) induces reactivation of the virus [166]. Interestingly, both LANA and BZLF1 reveal functional similarities to HAdV E1B-55K, for example in regulating gene transcription (reviewed in [212], [216]). LANA is also involved in inhibition of p53 and thereby blocking of apoptosis (reviewed in [212]). Studies together with the recently described humanized mouse model for persistent HAdV infections strongly indicate that the virus is able to induce persistent infections [33]. Early in life, around 80 % of the human population are infected with HAdV-C. When Garnett *et al.* analyzed tissues from tonsillectomies and adenoidectomies, they found HAdV DNA from species C in T-lymphocytes from 79 % of the samples. In addition, they found the highest amount of viral DNA in a 2-year-old donor [31]. In a later study, they could even reactivate replicating HAdVs from donor samples upon *in-vitro* stimulation [32]. Therefore, it is possible that HAdV-C E1B-55K SUMOylation and the regulation of its functions by this PTM could have a role in the establishment of a persistent infection by HAdV. Interestingly and contrary to other HAdV species, E1B-55K wt from species C is less SUMOylated (Fig. 14). The K101 residue of HAdV-C5 E1B-55K could promote viral persistence in infected cells by reducing the SUMOylation of the protein. E1B-55K from other species lacking K101 might therefore be less likely to induce persistence. Additional experiments in cellular systems modeling persistence and eventually our humanized mouse model are needed to further elucidate this theory.

Taken together, we have shown for the first time that SUMOylation of E1B-55K is conserved throughout the tested species. Our results provide further insights into conserved functions but also differences of HAdV E1B-55K. Furthermore, we identify K101 as a potential regulator of E1B-55K SUMOylation that is specific to HAdV-C. We suggest that HAdV E1B-55K from different species evolved diverse strategies to modulate the infected cell. In the case of HAdV-C5, these strategies might allow persistence.

6 Literature

1. **Rowe WP, Huebner RJ, Gilmore LK, Parrott RH, Ward TG.** Isolation of a Cytopathogenic Agent from Human Adenoids Undergoing Spontaneous Degeneration in Tissue Culture. *Exp Biol Med* 1953;84:570–573.
2. **Enders JF, Bell JA, Dingle JH, Francis T, Hilleman MR, et al.** Adenoviruses: group name proposed for new respiratory-tract viruses. *Science* 1956;124:119–20.
3. **Hilleman MR, Werner JH.** Recovery of new agent from patients with acute respiratory illness. *Proc Soc Exp Biol Med* 1954;85:183–8.
4. **Berk AJ.** Adenoviridae: The Viruses and Their Replication. In: Knipe D, Howley P (editors). *Fields Virology*. New York: Lippincott-Raven. pp. 2265–2300.
5. **Davison A, Benkó M, Harrach B.** Genetic content and evolution of adenoviruses. *J Gen Virol* 2003;84:2895–2908.
6. **Benkő M, Harrach B.** A proposal for a new (third) genus within the family Adenoviridae. *Arch Virol* 1998;143:829–37.
7. **Benkő M, Elo P, Ursu K, Ahne W, LaPatra SE, et al.** First Molecular Evidence for the Existence of Distinct Fish and Snake Adenoviruses. *J Virol* 2002;76:10056–10059.
8. **Harrach B, Benkő M, Both G, Brown M, Davison A, et al.** Adenoviridae - 9th report of the International Committee on Taxonomy of Viruses. In: King AMQ, Adams MJ, Carstens EB, Lefkowitz EJ (editors). *Virus Taxonomy*. Oxford: Elsevier; 2012. pp. 125–141.
9. **Hage E, Liebert UG, Bergs S, Ganzenmueller T, Heim A.** Human mastadenovirus type 70: a novel, multiple recombinant species D mastadenovirus isolated from diarrhoeal faeces of a haematopoietic stem cell transplantation recipient. *J Gen Virol* 2015;96:2734–2742.
10. **Bailey A, Mautner V.** Phylogenetic Relationships among Adenovirus Serotypes. *Virology* 1994;205:438–452.
11. **Jones MS, Harrach B, Ganac RD, Gozum MMA, Dela Cruz WP, et al.** New adenovirus species found in a patient presenting with gastroenteritis. *J Virol* 2007;81:5978–84.

12. **Rosen L.** A Hemagglutination-Inhibition Technique For Typing Adenoviruses. *Am J Hyg* 1960;71:120–128.
13. **Lion T.** Adenovirus Infections in Immunocompetent and Immunocompromised Patients. *Clin Microbiol Rev* 2014;27:441–462.
14. **Dicks MDJ, Spencer AJ, Edwards NJ, Wadell G, Bojang K.** A Novel Chimpanzee Adenovirus Vector with Low Human Seroprevalence: Improved Systems for Vector Derivation and Comparative Immunogenicity. *PLoS One* 2012;7:40385.
15. **Tatsis N, Ertl HCJ.** Adenoviruses as Vaccine Vectors. *Mol Ther* 2004;10:616–629.
16. **Russell WC.** Adenoviruses: update on structure and function. *J Gen Virol* 2009;90:1–20.
17. **Wood DJ.** Adenovirus gastroenteritis. *Br Med J* 1988;296:229–230.
18. **Matsushima Y, Shimizu H, Kano A, Nakajima E, Ishimaru Y, et al.** Genome Sequence of a Novel Virus of the Species Human Adenovirus D Associated with Acute Gastroenteritis. *Genome Announc* 2013;1:e00068-12.
19. **Yolken RH, Lawrence F, Leister F, Takiff HE, Strauss SE.** Gastroenteritis associated with enteric type adenovirus in hospitalized infants. *J Pediatr* 1982;101:21–26.
20. **Jawetz E, Kimura S, Nicholas AN, Thygeson P, Hanna L.** New type of APC virus from epidemic keratoconjunctivitis. *Science* 1955;122:1190–1.
21. **Numazaki Y, Kumasaka T, Yano N, Yamanaka M, Miyazawa T, et al.** Further Study on Acute Hemorrhagic Cystitis Due to Adenovirus Type 11. *N Engl J Med* 1973;289:344–347.
22. **Dingle JH, Langmuir AD.** Epidemiology of acute, respiratory disease in military recruits. *Am Rev Respir Dis* 1968;97:Suppl:1-65.
23. **Savón C, Acosta B, Valdés O, Goyenechea A, Gonzalez G, et al.** A myocarditis outbreak with fatal cases associated with adenovirus subgenera C among children from Havana City in 2005. *J Clin Virol* 2008;43:152–7.
24. **Siminovich M, Murtagh P.** Acute Lower Respiratory Tract Infections by Adenovirus in Children: Histopathologic Findings in 18 Fatal Cases. *Pediatr Dev Pathol* 2011;14:214–217.
25. **Wold WSM, Ison MG.** Adenoviruses. In: Knipe DM, Howley PM (editors). *Fields Virology*. Lippincott Williams & Wilkins; 2013. pp. 1732–

- 1767.
26. **Lindemans CA, Leen AM, Boelens JJ.** How I treat adenovirus in hematopoietic stem cell transplant recipients. *Blood* 2010;116:5476–85.
 27. **Al-Herz W, Moussa MAA.** Survival and Predictors of Death Among Primary Immunodeficient Patients: A Registry-Based Study. *J Clin Virol* 2012;32:467–473.
 28. **Wigger HJ, Blanc WA.** Fatal Hepatic and Bronchial Necrosis in Adenovirus Infection with Thymic A lymphoplasia. *N Engl J Med* 1966;275:870–874.
 29. **Myerowitz RL, Stalder H, Oxman MN, Levin MJ, Moore M, et al.** Fatal Disseminated Adenovirus Infection in a Renal Transplant Recipient. *Am J Med* 1975;59:591–598.
 30. **Kojaoghlanian T, Flomenberg P, Horwitz MS.** The impact of adenovirus infection on the immunocompromised host. *Rev Med Virol* 2003;13:155–171.
 31. **Garnett CT, Erdman D, Xu W, Gooding LR.** Prevalence and Quantitation of Species C Adenovirus DNA in Human Mucosal Lymphocytes. *J Virol* 2002;76:10608–10616.
 32. **Garnett CT, Talekar G, Mahr JA, Huang W, Zhang Y, et al.** Latent Species C Adenoviruses in Human Tonsil Tissues. *J Virol* 2009;83:2417–28.
 33. **Rodríguez E, Ip WH, Kolbe V, Hartmann K, Pilnitz-Stolze G, et al.** Humanized Mice Reproduce Acute and Persistent Human Adenovirus Infection. *J Infect Dis* 2017;215:70–79.
 34. **Bachenheimer S, Darnell JE.** Adenovirus-2 mRNA is transcribed as part of a high-molecular-weight precursor RNA. *Cell Biol* 1975;72:4445–4449.
 35. **Berget SM, Moore C, Sharp PA.** Spliced segments at the 5' terminus of adenovirus 2 late mRNA. 1977. *Rev Med Virol*;10:356-62; discussion 355–6.
 36. **Yabe Y, Trentin JJ, Taylor G.** Cancer induction in hamsters by human type 12 adenovirus. Effect of age and of virus dose. *Proc Soc Exp Biol Med* 1962;111:343–4.
 37. **Stewart PL, Fuller SD, Burnett RM.** Difference imaging of adenovirus: bridging the resolution gap between X-ray crystallography and electron microscopy. *EMBO J* 1993;12:2589–2599.
 38. **Gaggar A, Shayakhmetov DM, Lieber A.** CD46 is a cellular receptor for group B adenoviruses. *Nat Med* 2003;9:1408–1412.

39. **Bergelson JM, Cunningham JA, Droguett G, Kurt-Jones EA, Krithivas A, et al.** Isolation of a Common Receptor for Coxsackie B viruses and Adenoviruses 2 and 5. *Science* 1997;275:1320–3.
40. **Vellinga J, Van der Heijdt S, Hoeben RC.** The adenovirus capsid: major progress in minor proteins. *J Gen Virol* 2005;86:1581–1588.
41. **Schreiner S, Wimmer P, Dobner T.** Adenovirus degradation of cellular proteins. *Future Microbiol* 2012;7:211–225.
42. **Corden J, Engelking HM, Pearson GD.** Chromatin-like organization of the adenovirus chromosome. *Biochemistry* 1976;73:401–404.
43. **Chatterjee PK, Vayda ME, Flint SJ.** Interactions Among the Three Adenovirus Core Proteins. *J Virol* 1985;55:379–386.
44. **Rekosh DM, Russell WC, Bellet AJ, Robinson AJ.** Identification of a protein linked to the ends of adenovirus DNA. *Cell* 1977;11:283–95.
45. **Girard M, Bouché J-P, Marty L, Revet B, Berthelot N.** Circular adenovirus DNA-protein complexes from infected HeLa cell nuclei. *Virology* 1977;83:34–55.
46. **Tamanoi F, Stillman BW.** Function of adenovirus terminal protein in the initiation of DNA replication. *PNAS* 1982;79:2221–2225.
47. **Reddy VS, Nemerow GR.** Structures and organization of adenovirus cement proteins provide insights into the role of capsid maturation in virus entry and infection. *PNAS* 2014;111:11715–11720.
48. **Meier O, Greber UF.** Adenovirus endocytosis. *J Gene Med* 2003;5:451–462.
49. **Tomko RP, Johansson CB, Totrov M, Abagyan R, Frisén J, et al.** Expression of the Adenovirus Receptor and Its Interaction with the Fiber Knob. *Exp Cell Res* 2000;255:47–55.
50. **Amstutz B, Gastaldelli M, Kälin S, Imelli N, Boucke K, et al.** Subversion of CtBP1-controlled macropinocytosis by human adenovirus serotype 3. *EMBO J* 2008;27:956–969.
51. **Kälin S, Amstutz B, Gastaldelli M, Wolfrum N, Boucke K, et al.** Macropinocytotic Uptake and Infection of Human Epithelial Cells with Species B2 Adenovirus Type 35. *J Virol* 2010;84:5336–5350.
52. **Leopold PL, Kreitzer G, Miyazawa N, Rempel S, Pfister KK, et al.** Dynein- and Microtubule-Mediated Translocation of Adenovirus Serotype 5 Occurs after Endosomal Lysis. *Hum Gene Ther* 2000;11:151–165.
53. **Nevins J, Ginsberg H, Blanchard J, Wilson M, Darnell J.** Regulation of

- the Primary Expression of the Early Adenovirus Transcription Units. *J Virol* 1979;32:727–733.
54. **Ghosh MK, Harter ML.** A Viral Mechanism for Remodeling Chromatin Structure in G0 Cells. *Mol Cell* 2003;12:255–260.
 55. **Bagchi S, Raychaudhuri P, Nevins JR.** Adenovirus E1A proteins can dissociate heteromeric complexes involving the E2F transcription factor: A novel mechanism for E1A trans-activation. *Cell* 1990;62:659–669.
 56. **Cuconati A, Degenhardt K, Sundararajan R, Ansel A, White E.** Bak and Bax Function To Limit Adenovirus Replication through Apoptosis Induction. *J Virol* 2002;76:4547–4558.
 57. **Chiou SK, Tseng CC, Rao L, White E.** Functional Complementation of the Adenovirus E1B 19-Kilodalton Protein with Bcl-2 in the Inhibition of Apoptosis in Infected Cells. *J Virol* 1994;68:6553–6566.
 58. **Sarnow P, Ho YS, Williamst J, Levine AJ.** Adenovirus E1b-58kd Tumor Antigen and SV40 Large Tumor Antigen Are Physically Associated with the Same 54 kd Cellular Protein in Transformed Cells. *Cell* 1982;28:387–394.
 59. **Müller S, Dobner T.** The adenovirus E1B-55K oncoprotein induces SUMO modification of p53. *Cell Cycle* 2008;7:754–758.
 60. **Pennella M a, Liu Y, Woo JL, Kim C a, Berk AJ.** Adenovirus E1B 55-Kilodalton Protein Is a p53-SUMO1 E3 Ligase That Represses p53 and Stimulates Its Nuclear Export through Interactions with Promyelocytic Leukemia Nuclear Bodies. *J Virol* 2010;84:12210–12225.
 61. **Querido E, Blanchette P, Yan Q, Kamura T, Morrison M, et al.** Degradation of p53 by adenovirus E4orf6 and E1B55K proteins occurs via a novel mechanism involving a Cullin-containing complex. *Genes Dev* 2001;15:3104–17.
 62. **Querido E, Marcellus RC, Lai A, Charbonneau R, Teodoro JG, et al.** Regulation of p53 Levels by the E1B 55-Kilodalton Protein and E4orf6 in Adenovirus-Infected Cells. *J Virol* 1997;71:3788–3798.
 63. **Burgert H-G, Kvist S.** An Adenovirus Type 2 Glycoprotein Blocks Cell Surface Expression of Human Histocompatibility Class I Antigens. *Cell* 1985;41:987–997.
 64. **Burgert H-G, Maryanski JL, Kvist S.** E3/19K protein of adenovirus type 2 inhibits lysis of cytolytic T lymphocytes by blocking cell-surface

- expression of histocompatibility class I antigens. *Immunology* 1987;84:1356–1360.
65. **Evans JD, Hearing P.** Relocalization of the Mre11-Rad50-Nbs1 Complex by the Adenovirus E4 ORF3 Protein Is Required for Viral Replication. *J Virol* 2005;79:6207–6215.
 66. **Carvalho T, Seeler J-S, Öhman K, Jordan P, Pettersson U, et al.** Targeting of Adenovirus E1A and E4-ORF3 Proteins to Nuclear Matrix-associated PML Bodies. *J Cell Biol* 1995;131:45–56.
 67. **Harada JN, Shevchenko A, Shevchenko A, Pallas DC, Berk AJ.** Analysis of the Adenovirus E1B-55K-Anchored Proteome Reveals Its Link to Ubiquitination Machinery. *J Virol* 2002;76:9194–206.
 68. **Stracker TH, Carson CT, Weitzman MD.** Adenovirus oncoproteins inactivate the Mre11-Rad50-NBS1 DNA repair complex. *Nature* 2002;418:348–352.
 69. **Schreiner S, Kinkley S, Bürck C, Mund A, Wimmer P, et al.** SPOC1-Mediated Antiviral Host Cell Response Is Antagonized Early in Human Adenovirus Type 5 Infection. *PLoS Pathog* 2013;9:e1003775.
 70. **Marton MJ, Baim SB, Ornelles DA, Shenk T.** The Adenovirus E4 17-Kilodalton Protein Complexes with the Cellular Transcription Factor E2F, Altering Its DNA-Binding Properties and Stimulating E1A-Independent Accumulation of E2 mRNA. *J Virol* 1990;64:2345–59.
 71. **Nevins JR, Darnell JE.** Groups of Adenovirus Type 2 mRNA's Derived from a Large Primary Transcript: Probable Nuclear Origin and Possible Common 3' Ends. *J Virol* 1978;25:811–823.
 72. **Shaw AR, Ziff EB.** Transcripts from the adenovirus-2 major late promoter yield a single early family of 3' coterminal mRNAs and five late families. *Cell* 1980;22:905–16.
 73. **Beltz GA, Flint SJ.** Inhibition of HeLa Cell Protein Synthesis During Adenovirus Infection Restriction of Cellular Messenger RNA Sequences to the Nucleus. *J Mol Biol* 1979;131:353373.
 74. **Krätzer F, Rosorius O, Heger P, Hirschmann N, Dobner T, et al.** The adenovirus type 5 E1B-55K oncoprotein is a highly active shuttle protein and shuttling is independent of E4orf6, p53 and Mdm2. *Oncogene* 2000;19:850–857.
 75. **Endter C, Kzhyshkowska J, Stauber R, Dobner T.** SUMO-1 modification

- required for transformation by adenovirus type 5 early region 1B 55-kDa oncoprotein. *PNAS* 2001;98:11312–11317.
76. **Kao CC, Yew PR, Berk AJ.** Domains Required for in Vitro Association between the Cellular p53 and the Adenovirus 2 E1B 55K Proteins. *Virology* 1990;179:806–814.
 77. **Rubenwolf S, Schütt H, Nevels M, Wolf H, Dobner T.** Structural Analysis of the Adenovirus Type 5 E1B 55-Kilodalton-E4orf6 Protein Complex. *J Virol* 1997;71:1115–1123.
 78. **Härtl B, Zeller T, Blanchette P, Kremmer E, Dobner T.** Adenovirus type 5 early region 1B 55-kDa oncoprotein can promote cell transformation by a mechanism independent from blocking p53-activated transcription. *Oncogene* 2008;27:3673–84.
 79. **Blanchette P, Cheng CY, Yan Q, Ketner G, Ornelles DA, et al.** Both BC-Box Motifs of Adenovirus Protein E4orf6 Are Required To Efficiently Assemble an E3 Ligase Complex That Degrades p53. *Mol Cell Biol* 2004;24:9619–9629.
 80. **Teodoro JG, Halliday T, Whalen SG, Takayesu D, Graham FL, et al.** Phosphorylation at the Carboxy Terminus of the 55-Kilodalton Adenovirus Type 5 E1B Protein Regulates Transforming Activity. *J Virol* 1994;68:776–786.
 81. **Ching W, Dobner T, Koyuncu E.** The Human Adenovirus Type 5 E1B 55-Kilodalton Protein Is Phosphorylated by Protein Kinase CK2. *J Virol* 2012;86:2400–2415.
 82. **Zantema A, Fransen JAM, Davis-Olivier A, Ramaekers FCS, Vooijs GP, et al.** Localization of the E1B Proteins of Adenovirus 5 in Transformed Cells, as Revealed by Interaction with Monoclonal Antibodies. *Virology* 1985;142:44–58.
 83. **Garcia-Mata R, Gao YS, Sztul E.** Hassles with Taking Out the Garbage: Aggravating Aggresomes. *Traffic* 2002;3:388–396.
 84. **Martin MED, Berk AJ.** Adenovirus E1B 55K Represses p53 Activation In Vitro. *J Virol* 1998;72:3146–3154.
 85. **Yew PR, Liu X, Berk AJ.** Adenovirus E1B oncoprotein tethers a transcriptional repression domain to p53. *Genes Dev* 1994;8:190–202.
 86. **Sarnow P, Hearing P, Anderson CW, Halbert DN, Shenk T, et al.** Adenovirus Early Region 1B 58,000-Dalton Tumor Antigen Is Physically

- Associated with an Early Region 4 25,000-Dalton Protein in Productively Infected Cells. *J Virol* 1984;49:692–700.
87. **Baker A, Rohleder KJ, Hanakahi L a, Ketner G.** Adenovirus E4 34k and E1b 55k Oncoproteins Target Host DNA ligase IV for Proteasomal Degradation. *J Virol* 2007;81:7034–7040.
 88. **Orazio NI, Naeger CM, Karlseder J, Weitzman MD.** The Adenovirus E1b55K/E4orf6 Complex Induces Degradation of the Bloom Helicase during Infection. *J Virol* 2011;85:1887–1892.
 89. **Dallaire F, Blanchette P, Groitl P, Dobner T, Branton PE.** Identification of Integrin 3 as a New Substrate of the Adenovirus E4orf6/E1B 55-Kilodalton E3 Ubiquitin Ligase Complex. *J Virol* 2009;83:5329–5338.
 90. **Schreiner S, Wimmer P, Sirma H, Everett RD, Blanchette P, et al.** Proteasome-Dependent Degradation of Daxx by the Viral E1B-55K Protein in Human Adenovirus-Infected Cells. *J Virol* 2010;84:7029–7038.
 91. **Halbert DN, Cutt JR, Shenk T.** Adenovirus Early Region 4 Encodes Functions Required for Efficient DNA Replication, Late Gene Expression, and Host Cell Shutoff. *J Virol* 1985;56:250–257.
 92. **Weinberg DH, Ketner G.** Adenoviral Early Region 4 Is Required for Efficient Viral DNA Replication and for Late Gene Expression. *J Virol* 1986;57:833–838.
 93. **Blanchette P, Kindsmüller K, Groitl P, Dallaire F, Speiseder T, et al.** Control of mRNA Export by Adenovirus E4orf6 and E1B55K Proteins During Productive Infection Requires E4orf6 Ubiquitin Ligase Activity. *J Virol* 2008;82:2642–51.
 94. **Woo JL, Berk AJ.** Adenovirus Ubiquitin-Protein Ligase Stimulates Viral Late mRNA Nuclear Export. *J Virol* 2007;81:575–87.
 95. **Van Damme E, Laukens K, Dang TH, Van Ostade X.** A manually curated network of the PML nuclear body interactome reveals an important role for PML-NBs in SUMOylation dynamics. *Int J Biol Sci* 2010;6:51–67.
 96. **Wimmer P, Schreiner S, Everett RD, Sirma H, Groitl P, et al.** SUMO modification of E1B-55K oncoprotein regulates isoform-specific binding to the tumour suppressor protein PML. *Oncogene* 2010;29:5511–5522.
 97. **Berscheminski J, Brun J, Speiseder T, Wimmer P, Ip WH, et al.** Sp100A is a tumor suppressor that activates p53-dependent transcription and counteracts E1A/E1B-55K-mediated transformation. *Oncogene* 2015;1–12.

98. **Berscheminski J, Wimmer P, Brun J, Ip WH, Groitl P, et al.** Sp100 Isoform-Specific Regulation of Human Adenovirus 5 Gene Expression. *J Virol* 2014;88:6076–6092.
99. **Bürck C, Mund A, Berscheminski J, Kieweg L, Müncheberg S, et al.** KAP1 Is a Host Restriction Factor That Promotes Human Adenovirus E1B-55K SUMO Modification. *J Virol* 2015;JVI.01836-15.
100. **Cheng CY, Gilson T, Dallaire F, Ketner G, Branton PE, et al.** The E4orf6/E1B55K E3 Ubiquitin Ligase Complexes of Human Adenoviruses Exhibit Heterogeneity in Composition and Substrate Specificity. *J Virol* 2011;85:765–775.
101. **Cheng CY, Gilson T, Wimmer P, Schreiner S, Ketner G, et al.** Role of E1B55K in E4orf6/E1B55K E3 Ligase Complexes Formed by Different Human Adenovirus Serotypes. *J Virol* 2013;87:6232–45.
102. **Forrester NA, Sedgwick GG, Thomas A, Blackford AN, Speiseder T, et al.** Serotype-Specific Inactivation of the Cellular DNA Damage Response during Adenovirus Infection. *J Virol* 2011;85:2201–2211.
103. **Blanchette P, Wimmer P, Dallaire F, Cheng CY, Branton PE.** Aggresome Formation by the Adenoviral Protein E1B55K Is Not Conserved among Adenovirus Species and Is Not Required for Efficient Degradation of Nuclear Substrates. *J Virol* 2013;87:4872–4881.
104. **Graham F, Rowe DT, McKinnon R, Bacchetti S, Ruben M, et al.** Transformation by Human Adenoviruses. *J Cell Physiol Suppl* 1984;163:151–163.
105. **Freeman AE, Black PH, Vanderpool EA, Henry PH, Austin JB, et al.** Transformation of Primary Rat Embryo Cells by Adenovirus Type 2. *PNAS* 1967;58:1205–1212.
106. **Houweling A, Van Den Elsen PJ, Van Der Eb AJ.** Partial Transformation of Primary Rat Cells by the Leftmost 4.5% of Adenovirus 5 DNA. *Virology* 1980;105:537–550.
107. **McBride WD, Wiener A.** In Vitro Transformation of Hamster Kidney Cells by Human Adenovirus Type 12. *Proc Soc Exp Biol Med* 1964;115:870–4.
108. **Lowe SW, Ruley HE.** Stabilization of the p53 tumor suppressor is induced by adenovirus-5 E1A and accompanies apoptosis. *Genes Dev* 1993;7:535–545.

109. **Querido E, Teodoro JG, Branton PE.** Accumulation of p53 Induced by the Adenovirus E1A Protein Requires Regions Involved in the Stimulation of DNA Synthesis. *J Virol* 1997;71:3526–3533.
110. **Debbas M, White E.** Wild-type p53 mediates apoptosis by E1A, which is inhibited by E1B. *Genes Dev* 1993;7:546–554.
111. **Schreiner S, Wimmer P, Groitl P, Chen S-Y, Blanchette P, et al.** Adenovirus Type 5 Early Region 1B 55K Oncoprotein-Dependent Degradation of Cellular Factor Daxx Is Required for Efficient Transformation of Primary Rodent Cells. *J Virol* 2011;85:8752–8765.
112. **Endter C, Dobner T.** Cell Transformation by Human Adenoviruses. *Curr Top Microbiol Immunol* 2004;273:163–214.
113. **Kosulin K, Haberler C, Hainfellner JA, Amann G, Lang S, et al.** Investigation of Adenovirus Occurrence in Pediatric Tumor Entities. *J Virol* 2007;81:7629–7635.
114. **Kuwano K, Kawasaki M, Kunitake R, Hagimoto N, Nomoto Y, et al.** Detection of group C adenovirus DNA in small-cell lung cancer with the nested polymerase chain reaction. *J Cancer Res Clin Oncol* 1997;123:377–82.
115. **Kosulin K, Rauch M, Ambros PF, Pötschger U, Chott A, et al.** Screening for adenoviruses in haematological neoplasia: High prevalence in mantle cell lymphoma. *Eur J Cancer* 2014;50:622–7.
116. **Kosulin K, Hoffmann F, Clauditz TS, Wilczak W, Dobner T.** Presence of Adenovirus Species C in Infiltrating Lymphocytes of Human Sarcoma. *PLoS One* 2013;8:e63646.
117. **Speiseder T, Hofmann-Sieber H, Rodríguez E, Schellenberg A, Akyüz N, et al.** Efficient Transformation of Primary Human Mesenchymal Stromal Cells by Adenovirus Early Region 1 Oncogenes. *J Virol* 2017;91:1782–1798.
118. **Ciechanover A.** The ubiquitin-proteasome pathway: on protein death and cell life. *EMBO J* 1998;17:7151–7160.
119. **Haglund K, Dikic I.** Ubiquitylation and cell signaling. *EMBO J* 2005;24:3353–3359.
120. **Johnson ES.** Protein Modification by SUMO. *Annu Rev Biochem* 2004;73:355–382.
121. **Ribet D, Cossart P.** Ubiquitin, SUMO, and NEDD8: Key Targets of Bacterial Pathogens. *Trends Cell Biol* 2018;28:926–940.

122. **Everett RD, Boutell C, Hale BG.** Interplay between viruses and host sumoylation pathways. *Nat Rev Microbiol* 2013;11:400–411.
123. **Goldknopf IL, Busch H.** Isopeptide linkage between nonhistone and histone 2A polypeptides of chromosomal conjugate-protein A24. *Biochemistry* 1977;74:864–868.
124. **Hay RT.** SUMO: A history of modification. *Mol Cell* 2005;18:1–12.
125. **Schneider E, Kartarius S, Schuster N, Montenarh M.** The cyclin H/cdk7/Mat1 kinase activity is regulated by CK2 phosphorylation of cyclin H. *Oncogene* 2002;21:5031–5037.
126. **Montenarh, Mathias.** Protein kinase CK2 in DNA damage and repair. *Transl Cancer Res* 2016;5:49–63.
127. **Ahmad KA, Wang G, Unger G, Slaton J, Ahmed K.** Protein Kinase CK2- A Key Suppressor of Apoptosis. *Adv Enzym Regul* 2008;48:179–187.
128. **Meggio F, Pinna LA.** One-thousand-and-one substrates of protein kinase CK2? *FASEB J* 2003;17:349–368.
129. **Trembley JH, Wang G, Unger G, Slaton J, Ahmed K, et al.** CK2: A key player in cancer biology. *Cell Mol Life Sci* 2009;66:1858–1867.
130. **Medina-Palazon C, Gruffat H, Mure F, Filhol O, Vingtdeux-Didier V, et al.** Protein Kinase CK2 Phosphorylation of EB2 Regulates Its Function in the Production of Epstein-Barr Virus Infectious Viral Particles. *J Virol* 2007;81:11850–11860.
131. **Franck N, Le Seyec J, Guguen-Guillouzo C, Erdtmann L.** Hepatitis C Virus NS2 Protein Is Phosphorylated by the Protein Kinase CK2 and Targeted for Degradation to the Proteasome. *J Virol* 2005;79:2700–2708.
132. **Niefind K, Pütter M, Guerra B, Issinger O-G, Schomburg D.** GTP plus water mimic ATP in the active site of protein kinase CK2. *Nat Struct Biol* 1999;6:1100–1103.
133. **Allfrey VG, Mirsky AE.** Structural modifications of histones and their possible role in the regulation of RNA synthesis. *Science* 1964;144:559.
134. **Drazic A, Myklebust LM, Ree R, Arnesen T.** The world of protein acetylation. *Biochim Biophys Acta* 2016;1864:1372–1401.
135. **Li M, Luo J, Brooks CL, Gu W.** Acetylation of p53 Inhibits Its Ubiquitination by Mdm2. *J Biol Chem* 2002;277:50607–50611.
136. **Van Rechem C, Boulay G, Pinte S, Stankovic-Valentin N, Guérardel C, et al.** Differential Regulation of HIC1 Target Genes by CtBP and NuRD,

- via an Acetylation/SUMOylation Switch, in Quiescent versus Proliferating Cells. *Mol Cell Biol* 2010;30:4045–4059.
137. **Guan D, Lim JH, Peng L, Liu Y, Lam M, et al.** Deacetylation of the tumor suppressor protein PML regulates hydrogen peroxide-induced cell death. *Cell Death Dis* 2014;5:e1340.
138. **Matunis MJ, Coutavas E, Blobel G.** A Novel Ubiquitin-like Modification Modulates the Partitioning of the Ran-GTPase-activating Protein RanGAP1 between the Cytosol and the Nuclear Pore Complex. *J Cell Biol* 1996;135:1457–1470.
139. **Mahajan R, Delphin C, Guan T.** A Small Ubiquitin-Related Polypeptide Involved in Targeting RanGAP1 to Nuclear Pore Complex Protein RanBP2. *Cell* 1997;88:97–107.
140. **Saitoh H, Hinchey J.** Functional Heterogeneity of Small Ubiquitin-related Protein Modifiers SUMO-1 versus SUMO-2/3. *J Biol Chem* 2000;275:6252–6258.
141. **Tatham MH, Jaffray E, Vaughan OA, Desterro JMP, Botting CH, et al.** Polymeric Chains of SUMO-2 and SUMO-3 Are Conjugated to Protein Substrates by SAE1/SAE2 and Ubc9. *J Biol Chem* 2001;276:35368–35374.
142. **Bohren KM, Nadkarni V, Song JH, Gabbay KH, Owerbach D.** A M55V Polymorphism in a Novel SUMO Gene (SUMO-4) Differentially Activates Heat Shock Transcription Factors and Is Associated with Susceptibility to Type I Diabetes Mellitus. *J Biol Chem* 2004;279:27233–27238.
143. **Su H-L, Li SSL.** Molecular features of human ubiquitin-like SUMO genes and their encoded proteins. *Gene* 2002;296:65–73.
144. **Liang Y-C, Lee C-C, Yao Y-L, Lai C-C, Lienhard Schmitz M, et al.** SUMO5, a Novel Poly-SUMO Isoform, Regulates PML Nuclear Bodies. *Sci Rep* 2016;6:26509.
145. **Rodriguez MS, Dargemont C, Hay RT.** SUMO-1 Conjugation in Vivo Requires Both a Consensus Modification Motif and Nuclear Targeting. *J Biol Chem* 2001;276:12654–12659.
146. **Johnson ES, Schwienhorst I.** The ubiquitin-like protein Smt3p is activated for conjugation to other proteins by an Aos1p/Uba2p heterodimer. *EMBO J* 1997;16:5509–5519.
147. **Desterro JMP, Rodriguez MS, Kemp GD, Hay RT.** Identification of the Enzyme Required for Activation of the Small Ubiquitin-like Protein

- SUMO-1. *J Biol Chem* 1999;274:10618–10624.
148. **Desterro JMP, Thomson J, Hay RT.** Ubch9 conjugates SUMO but not ubiquitin. *FEBS Lett* 1997;417:297–300.
 149. **Okuma T, Honda R, Ichikawa G, Tsumagari N, Yasuda H.** In Vitro SUMO-1 Modification Requires Two Enzymatic Steps, E1 and E2. *Biochem Biophys Res Commun* 1999;254:693–698.
 150. **Geiss-Friedlander R, Melchior F.** Concepts in sumoylation: a decade on. *Nat Rev Mol Cell Biol* 2007;8:947–956.
 151. **Kotaja N, Karvonen U, Jänne OA, Palvimo JJ.** PIAS Proteins Modulate Transcription Factors by Functioning as SUMO-1 Ligases. *Mol Cell Biol* 2002;22:5222–5234.
 152. **Pichler A, Gast A, Seeler JS, Dejean A, Melchior F.** The Nucleoporin RanBP2 Has SUMO1 E3 Ligase Activity. *Cell* 2002;108:109–120.
 153. **Kagey MH, Melhuish TA, Wotton D.** The Polycomb Protein Pc2 Is a SUMO E3. *Cell* 2003;113:127–137.
 154. **Li S-J, Hochstrasser M.** A new protease required for cell-cycle progression in yeast. *Nature* 1999;398:246–251.
 155. **Gong L, Millas S, Maul GG, Yeh ETH.** Differential Regulation of Sentrinized Proteins by a Novel Sentrin-specific Protease. *J Biol Chem* 2000;275:3355–3359.
 156. **Hewitt EW, Duncan L, Mufti D, Baker J, Stevenson PG, et al.** Ubiquitylation of MHC class I by the K3 viral protein signals internalization and TSG101-dependent degradation. *EMBO J* 2002;21:2418–2429.
 157. **Huibregtse JM, Scheffner M, Howley PM.** A cellular protein mediates association of p53 with the E6 oncoprotein of human papillomavirus types 16 or 18. *EMBO J* 1991;10:4129–4135.
 158. **Scheffner M, Huibregtse JM, Vierstra RD, Howley PM.** The HPV-16 E6 and E6-AP complex functions as a ubiquitin-protein ligase in the ubiquitination of p53. *Cell* 1993;75:495–505.
 159. **Martinez-Zapien D, Ruiz FX, Poirson J, Mitschler A, Ramirez-Ramos J, et al.** Structure of the E6/E6AP/p53 complex required for HPV-mediated degradation of p53. *Nature* 2016;529:541–545.
 160. **Boutell C, Cuchet-Lourenço D, Vanni E, Orr A, Glass M, et al.** A Viral Ubiquitin Ligase Has Substrate Preferential SUMO Targeted Ubiquitin

- Ligase Activity that Counteracts Intrinsic Antiviral Defence. *PLoS Pathog* 2011;7:e1002245.
161. **Sohn S-Y, Hearing P.** The adenovirus E4-ORF3 protein functions as a SUMO E3 ligase for TIF-1 γ sumoylation and poly-SUMO chain elongation. *PNAS* 2016;113:6725–30.
 162. **Chang P-C, Izumiya Y, Wu C-Y, Fitzgerald LD, Campbell M, et al.** Kaposi's Sarcoma-associated Herpesvirus (KSHV) Encodes a SUMO E3 ligase That Is SIM-dependent and SUMO-2/3-specific. *J Biol Chem* 2010;285:5266–5273.
 163. **De La Cruz-Herrera CF, Shire K, Siddiqi UZ, Frappier L.** A genome-wide screen of Epstein-Barr virus proteins that modulate host SUMOylation identifies a SUMO E3 ligase conserved in herpesviruses. *PLoS Pathog* 2018;14:e1007176.
 164. **Wilson VG, Rangasamy D.** Viral interaction with the host cell sumoylation system. *Virus Res* 2001;81:17–27.
 165. **Hofmann H, Flöss S, Stamminger T.** Covalent Modification of the Transactivator Protein IE2-p86 of Human Cytomegalovirus by Conjugation to the Ubiquitin-Homologous Proteins SUMO-1 and hSMT3b. *J Virol* 2000;74:2510–2524.
 166. **Hagemeier SR, Dickerson SJ, Meng Q, Yu X, Mertz JE, et al.** Sumoylation of the Epstein-Barr Virus BZLF1 Protein Inhibits Its Transcriptional Activity and Is Regulated by the Virus-Encoded Protein Kinase. *J Virol* 2010;84:4383–4394.
 167. **Chen S-C, Chang L-Y, Wang Y-W, Chen Y-C, Weng K-F, et al.** Sumoylation-promoted Enterovirus 71 3C Degradation Correlates with a Reduction in Viral Replication and Cell Apoptosis. *J Biol Chem* 2011;286:31373–31384.
 168. **Gurer C, Berthoux L, Luban J.** Covalent Modification of Human Immunodeficiency Virus Type 1 p6 by SUMO-1. *J Virol* 2005;79:910–917.
 169. **Kindsmüller K, Groitl P, Härtl B, Blanchette P, Hauber J, et al.** Intranuclear targeting and nuclear export of the adenovirus E1B-55K protein are regulated by SUMO1 conjugation. *PNAS* 2007;104:6684–6689.
 170. **Wimmer P, Blanchette P, Schreiner S, Ching W, Groitl P, et al.** Cross-talk between phosphorylation and SUMOylation regulates transforming activities of an adenoviral oncoprotein. *Oncogene* 2012;32:1626–1637.

171. **Endter C, Härtl B, Spruss T, Hauber J, Dobner T.** Blockage of CRM1-dependent nuclear export of the adenovirus type 5 early region 1B 55-kDa protein augments oncogenic transformation of primary rat cells. *Oncogene* 2005;24:55–64.
172. **Hanahan D, Meselson M.** Plasmid screening at high colony density. *Methods Enzymol* 1983;100:333–42.
173. **Giard DJ, Aaronson SA, Todaro GJ, Arnstein P, Kersey JH, et al.** In Vitro Cultivation of Human Tumors: Establishment of Cell Lines Derived From a Series of Solid Tumors. *J Natl Cancer Inst* 1973;51:1417–1423.
174. **Mitsudomi T, Steinberg SM, Nau MM, Carbone D, D'Amico D, et al.** p53 gene mutations in non-small-cell lung cancer cell lines and their correlation with the presence of ras mutations and clinical features. *Oncogene* 1992;7:171–80.
175. **Gey GO, Coffman WD, Kubicek MT.** Tissue culture studies of the proliferative capacity of cervical carcinoma and normal epithelium. *Cancer Res* 1952;12:264–265.
176. **Tatham MH, Rodriguez MS, Xirodimas DP, Hay RT.** Detection of protein SUMOylation in vivo. *Nat Protoc* 2009;4:1363–1371.
177. **Sarnow P, Sullivan CA, Levine AJ.** A Monoclonal Antibody Detecting the Adenovirus Type 5 Elb-58Kd Tumor Antigen: Characterization of the E1b-58Kd Tumor Antigen in Adenovirus-Infected and -Transformed Cell. *Virology* 1982;120:510–517.
178. **Kindsmüller K, Schreiner S, Leinenkugel F, Groitl P, Kremmer E, et al.** A 49-Kilodalton Isoform of the Adenovirus Type 5 Early Region 1B 55-Kilodalton Protein Is Sufficient To Support Virus Replication. *J Virol* 2009;83:9045–56.
179. **Reich NC, Sarnow P, Duprey E, Levine AJ.** Monoclonal antibodies which recognize native and denatured forms of the adenovirus DNA-binding protein. *Virology* 1983;128:480–4.
180. **Vojtěšek B, Bártek J, Midgley CA, Lane DP.** An immunochemical analysis of the human nuclear phosphoprotein p53. New monoclonal antibodies and epitope mapping using recombinant p53. *J Immunol Methods* 1992;151:237–44.
181. **Schindelin J, Arganda-Carreras I, Frise E, Kaynig V, Longair M, et al.** Fiji: an open-source platform for biological-image analysis. *Nat Methods*

- 2012;9:676–82.
182. **Ren J, Gao X, Jin C, Zhu M, Wang X, et al.** Systematic study of protein sumoylation: Development of a site-specific predictor of SUMOsp 2.0. *Proteomics* 2009;9:3409–3412.
 183. **Zhao Q, Xie Y, Zheng Y, Jiang S, Liu W, et al.** GPS-SUMO: a tool for the prediction of sumoylation sites and SUMO-interaction motifs. *Nucleic Acids Res* 2014;42:W325-30.
 184. **Bradford MM.** A Rapid and Sensitive Method for the Quantitation of Microgram Quantities of Protein Utilizing the Principle of Protein-Dye Binding. *Anal Biochem* 1976;72:248–254.
 185. **Laemmli UK.** Cleavage of structural proteins during the assembly of the head of bacteriophage T4. *Nature* 1970;227:680–5.
 186. **Tammsalu T, Matic I, Jaffray EG, Ibrahim AFM, Tatham MH, et al.** Proteome-wide identification of SUMO modification sites by mass spectrometry. *Nat Protoc* 2015;10:1374–1388.
 187. **Cheng X, Kao H-Y.** Post-translational modifications of PML: consequences and implications. *Front Oncol* 2013;2:1–10.
 188. **Dosch T, Horn F, Schneider G, Krätzer F, Dobner T, et al.** The Adenovirus Type 5 E1B-55K Oncoprotein Actively Shuttles in Virus-Infected Cells, Whereas Transport of E4orf6 Is Mediated by a CRM1-Independent Mechanism. *J Virol* 2001;75:5677–5683.
 189. **Ornelles DA, Shenk T.** Localization of the Adenovirus Early Region 1B 55-Kilodalton Protein during Lytic Infection: Association with Nuclear Viral Inclusions Requires the Early Region 4 34-Kilodalton Protein. *J Virol* 1991;65:424–9.
 190. **Yew PR, Berk AJ.** Inhibition of p53 transactivation required for transformation by adenovirus early 1B protein. *Nature* 1992;357:82–85.
 191. **Matsuzaki H, Daitoku H, Hatta M, Aoyama H, Yoshimochi K, et al.** Acetylation of Foxo1 alters its DNA-binding ability and sensitivity to phosphorylation. *PNAS* 2005;102:11278–83.
 192. **Teodoro JG, Branton PE.** Regulation of p53-Dependent Apoptosis, Transcriptional Repression, and Cell Transformation by Phosphorylation of the 55-Kilodalton E1B Protein of Human Adenovirus Type 5. *J Virol* 1997;71:3620–3627.
 193. **Berk AJ.** Recent lessons in gene expression, cell cycle control, and cell

- biology from adenovirus. *Oncogene* 2005;24:7673–7685.
194. **Kerscher O.** SUMO junction - what's your function? New insights through SUMO-interacting motifs. *EMBO Rep* 2007;8:550–555.
 195. **Sieber T, Scholz R, Spoerner M, Schumann F, Kalbitzer HR, et al.** Intrinsic disorder in the common N-terminus of human adenovirus 5 E1B-55K and its related E1BN proteins indicated by studies on E1B-93R. *Virology* 2011;418:133–143.
 196. **Lori C, Lantella A, Pasquo A, Alexander LT, Knapp S, et al.** Effect of Single Amino Acid Substitution Observed in Cancer on Pim-1 Kinase Thermodynamic Stability and Structure. *PLoS One* 2013;8:e64824.
 197. **Miyauchi Y, Yogosawa S, Honda R, Nishida T, Yasuda H.** Sumoylation of Mdm2 by Protein Inhibitor of Activated STAT (PIAS) and RanBP2 Enzymes. *J Biol Chem* 2002;277:50131–50136.
 198. **Du JX, Bialkowska AB, McConnell BB, Yang VW.** SUMOylation Regulates Nuclear Localization of Krüppel-like Factor 5. *J Biol Chem* 2008;283:31991–32002.
 199. **Wilson VG, Rangasamy D.** Intracellular Targeting of Proteins by Sumoylation. *Exp Cell Res* 2001;271:57–65.
 200. **Comerford KM, Leonard MO, Karhausen J, Carey R, Colgan SP, et al.** Small ubiquitin-related modifier-1 modification mediates resolution of CREB-dependent responses to hypoxia. *PNAS* 2003;100:986–991.
 201. **Lin X, Sun B, Liang M, Liang Y-Y, Gast A, et al.** Opposed Regulation of Corepressor CtBP by SUMOylation and PDZ Binding. *Mol Cell* 2003;11:1389–1396.
 202. **Ullman AJ, Hearing P.** Cellular Proteins PML and Daxx Mediate an Innate Antiviral Defense Antagonized by the Adenovirus E4 ORF3 Protein. *J Virol* 2008;82:7325–7335.
 203. **Muromoto R, Sugiyama K, Yamamoto T, Oritani K, Shimoda K, et al.** Physical and functional interactions between Daxx and TSG101. *Biochem Biophys Res Commun* 2004;316:827–833.
 204. **He M, Zhang L, Wang X, Huo L, Sun L, et al.** Systematic Analysis of the Functions of Lysine Acetylation in the Regulation of Tat Activity. *PLoS One* 2013;8:e67186.
 205. **Haupt Y, Maya R, Kazaz A, Oren M.** Mdm2 promotes the rapid degradation of p53. *Nature* 1997;387:296–299.

206. **Kubbutat MHG, Jones SN, Vousden KH.** Regulation of p53 stability by Mdm2. *Nature* 1997;387:299–303.
207. **Honda R, Tanaka H, Yasuda H.** Oncoprotein MDM2 is a ubiquitin ligase E3 for tumor suppressor p53. *FEBS Lett* 1997;420:25–27.
208. **Liu Y, Colosimo AL, Yang X-J, Liao D.** Adenovirus E1B 55-Kilodalton Oncoprotein Inhibits p53 Acetylation by PCAF. *Mol Cell Biol* 2000;20:5540–5553.
209. **Lischka P, Rosorius O, Trommer E, Stamminger T.** A novel transferable nuclear export signal mediated CRM1-independent nucleocytoplasmic shuttling of the human cytomegalovirus transactivator protein pUL69. *EMBO J* 2001;20:7271–7283.
210. **Kutay U, Bischoff FR.** Export of Importin from the Nucleus Is Mediated by a Specific Nuclear Transport Factor. *Cell* 1997;90:1061–1071.
211. **Kutay U, Lipowsky G, Izaurralde E, Bischoff FR, Schwarzmaier P, et al.** Identification of a tRNA-Specific Nuclear Export Receptor. *Mol Cell* 1998;1:359–369.
212. **Verma SC, Lan K, Robertson E.** Structure and Function of Latency-Associated Nuclear Antigen. *Curr Top Microbiol Immunol* 2007;312:101–136.
213. **Cai Q, Cai S, Zhu C, Verma SC, Choi JY, et al.** A Unique SUMO-2-Interacting Motif within LANA Is Essential for KSHV Latency. *PLoS Pathog* 2013;9:1–14.
214. **Campbell M, Izumiya Y.** Post-translational modifications of Kaposi's sarcoma-associated herpesvirus regulatory proteins - SUMO and KSHV. *Front Microbiol* 2012;3:1–13.
215. **Rooney CM, Rowe DT, Ragot T, Farrell PJ.** The Spliced BZLF1 Gene of Epstein-Barr Virus (EBV) Transactivates an Early EBV Promoter and Induces the Virus Productive Cycle. *J Virol* 1989;3109–3116.
216. **Takada K, Shimizu N, Sakuma S, Ono Y.** trans Activation of the Latent Epstein-Barr Virus (EBV) Genome after Transfection of the EBV DNA Fragment. *J Virol* 1986;1016–1022.

Zusammenfassung

E1B-55K (*early region 1B 55 kDa*) der humanen Adenoviren Spezies C Typ 5 (HAdV-C5) ist ein frühes multifunktionelles Protein, das eine entscheidende Rolle während des gesamten viralen Replikationszyklus spielt. Das erste exprimierte virale Protein E1A unterstützt die virale Replikation durch die Induktion der S-Phase. Dabei wird das zelluläre pro-apoptotische Protein p53 stabilisiert. E1B-55K entwickelte mehrere Mechanismen, um dieser Stabilisierung entgegenzuwirken. Zum einen dient E1B-55K als E3-SUMO-Ligase für p53 und transportiert das Protein aus dem Nukleus, um die Aktivierung der pro-apoptotischen p53-abhängigen Gene zu inhibieren. Zum anderen bildet E1B-55K zusammen mit E4orf6 und weiteren zellulären Proteinen einen E3-Ubiquitin-Ligase Komplex, der neben p53 auch andere zelluläre Faktoren abbaut. Dazu gehören unter anderem Mre11, SPOC-1 und Daxx, die sowohl an der DNA-Schadensantwort (*DNA damage response; DDR*) als auch an der Transkriptionsregulierung beteiligt sind. Diese anti-apoptotischen und proviralen Funktionen führen zum onkogenen Potential von E1B-55K. Darüber hinaus erhöhen post-translationale Modifikationen (PTMs) an E1B-55K seine funktionelle Vielfalt, die wiederum durch gegenseitige Regulation der PTMs nochmal erhöht wird. Interessanterweise werden viele Funktionen von E1B-55K durch SUMOylierung reguliert, was darauf schließen lässt, dass diese Modifikation ein essentieller Bestandteil für das Protein ist. Um diesen Sachverhalt noch besser zu verstehen, wurde E1B-55K mittels Massenspektrometrie genauer untersucht. Dabei wurde unter anderem ein Lysin an Position 101 (K101) als potentielles neues SUMO-Konjugationsmotiv (*SUMO conjugation motif; SCM*) entdeckt. Die Nähe von K101 zum eigentlichen SCM um das Lysin 104 (K104) machte diese Position besonders interessant. Daher ist K101 Gegenstand der Untersuchungen dieser Arbeit.

Im ersten Teil wurde K101 als Regulator der E1B-55K SUMOylierung identifiziert. Untersuchungen dieses Lysins durch einen Aminosäureaustausch (K101R) zeigten eine erhöhte SUMOylierung von E1B-55K. Übereinstimmend mit früheren Studien an E1B-55K Mutanten, die eine erhöhte SUMOylierung zeigen, wies E1B-55K K101R eine vermehrt nukleare Lokalisation auf. Außerdem zeigten Infektionsexperimente mit E1B-55K K101R, dass es in

Strukturen lokalisiert, die mutmaßlich virale Replikationszentren (*replication center*; RC) darstellen. Funktionell ging die erhöhte SUMOylierung der K101R-Mutante mit einer verstärkten Hemmung der p53-abhängigen Transkription sowie einer erhöhten Fokusformation in Transformationsexperimenten einher.

Der zweite Teil dieser Arbeit befasste sich mit E1B-55K von weiteren HAdV Spezies. Zunächst wurde ein konserviertes SCM in nahezu allen Spezies identifiziert. Zudem wurde gezeigt, dass K101 spezifisch für HAdV der Spezies C ist, da alle anderen HAdV Spezies ein Arginin an entsprechender Stelle aufwiesen. Vergleichbar mit HAdV-C5 E1B-55K K101R wurden die Proteine fast aller untersuchten Spezies stark SUMOyliert und lokalisierten meist im Nukleus. Ein Vergleich von E1B-55K der verschiedenen Spezies hinsichtlich der SUMO-anhängigen Funktionen zeigt, dass die Hemmung der p53-vermittelten Transkription eher konserviert, während seine Funktion als E3-SUMO1-Ligase nicht konserviert zu sein scheint. Die Ergebnisse dieser Arbeit zeigen, dass E1B-55K speziesübergreifende konservierte Funktionen entwickelt hat, die allerdings je nach Spezies und mutmaßlich Pathogenität ein wenig voneinander abweichen.

Publications

I Publications in scientific journals

- Rodríguez E, Ip WH, Kolbe V, Hartmann K, Pilnitz-Stolze G, Tekin-Bubenheim N, Gómez-Medina S, Muñoz-Fontela C, Krasemann S, Dobner T. Humanized Mice Reproduce Acute and Persistent Human Adenovirus Infection. *J Infect Dis* 2017;215:70–79.
- Kolbe V, Kieweg-Thompson L, Bezgovsek J, Gruhne J, Schreiner S, Tatham MH, Hay RT, Dobner T. SUMO-2 conjugation is highly conserved in large E1B proteins from different human Adenovirus species. (*manuscript in preparation*).

II Oral presentations at scientific meetings

- 12th International Adenovirus Meeting, Barsinghausen, Germany, 2016
- DNA Tumor Virus Meeting, Birmingham, United Kingdom, 2017
- 1st Ad-Obese Workshop, San José Vista Hermosa, Mexico, 2018

III Poster presentations at scientific meetings

- 26th Annual Meeting of the Society of Virology, Münster, Germany, 2016
- HPI Scientific Retreat, Hamburg, Germany, 2016
- EMBO conference Ubiquitin and SUMO, Cavtat, Croatia, 2017
- 13th International Adenovirus Meeting, San José Vista Hermosa, Mexico, 2018
- HPI Scientific Retreat, Hamburg, Germany, 2018

Danksagung

Zuallererst möchte ich meinem Doktorvater und Erstgutachter Thomas Dobner dafür danken, dass er mir die Möglichkeit gegeben hat, meine Doktorarbeit in seiner Abteilung zu schreiben. Vielen Dank für Deine Unterstützung, den wissenschaftlichen Austausch und den Freiraum, eigenverantwortlich zu arbeiten.

Außerdem möchte ich Nicole Fischer für die Übernahme meines Zweitgutachtens danken. Danke für die vielen wertvollen Besprechungen und Anregungen von Deiner Seite.

Vielen Dank an Julia Kehr für die Übernahme des Vorsitzes während meiner Disputation und an Joachim Hauber für die Mitwirkung in der Prüfungskommission.

Ein großer Dank gilt Wing-Hang Ip und Estefanía Rodríguez-Burgos. Danke, dass Ihr diese Arbeit – trotz der Feiertage – gelesen habt und mir mit vielen hilfreichen Verbesserungen und Kommentaren zur Seite gestanden habt. Vielen Dank an Timothy Soh. Danke, dass Du die Arbeit noch einmal gelesen hast und für die Übernahme des Sprachgutachtens.

Der gesamten Abteilung Dobner möchte ich für die vier tollen Jahre am HPI danken. Vielen Dank insbesondere an Sarah Müncheberg, Tina Meyer, Wing-Hang Ip, Nora Freudenberger, Carolin Bürck, Julia Gruhne, Steewen Krohne, Michael Melling, Marie Fiedler, Britta Wilkens und Edda Renz für Eure Unterstützung im Labor, zahlreiche (wissenschaftliche) Diskussionen, die gute Arbeitsatmosphäre und viele lustige Momente zusammen.

Zuletzt noch ein großer Dank an meine Freunde, meine Familie und meinen Freund Niels. Ohne Eure Hilfe und Unterstützung hätte ich es nicht geschafft. Ihr seid super!